

**Characterization of Semi-insulating Liquid Encapsulated Czochralski  
Gallium Arsenide**

**By**

**Hiroshi Kato**

**B.Sc., The University of British Columbia 1985**

**A THESIS SUBMITTED IN PARTIAL FULFILMENT OF  
THE REQUIREMENTS FOR THE DEGREE OF  
MASTER OF APPLIED SCIENCE**

**in**

**THE FACULTY OF GRADUATE STUDIES**

**Department of Electrical Engineering**

**We accept this thesis as conforming**

**to the required standard**

**THE UNIVERSITY OF BRITISH COLUMBIA  
May 1994**

**© Hiroshi Kato, 1994**

In presenting this thesis in partial fulfilment of the requirements for an advanced degree at the University of British Columbia, I agree that the Library shall make it freely available for reference and study. I further agree that permission for extensive copying of this thesis for scholarly purposes may be granted by the head of my department or by his or her representatives. It is understood that copying or publication of this thesis for financial gain shall not be allowed without my written permission.

Department of ELECTRICAL ENGINEERING

The University of British Columbia  
Vancouver, Canada

Date July 7<sup>th</sup>, 1994

## **Abstract**

Deep levels in semi-insulating gallium arsenide (SI GaAs) have been associated with effects such as threshold voltage variations, sidegating and low frequency oscillations in transistors fabricated using this material. The distribution of deep levels is not uniform, which is a key concern to IC manufacturers. Techniques such as altering the stoichiometry of the melt, characterization of crucibles and encapsulants used in crystal growth and boule annealing have been used to improve the uniformity of wafers by GaAs suppliers.

The work to be described was part of a project in which optical transient current spectroscopy (OTCS) was used to investigate deep levels in GaAs wafers manufactured by Johnson Matthey in Trail, B.C. using a high pressure liquid encapsulated Czochralski (LEC) method. Part of the present work involved development of a scanning OTCS system to map variations across wafers. The inhomogeneities in LEC material display both microscopic and macroscopic features. The dimensions of dislocation networks are in the range of several tens of microns. On a macroscopic scale, the density of dislocations displays a radial dependence with concentrations being higher near the centre and outer edges of a wafer. Dislocations have been suspected to getter impurities. Previously published scanning OTCS experiments had examined macroscopic variations. The goal of the work was to map variations in the magnitude of OTCS signals with lateral resolution comparable to that of dislocation networks. The system consisted of a pulsed laser which was focussed onto the surface of GaAs wafers.

"Sandwich" type electrical contacts with one electrode semi-transparent were made to the specimen to monitor the photo-generated current in the sample. The stage used to support the sample was temperature controlled and could be stepped laterally with respect to the light spot in 0.1 micron steps. The magnitude of the exponentially decaying components of the photo-current pulses were examined using a double gated technique. Lateral variations in the OTCS signal similar in scale to dislocation networks were observed. In practice, it was difficult to correlate OTCS signals to an energy level corresponding to deep levels. Moreover the transient signals which were observed using the scanning OTCS apparatus were different from those typically encountered in non-scanning experiments conducted in this laboratory and reported in literature. To examine some of these differences, copper, which has been reported to create several deep levels in GaAs, was intentionally introduced into specimens of SI GaAs and measured using OTCS methods.

The remainder of the thesis deals with studies of copper as a contaminant of GaAs wafers. Copper was chosen because it is believed to be present in significant quantities in materials used in device fabrication and has been associated with problems in device performance[Hiramoto, 1988]. The effects of copper in GaAs have been studied by a number of groups[Tin, 1987][Venter, 1992][Moore,1992]. Various means were investigated to introduce minute quantities of copper sufficient to measurably alter electrical characteristics but not change gross features such as the high resistivity or physical appearance of the material. Results from OTCS measurements using a variety of experimental conditions were compared for both copper-treated and "as-received" GaAs substrates. The OTCS signatures found in this work were comparable to those reported in the literature, but a unique signal

due to the presence of copper was not determined. Comparisons of copper contaminated and untreated material were also made using cathodoluminescence and by measuring the current-voltage characteristics of ohmic and rectifying contacts made to the samples. In addition, the variation in current under illumination and in the dark were examined as a function of sample temperature.

## Table of Contents

Abstract .....	ii
Table of Contents .....	v
List of Tables .....	vii
List of Figures .....	viii
Acknowledgements .....	xi
<b>Chapter 1</b> Introduction .....	1
<b>Chapter 2</b> Previous Work on Optical Transient Current Spectroscopy	
2-1 Introduction .....	7
2-2 Review of Techniques Used to Map Defects in GaAs .....	9
2-2.1 Etch Pit Density .....	10
2-2.2 Infra-red Transmission .....	11
2-2.3 Photo-resistivity .....	11
2-2.4 Scanning DLTS .....	12
2-2.5 Scanning OTCS .....	12
2-2.6 Cathodoluminescence and Photoluminescence .....	13
2-3 Summary .....	13
<b>Chapter 3</b> Design of a Scanning OTCS System	
3-1 Introduction .....	15
3-2 Optical System .....	16
3-3 Translation Stage .....	17
3-4 Temperature Controlled Stage .....	17
3-5 Current Measurement and Data Collection .....	18
3-6 Experimental Method .....	20
3-7 Results of Scans .....	21
<b>Chapter 4</b> Preparation of Copper Diffused Samples	
4-1 Introduction .....	30
4-2 Literature Review of Diffusion of Copper in GaAs .....	31
4-2.1 Cathodoluminescence Studies of Copper in GaAs .....	35
4-3 Experimental Work .....	39
4-3.1 Introduction of Copper by Immersion in CuSO <sub>4</sub> Solution .....	42
4-3.2 Copper Deposition using Thermal Evaporation .....	46
4-3.2.1 Heat Treatments in a Tube Furnace .....	46
4-3.2.2 Heat Treatments Using Rapid Thermal Annealing Methods .....	50
4-4 Summary .....	57

<b>Chapter 5</b>	<b>The Effect of Copper on Current-Voltage Characteristics</b>	
5-1	Introduction	59
5-2	Methods Used to Form Contacts Reported in Literature	61
5-3	Fabrication of Samples	62
5-3.1	Heat Treatments in a Tube Furnace	64
5-3.2	Heat Treatments Using Rapid Thermal Annealing Methods	65
5-3.2.1	Planar Ohmic Electrodes	66
5-3.2.2	Results of Measurements	68
5-3.2.3	Planar Schottky Contacts	78
5-3.2.4	Results of Measurements	79
5-3.2.5	Effect of Temperature on I-V Behaviour	84
5-3.2.6	Temporal Variation in Current	88
5-3.2.7	Parallel Plate Structures	89
5-4	Conclusion	91
<b>Chapter 6</b>	<b>Comparison of Non-scanning Optical Transient Current Spectroscopy Applied to Copper Doped and Undoped GaAs</b>	
6-1	Non-scanning OTCS	94
6-1.1	Survey of Literature	96
6-2	Experimental Results	98
6-2.1	Co-planar Schottky Electrodes	98
6-2.2	Co-planar Ohmic Electrodes	99
6-2.3	Parallel Plate Electrodes	100
6-2.4	Effect of the Illumination Wavelength	102
6-2.5	Negative Transients	102
6-2.6	Exponential Fitting	107
6-3	Conclusion	108
<b>Chapter 7</b>	<b>Conclusion and Suggestions for Future Work</b>	110
<b>References</b>		111
<b>Appendix A</b>	<b>Fabrication Procedures</b>	121
<b>Appendix B</b>	<b>C Program for Performing Scanning OTCS</b>	123

## List of Tables

4-1	Studies of Copper in Undoped GaAs . . . . .	33
4-2	Reported Diffusion Constants and Solubilities of Copper in GaAs . . . . .	34
4-3	Estimates of Diffusion Constants of Samples Heated at 500°C to 600°C . . . . .	53
5-1	Types of Electrodes Used in Reported OTCS Work . . . . .	62
5-2	Resistance Parameters in Planar Ohmic Contacts . . . . .	74
5-3	Resistance Parameters in Planar Ohmic Contacts Under Illumination and in the Dark . . . . .	76
6-1	Copper Levels Reported in Literature . . . . .	97
6-2	Levels Detected Using Planar Al Electrodes and Double Gated Analysis . . . . .	99
6-3	Levels Detected Using Planar AuGe Electrodes and Double Gated Analysis . . . . .	99
6-4	Levels Detected Using Parallel Plate Electrodes and Double Gated Analysis . . . . .	102

## List of Figures

3-1	A Schematic Diagram of the Scanning OTCS Apparatus . . . . .	19
3-2(a)	Photo-current Map of 2500Å Thick Al Test Grid . . . . .	21
3-2(b)	OTCS Signal Map of 2500Å Thick Al Test Grid . . . . .	22
3-3(a)	OTCS Scan of 200µm x 200µm Area, $t_1=2\text{ms}$ and $t_2=10\text{ms}$ , 10 x Averaging . .	24
3-3(b)	Repeat Scan of Same Area as Fig. 3-2(a) using the Same Parameters . . . . .	25
3-4(a)	Topographical Map of Regions with the Largest Signal in Fig. 3-2(a) . . . . .	26
3-4(b)	Topographical Map of Regions with the Largest Signal in Fig. 3-2(b) . . . . .	27
3-5	An Example of a Cathodoluminescence Contrast Image . . . . .	28
4-1	Interaction of the Electron Beam With GaAs . . . . .	37
4-2	Schematic Diagram of the Apparatus Used to Obtain CL Images . . . . .	41
4-3	CL Image of Surface of GaAs Partially Immersed in $\text{CuSO}_4$ and Heated at 850°C . . . . .	43
4-4(a)	Profilometer Scan of Copper Film-GaAs Boundary Prior to Heat Treatment . . .	47
4-4(b)	Profilometer Scan of Copper Film-GaAs Boundary After Heat Treatment . . . . .	47
4-5	CL Image of Cleaved Edge of a GaAs Wafer at the Boundary of the Copper Film Heated at 500°C for 4 hrs . . . . .	49
4-6(a)	CL Image of Cleaved Edge of a GaAs Wafer at the Boundary of the Copper Film Heated at 950°C for 5 s . . . . .	51
4-6(b)	CL Image of Cleaved Edge of a GaAs Wafer Heated at 950°C for 5 s . . . . .	52
4-7(a)	CL Image of Cleaved Edge of a GaAs wafer Heated at 500°C for 50 s . . . . .	54
4-7(b)	CL Image of Cleaved Edge of a GaAs wafer Heated at 550°C for 50 s . . . . .	55
4-7(c)	CL Image of Cleaved Edge of a GaAs wafer Heated at 600°C for 50 s . . . . .	56
5-1	Electrode Geometry of Specimens . . . . .	63

5-2	I-V Plots of Copper Treated and Untreated Specimens Heated at 950° for 5 s .	65
5-3(a)	I-V Plots of AuGe\Ni\Au Electrodes, Control Sample Heated at 600° for 50 s .	69
5-3(b)	I-V Plots of AuGe\Ni\Au Electrodes, Cu Treated Sample Heated at 600° for 50 s . . . . .	70
5-4(a)	Resistance as a Function of Electrode Separation for Specimens Heated at 500°C for 50 s . . . . .	72
5-4(b)	Resistance as a Function of Electrode Separation for Specimens Heated at 600°C for 50 s . . . . .	73
5-5	Resistance as a Function of Electrode Separation under Illumination and In the Dark for Specimens Heated at 600° C for 50 s . . . . .	75
5-6(a)	I-V Plots for AuGe Metallizations Prior to Sintering for Cu Treated and Control Specimens . . . . .	77
5-6(b)	I-V Plots for AuGe Metallizations After Sintering for Cu Treated and Control Specimens . . . . .	77
5-7(a)	I-V Characteristics of Al Electrodes on GaAs with no Heat Treatment . . . . .	80
5-7(b)	I-V Characteristics of Al Electrodes on GaAs Heated at 450°C for 50 s . . . . .	80
5-7(c)	I-V Characteristics of Al Electrodes on GaAs Heated at 500°C for 50 s . . . . .	81
5-7(d)	I-V Characteristics of Al Electrodes on GaAs Heated at 550°C for 50 s . . . . .	81
5-7(e)	I-V Characteristics of Al Electrodes on GaAs Heated at 600°C for 50 s . . . . .	82
5-7(f)	I-V Characteristics of Al Electrodes on GaAs Heated at 650°C for 23 s . . . . .	82
5-7(g)	I-V Characteristics of Al Electrodes on GaAs Heated at 750°C for 13 s . . . . .	83
5-7(h)	I-V Characteristics of Al Electrodes on GaAs Heated at 850°C for 5 s . . . . .	83
5-8(a)	Control Sample Heated at 550°C, I-V Characteristics Measured at 250K . . . . .	85
5-8(b)	Control Sample Heated at 550°C, I-V Characteristics Measured at 300K . . . . .	86
5-8(c)	Control Sample Heated at 550°C, I-V Characteristics Measured at 350K . . . . .	87

5-9	Temporal Variation in the Current with Constant Applied Voltage . . . . .	88
5-10(a)	I-V Plots of Parallel Plate Electrode Samples Prior to OTCS Measurements . . . . .	.90
5-10(b)	I-V Plots of Parallel Plate Electrode Samples After OTCS Measurements . . . . .	.91
6-1(a)	OTCS Spectra of a Copper Treated Sample, $t_2=5t_1$ , $t_1$ incremented in 20 ms steps . . . . .	.100
6-1(b)	OTCS Spectra of an Untreated Sample, $t_2=5t_1$ , $t_1$ incremented in 20 ms steps . . . . .	.100
6-2(a)	Change in OTCS Spectra with Applied Voltage for 935nm Illumination .	104
6-2(b)	Change in OTCS Spectra with Applied Voltage for 660nm Illumination .	105
6-3	Arrhenius Plot for a Negative and Positive Peak . . . . .	106

## Acknowledgments

I would like to thank Dr. L. Young for his support, guidance and patience during this research. Generosity in allowing time off from work and use of facilities by Dr. N. Jaeger during the preparation of this thesis is greatly appreciated.

In addition I would like to thank C. Backhouse and D. Hui for their extensive assistance, allowing me to use their software routines for this work and helpful discussions. The assistance of A. Leugner, and all of the other members of the research group are also to be thanked.

The provision of GaAs wafers and valuable information on wafer characteristics by R. P. Bult of Johnson-Matthey is also greatly appreciated.

The moral support and understanding of J. Torrance outside of the laboratory was much needed and appreciated. I would especially like to thank my parents for their continual support.

# Chapter 1

## Introduction

Semi-insulating(SI) gallium arsenide(GaAs) is the starting material of choice for many applications in microwave and high-speed circuits as well as in opto-electronic devices. For high-speed operation, devices fabricated using SI GaAs benefit from the high electron mobility at low electric fields and high electrical resistivity of the substrate at room temperatures. In addition, because GaAs is an direct band gap semiconductor, it is suited for making infra-red light-emitting diodes and diode lasers for use in opto-electronic applications. However the commercial acceptance of SI GaAs manufactured using the liquid encapsulated Czochralski (LEC) method has been hampered by effects such as variation in threshold voltages, backgating, and low frequency oscillations in addition to higher substrate costs in comparison with silicon. The concern of device manufacturers with problems associated with defects in GaAs wafers was emphasized at a recent conference on semi-insulating III-V materials, where out of seven key problem areas in commercial manufacturing, five were due to variabilities in substrate[Jay, 1992]. For example, in GaAs circuits fabricated by Vitesse Semiconductor and Convex Computer Corporation, the supply voltages had to be kept low to avoid backgating problems[Jay,1992]. Threshold voltage uniformity is particularly critical for applications such as direct coupled FET logic circuits where the threshold voltage of enhancement devices are on the order of 0.5 V and threshold voltage variations of less than 0.025 V

are required for noise margins competitive with other logic circuits[Lehovec, 1981]. These effects are believed to be caused by undesired impurities and defects in the crystal which are not always distributed uniformly.

These defects influence the electrical behaviour of semiconducting materials by creating energy states within the band gap which trap and emit free carriers thereby changing the electrical conductivity. Energy levels in the band gap are referenced with respect to the edge of either the conduction or valence band. Levels which are close enough to the band edge such that they are fully ionized at temperatures near room temperature have been labelled as being shallow and levels more than a few  $kT$  from either band edge have been termed as being deep levels. In general the concentration of shallow levels is considered to be well controlled in the commercial manufacturing of electrical devices. The control of deep levels on the other hand has been more problematic. There are several reasons for this. First, deep levels are usually present in low concentrations, typically in the  $10^{15}$ - $10^{16}$  / $\text{cm}^2$  range. Second, many of these levels are created by undesired impurities and defects in the crystal lattice caused by unavoidable or undetermined conditions in the crystal growing and wafer polishing processes. Examples of these include mechanical stresses, temperature gradients and contamination of crucibles used in the crystal pulling process. Furthermore, defects are often redistributed by heating processes. This makes the task of linking defects to manufacturing steps difficult. However if links could be made, problematic process steps could be improved or eliminated. Reports in the literature indicate that there has been considerable difficulty in making direct correlations between deep levels identified

primarily by their transition energies and particular physical defects[Look, 1989].

Distinct patterns in the distribution of defects on the scale of microns to centimetres have been observed in wafers of LEC grown SI GaAs using a number of techniques including cathodoluminescence(CL), photoconductivity, infra-red transmission and mapping of electrical parameters[Eckstein, 1990][Look, 1987][Fillard, 1988][Miyazawa, 1986]. Some of these patterns have been associated with dislocation networks and non-uniformity in impurity concentrations which are believed to be introduced at various stages in the fabrication of electrical devices. Often, the spatial distribution of the defect will provide information on the nature and causes of a particular defect. For example in the manufacturing of crystals using the LEC method, dislocation networks are suspected to be created as a result of mechanical stresses and thermal gradients. A radially dependent pattern, believed to be similar to the distribution of stress in the crystal during the growing of the boule, is often seen in the distribution of dislocations in finished wafers[Kirkpatrick,1985].

Earlier projects carried out in this laboratory involved the characterization of LEC grown SI GaAs wafers manufactured by Johnson-Matthey with respect to suitability for use as a substrate in device fabrication. One of the goals of the project was to identify and correlate deep levels to their effects on the threshold voltage of transistors and the activation of implanted dopants. In work done by Hui in this laboratory, assisted by the author, the threshold voltages of transistors fabricated in a dense array on quadrants of 75 mm diameter wafers were mapped. Additionally, Hui studied a negative peak in the OTCS signal which is of significance to the variation of threshold voltages since it has

been reported to be associated with the activation efficiency of implanted dopants. A scanning OTCS system was constructed by Hui and Switlshoff to map the distribution of negative peaks.. This system was made using components available in the laboratory from previous unrelated experiments. Their findings indicated that the "negative peak" was related to surface damage. Due to limitations in lateral resolution, limited computer memory, effects of stress related to the use of chromium electrodes and limited temperature range of the system, the distribution of deep levels due to other defects were not imaged.

The first part of this thesis is a description of the work that went into developing an improved version of an OTCS system to map the distribution of deep levels in SI LEC grown GaAs. The system described in this thesis had advantages of greater lateral resolution, capacity to store more data combined with faster data collection and a greater range of temperature over which the measurements could be performed.

An outline of the organization of the thesis is as follows. To define design parameters for a scanning system, the work started with a literature survey of other work which used a variety of techniques used to map deep levels in SI GaAs. This overview, given in Chapter 2, helps to put the criteria used in the design of the scanning system into perspective. In Chapter 3, the design consideration and a description of the OTCS system which was constructed in this work is given along with results which illustrate the capabilities and limitations of the instrument.

It is recognized in the literature that experiments which are based on spectroscopic techniques do not always give the same deep level parameters. For example it is reported

that GaAs from a single crystal examined by four commercial, independent laboratories using deep level transient spectroscopy (DLTS) resulted in the ascribing of energies ranging from 0.717 to 0.835 eV to the main deep centre EL2[Look, 1989]. OTCS signals are sensitive to specimen geometry and experimental conditions[Hui, 1992.]. To calibrate the scanning system, copper, a well-studied impurity in GaAs, was intentionally introduced and examined using both scanning and non-scanning OTCS. Copper is of interest for several reasons. Copper is suspected to be present in significant quantities in chemicals and materials used in the fabrication of devices[Hiramoto, 1988]. The copper from these sources is believed to diffuse into the GaAs during process steps involving heating, and has been implicated in the variabilities in device performance. Deep levels due to copper have recently been used to alter the photoconductive properties of doped GaAs in power switches that are triggered using light pulses[Mazzola,1988][Roush,1993].

It is reported in the literature that the diffusion of copper in GaAs is complex and not well understood[Moore, 1992] and this caused some problems in the present work. Considerable effort was made to develop a doping process using the diffusion of copper. The introduction of copper was monitored by examining contrast in cathodoluminescence(CL) images, and by measuring the current voltage(I-V) dependence of electrodes placed on the GaAs. In addition the current and photocurrent properties were studied as a function of temperature. This work is reported in Chapters 4 and 5 respectively.

In Chapter 6 results of both scanning and non-scanning OTCS studies of copper are compared with reports in the literature. Non-scanning OTCS has the advantages of

greater sensitivity and larger temperature range because the measurements are performed in a cryostat. Moreover the conditions used in this apparatus are similar to those reported in the literature and a better comparison with published work could be made. In addition the effects of electrode material, geometry and experimental procedures used in the OTCS examinations are reported.

In Chapter 7, the work is summarized and suggestions for future work are made.

## Chapter 2

### Previous work on Scanning Optical Transient Current Spectroscopy

#### 2-1 Introduction

OTCS is a method which has been used to study deep levels in semi-insulating materials. In OTCS, the decay in photo-current after the removal of illumination is examined as a function of temperature. A constant voltage is applied across electrodes and the current through the sample is measured. When a semiconductor is illuminated, free carriers are generated and this increases the proportion of deep levels which are occupied. When the illumination ceases, the excess free electrons and holes recombine very rapidly but, the trap occupancy is restored to the dark level through the thermal emission of carriers and this process has time constants typically in the range of less than a millisecond to several seconds in GaAs. The transient current due to the release of carriers from a deep level in a depletion layer is given by Martin et. al., 1978 as :

$$I(t)=(qAW/2)(e_n n_t(t)+e_p(N_T-n_t(t)))$$

where  $q$  is the charge on the electron,  $A$ , the area of the contact,  $W$ , the width of the depletion layer,  $e_n$  and  $e_p$  are the respective emission rates of electrons and holes,  $N_T$  is the concentration of the level and  $n_t(t)$  is the number of levels occupied by electrons.

To optimize the sensitivity, a series of light pulses is used to generate a periodic signal which can then be averaged over a number of cycles. In Martin's original method, the

transient signal is quantified by measuring the current at two different times after the end of illumination and the difference in the magnitude of the current recorded. If an assumption is made that a given trap communicates with only one band the expression for the difference in current can be expressed by:

$$I(t_1) - I(t_2) = (qAW/2)[n_t(t_1)e_n - n_t(t_2)e_n]$$

for the case of an electron trap. For a given set of values for  $t_1$  and  $t_2$ , there will be a characteristic time constant, related to the emission rate by  $\tau = 1/e_n$ , which will result in a maximum for the above expression. From the first derivative,  $\tau$  can be found as a function of  $t_1$  and  $t_2$  and is given by:

$$\tau = \frac{t_1 e^{-t_1/\tau} - t_2 e^{-t_2/\tau}}{e^{-t_2/\tau} - e^{-t_1/\tau}}$$

Using the Shockley-Read-Hall expressions, the temperature dependence of the emission rate can be expressed by:

$$e_n(T) = \gamma T^2 \sigma_{na} \exp\left[-\frac{E_{na}}{kT}\right]$$

where  $E_{na}$  is the apparent activation energy of the trap level,  $\sigma_{na}$ , the extrapolated capture cross section at  $T = \infty$ . The activation energy can be found from the slope of a plot of  $\ln(T^2\tau)$  as a function of  $1/T$  and the intercept at  $1/T = 0$  gives  $\gamma_n \sigma_{na}$  where:

$$\gamma_n = \frac{16\pi m_n^* k^2 g_o}{h^3 g_1}$$

and is  $2.28 \times 10^{20} \text{ s}^{-1} \text{ cm}^{-2} \text{ K}^{-2}$  for electrons and  $\gamma_p$  is  $1.78 \times 10^{21} \text{ s}^{-1} \text{ cm}^{-2} \text{ K}^{-2}$  for holes [Martin et. al., 1978] [Mitonneau et. al., 1977].

Other models such as the neutral semiconductor and insulator model have been proposed by Young et. al., 1986 which give similar temperature dependence of the transient current.

In this work two separate OTCS systems were used to study LEC SI GaAs samples. One has the advantage of greater sensitivity and a wider range of temperature and is similar to systems which are reported in the literature. In the other the distribution of deep levels can be mapped across wafers. The non-scanning version was used to determine the experimental parameters to be used in the scanning experiments. In the following section both systems are described. The development of the version with mapping capability was a significant portion of this work. This chapter concludes by reviewing other methods of mapping defects in GaAs which were used to determine some of the requirements in the design of a scanning OTCS system.

## **2-2 Review of Techniques Used to Map Defects in GaAs**

In LEC grown SI GaAs the distribution of some defects has been shown to vary with a radial dependence. In studies, in which the density of the defects are examined across a diameter of a wafer, a "W" or "M" shaped distribution is often reported[Yoshie, 1985],[Dobrilla, 1985]. This non-uniformity in the wafer characteristics is one of the main problems with LEC grown material. It has been reported that the variation in the threshold voltage of transistors fabricated using the ion-implantation technique, can be correlated to the distribution of dislocations[Morrow, 1988]. It is believed that the effect of dislocations on the threshold voltage may involve gettering of impurities by the

dislocations. These impurities, in some cases, interact with other defects and are suspected to create additional energy levels[Moore, 1992]. The density of dislocations is given as a material specification by GaAs wafer manufacturers.

There are a number of methods by which dislocation densities have been mapped on wafers of GaAs. Some of the methods reported in the literature were examined prior to starting the work to help determine what criteria would be important for a scanning OTCS instrument. These are summarized in the following section.

### 2-2.1 Etch Pit Density

The most commonly used method of mapping dislocations is by etching a wafer in molten KOH. KOH is an anisotropic etchant for GaAs which etches much more rapidly near dislocations. After the etching, dislocations terminating at the surface of the wafer are visible as rectangular pits. The etch pit density has been found to form a distinct "W" shaped pattern[Yoshie, 1985][Young, 1988] with the highest concentration of dislocations near the centre and outer circumference of a circular wafer. This type of pattern has been associated with mechanical stresses present during the LEC crystal growth process. Typical etch pit densities quoted by manufacturers are in the thousands per  $\text{cm}^2$ .

This method gives no information on the electrical effects of these defects. Some problems are associated with this technique in quantifying the size of the etch pits indicating a dislocation rather than some other defect. Not all of the pits formed being uniform in size or shape. For example, if two dislocations are located close together, the

etch many create a large single pit instead of two distinct pits. This has led to disputes in deciding how pits of different shapes and sizes should be counted to determine the actual number of dislocations present.

### **2-2.2 Infra-red Transmission**

The absorption of infra-red light, by GaAs is sensitive to the concentration of deep levels in the band gap. When irradiated by light with a lower energy than the band gap, light is only absorbed in electron transitions which involve intermediate levels in the band gap. This has been used to map the distribution of EL2 in LEC grown material. Work done by Dobrilla and Blakemore, 1985, used a 0.5 mm diameter spot of light with a wavelength of 1.1  $\mu\text{m}$ . Wafers grown using several different techniques were examined. Wafers grown using the high pressure LEC growth technique were found to have a "W" shaped distribution in the variation in absorption with greater absorption near the centre and outer edges, similar to the pattern reported for etch pit densities.

### **2-2.3 Photo-resistivity**

Photo-resistivity measurements were performed by Look and Pimentel by illuminating perpendicular strips of light to form the equivalent of a Greek cross with the illuminated areas forming the conductive arms of the cross[Look, 1987]. van der Pauw measurements of these were made as the illuminated strips were moved from region to region to determine the variation in photoresistivity across a wafer. The lateral resolution in the reported results was 6mm. The samples displayed either a "W" or a "U" shaped

distribution in the variation of photo-resistivity.

#### 2-2.4 Scanning DLTS

Scanning DLTS has been used to image the deep level distribution in doped conductive layers[Breitenstein, 1985, 1987]. In this technique the capacitance of an electrode placed on a conductive layer of the semiconductor is monitored. One electrode was thin enough that a significant portion of the electrons in a scanning electron microscope would pass through the electrode into the semiconductor. The resulting generation of free carriers would perturb the trap occupancy level. The electron beam was pulsed and the resulting transients in the capacitance were examined.

#### 2-2.5 Scanning OTCS

Yoshie and Kamihara reported on a scanning OTCS system. In their work the technique was referred to as scanning photo-induced current transient spectroscopy (PICTS)[Yoshie, 1985]. Specimens with "Sandwich" type, ohmic electrodes with a semi-transparent front contact a  $1000\text{\AA}$  thick, were examined. Electrodes this thick would only allow a small portion of the light to be transmitted. In addition it may be quite difficult to form uniform contacts using this method. It is reported in the literature that different phases occur during the sintering process resulting in a roughened surface. In some cases the roughness is used as an indicator of successful sintering[Williams, 1990]. The distribution of three deep levels with energies of 0.14, 0.31 and 0.55 eV were examined across a 75 mm diameter SI GaAs wafer. The source of illumination was a 250W

tungsten halogen lamp, focussed to a spot size of roughly 1.2 mm. It was reported that the variation in concentration of the 0.14 eV level was clearly "W" shaped and correlated to the distribution in etch pit density. The other two levels only showed weak if any correlation to the etch pit distribution. Although the resolution of their system was limited by the relatively large light spot, the temperature range in which the sample could be examined was from 100 K to 350 K, a much larger range than the system constructed in our work. This was due to the specimen being placed in an evacuated cryostat.

### 2-2.6 Cathodoluminescence and Photoluminescence

In cathodoluminescence and photoluminescence, a specimen is irradiated with an electron beam and light respectively. The emission of light from the specimen after stimulation is examined. In both cases microscopic structures, some which are dislocation networks can be observed[Third, 1989][Jahn, 1991]. In photoluminescence maps variation in the concentration of EL2 has also been observed[Data from Johnson-Matthey].

### 2-3 Summary

In the literature, similar variations are reported in the density of dislocations and the density of EL2 centres. However the physical model for EL2 and dislocations are not related. The variation was reported to occur as two distinct patterns. In one the macroscopic density of the defects forms an annular shape with a higher concentration of defects near the centre and the outer circumference of a wafer. In the other, a microscopic pattern with features sizes in the order of a tens of microns is observed.

## Chapter 3

### Design of a Scanning OTCS System

#### 3-1 Introduction

The scanning OTCS system developed in this work was intended to map the distribution of deep levels associated with dislocation networks in "as received" wafers. The main components of the system were a temperature-controlled translation stage on which light from a pulsed laser was focussed into a small spot, a current amplifier for measuring the sample current and a PC to control the experiment. A GaAs wafer, or in most cases, a section of a wafer is placed on the stage and held in place by vacuum. Electrical contacts are made to the specimen and connected to a constant voltage supply and a transconductance amplifier. The stage is moved in such a way that the light spot is stepped over the region of study. The transient decay in the photocurrent as well as the net photocurrent is recorded point by point by a PC using an analog to digital converter (A/D) card.

The two criteria which were paramount in a scanning version of OTCS were the lateral resolution and the signal to noise ratio of the OTCS signal. With increasing resolution the volume of stimulation is smaller which results in a reduction in the magnitude of the OTCS signal.

### 3-2 Optical System

The optical system consisted of a 670 nm wavelength diode laser, manufactured by Laser Max, with a maximum power output of 5mW. The laser unit contains a four element lens with a high numerical aperture and a current regulator. The lens is placed within a few millimetres of the laser diode to collect as much of the divergent light as possible. The position of the lens is adjustable and can be used to either collimate or focus the output light into a spot.

Initially the collimated beam was directly focussed into a spot using a Bausch and Lomb 25X long working distance microscope objective lens. However the minimum spot size achievable with this configuration was about 50 microns in diameter.

The size of the light spot was measured by stepping a knife blade through the light beam at the narrowest point while monitoring the intensity of the light using a photodetector placed below the knife blade.

The light from a typical diode laser is difficult to focus into a small point due to the elliptical cross section of the beam shape and large divergence angle of the light as it emerges from the diode. To obtain an ideal beam, the beam may be circularized using anamorphic prism pairs[Melles-Griot Optics Guide 5]. These are moderately expensive. A simpler method was to focus the light through an small aperture which would then be imaged into a smaller spot by a microscope objective. For this work, the four element lens used to collect the diverging output of the diode laser was adjusted so that much of the light was focussed on an 80 micron pinhole placed approximately 5cm from the laser unit. A 25 x long working distance objective lens was then used to image the aperture

onto the surface of the specimen. The distance between the aperture and objective lens was 15 cm. The minimum measured spot size using this method was approximately 10 microns in diameter.

### **3-3 Translation Stage**

The motorized stage of a Micromanipulator model 6000 semi-automatic probe station was used as the translation stage. The system was modified so that the optical system could be fitted to a supporting beam originally designed to hold a microscope. The intended use of the semi-automatic probe station is to make electrical contacts to devices while they are still in an unpackaged state. The stage is capable of stepping in 0.1  $\mu\text{m}$  steps with a repeatability of  $\pm 3 \mu\text{m}$  across an approximately 15 x 15 cm area. The movement of the stage can be controlled by instructions from a computer through a GPIB bus.

### **3-4 Temperature Controlled Stage**

A model TP-350 temperature controlled stage manufactured by Temptronics was used. This unit is designed to be used with the probing station to examine the temperature dependence of device parameters. The temperature of the stage can be varied from 213 K to 473 K with  $\pm 0.5$  degree resolution and stability.

To control the humidity of the air surrounding the specimen during measurement and to shield the specimen from both light and electrical interference, the translation stage and optical system were enclosed in an aluminium box. The box was sealed using RTV

silicone sealant along the joints and neoprene foam gaskets around access panels. In addition the box included fittings to allow the purging of the box with compressed air passed through a tube filled with desiccant or nitrogen from a compressed gas cylinder.

The accessible temperature range was roughly 260 K to 350 K.

### **3-5 Current Measurement and Data Collection**

As mentioned above, the main criterion for measuring the OTCS signal is to balance the lateral resolution against the signal to noise ratio. One of the sources of noise in the measured signal is due to error in synchronizing the termination of the illumination and the start of the current transient measurement. In the prior work by Hui, 1989, the illumination pulses were created using a rotating wheel chopper. The light beam was divided using a cube splitter and monitored using a separate photo-diode. This apparatus has the disadvantage that the turn-off time of the light beam is dependent on the rotational speed of the chopper wheel as well as the optical beam diameter. In OTCS experiments the periods of illumination and dark are on the order of seconds in order to allow the free carrier concentrations to reach equilibrium. For such cases the turn-off time of the light pulse will vary for different illumination cycles. For this work the diode laser was switched. Although the turn-on time of the laser is intentionally slow to avoid damage to the laser diode by spikes in the drive current, the turn-off time is a few microseconds. Moreover the turn-off time is constant regardless of the periods of illumination and dark.

To measure the transient current, a Keithley 427 current amplifier was used. The dc bias on the output signal of this unit is manually adjustable and was set so that the

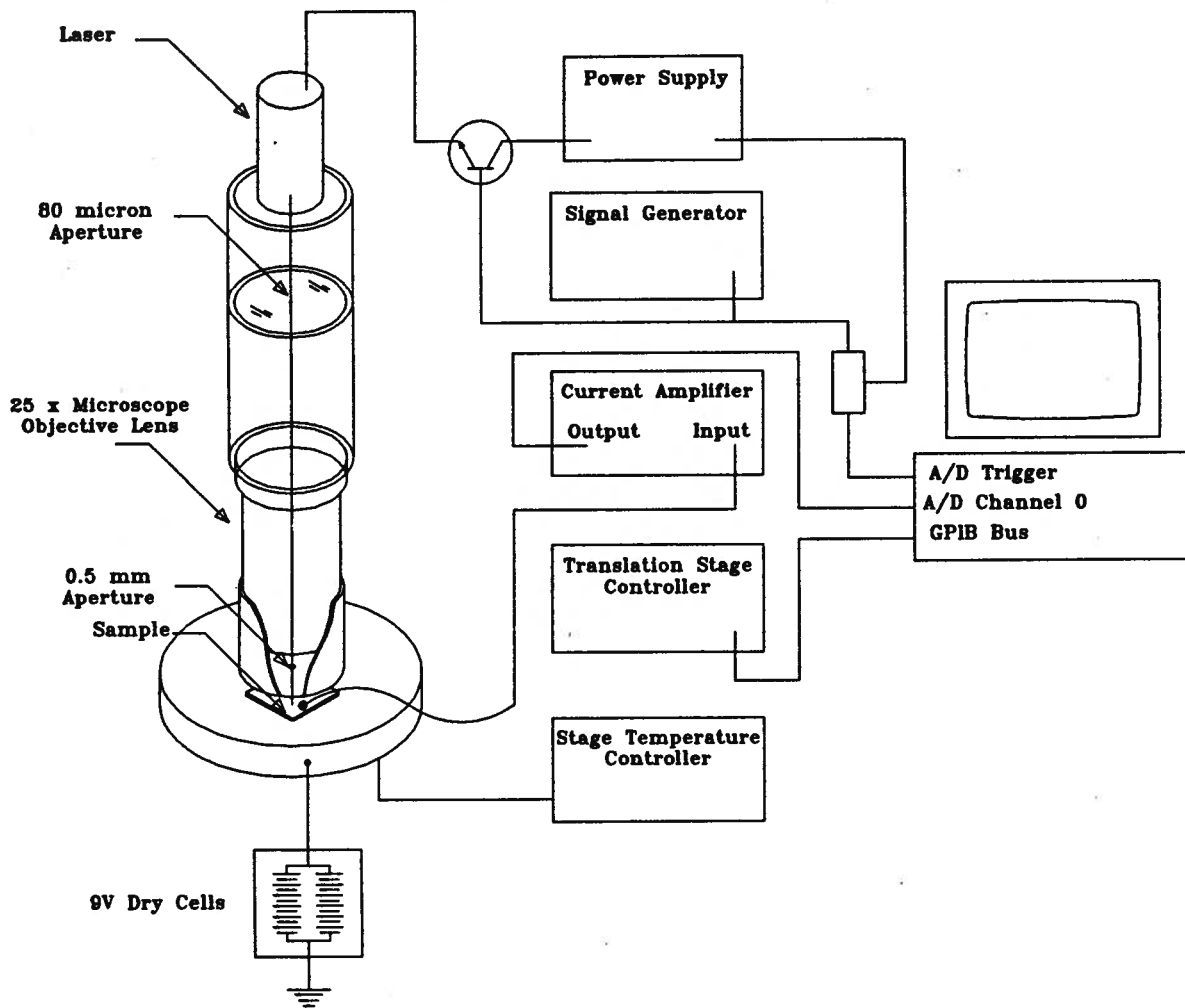
amplitude of the photocurrent was close to the dynamic range of the measuring instrument. This was done at the expense of not being able to monitor the dark current during measurement. Unlike typical OTCS measurements, the temperature is not intentionally varied in this case and the dark current should remain constant and therefore was not recorded.

To supply the bias voltage, a pair of 9 volt dry cells connected in parallel combined with a voltage divider was used as a low-cost method of applying a constant voltage with low noise. This portion of the apparatus is similar to that used in the non-scanning OTCS measurements.

However the method of synchronizing the data collection and the illumination pulses were different than in the non-scanning measurements. In the scanning experiments both the timing of the light pulses and the start time of the data collection were controlled by a signal generator. A signal generator was used to supply a square wave with a period on the order of a second. The output of the signal generator was connected to a transistor which switched the current supply to the laser. The output of the signal generator was also connected to the input of a TTL pulse generator. The falling edge of the square wave would cause the pulse generator to send a 300 ns pulse to the external trigger of a Data Translation DT-2828 A/D convertor to start the data collection.

The A/D had two channels with a resolution of 12 bits and maximum sampling frequency of 100K samples/s. Usually the entire transient was collected and the difference in the signal amplitude at two different times were averaged over 10 to 20

cycles and then stored in the PC memory. The storage of the entire transient was not done due to the excessive time it would take to average and store the data as well as the prohibitive amount of memory required for the large number of points required for high lateral resolution. A sketch of the apparatus constructed to perform scanning OTCS measurements is given in Figure 3-1.



A Schematic Diagram of the Scanning OTCS Apparatus

Fig. 3-1

### **3-6 Experimental Method**

For the scanning OTCS the choice of temperature to be used was made by first examining the transient photocurrent using an oscilloscope at one point while varying the temperature. The response of the temperature-controlled stage is slow and several minutes were taken for the temperature of the stage to reach steady state. The magnitude of the transient current was not found to reach a peak at a certain temperature as in the standard OTCS. Instead it was found to increase in a monotonic fashion with the temperature. However, when using the photo-current normalization as suggested by Yoshie, 1985, there was a peak in the OTCS signal. For the time constants in the range of 1 ms the temperature corresponding to the peak in the OTCS signal was near room temperature. Several scans were performed using these parameters.

### **3-7 Results of Scans**

To examine the resolution of the system special specimens were prepared with a 2000Å thick Al grid evaporated on top of the semi-transparent contact. The width of the lines used to form the grid were 100 μm. In Figure 3-2(a) a plot of the variation in the magnitude of the the photocurrent as the focussed light is scanned across this grid is given.

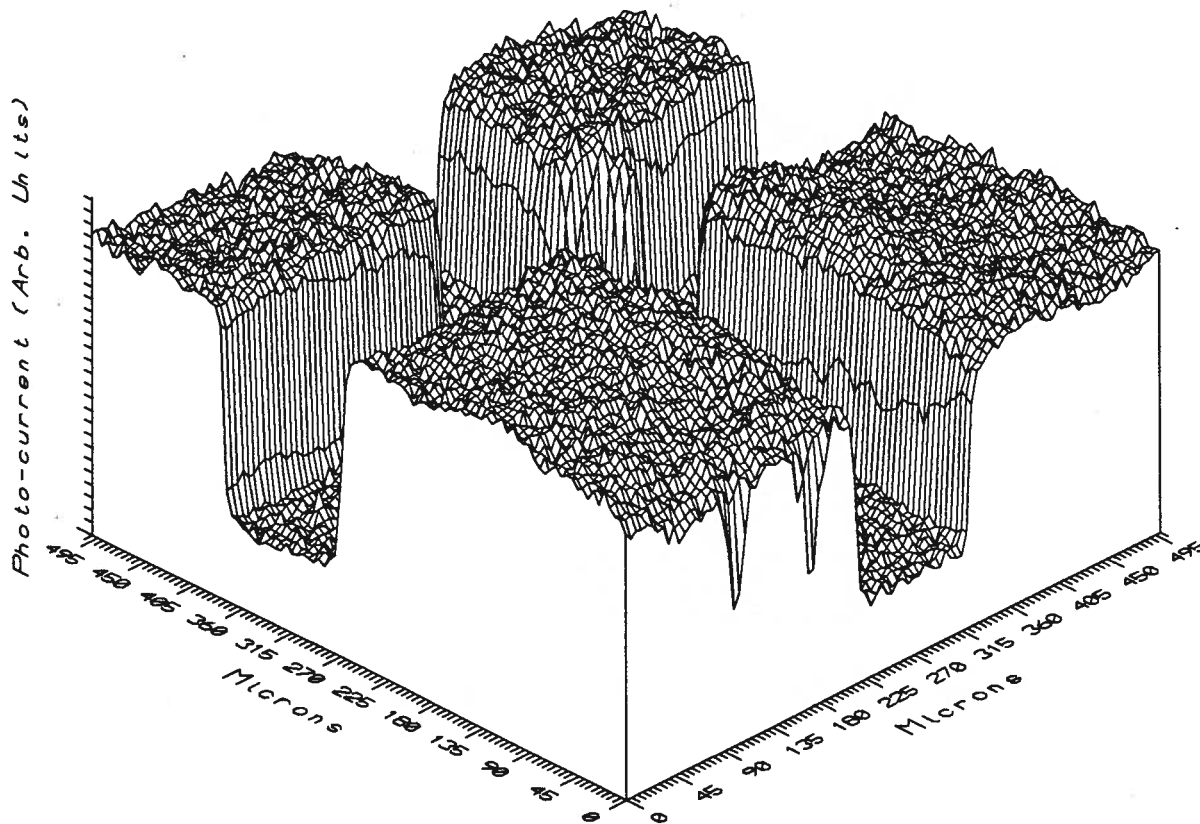
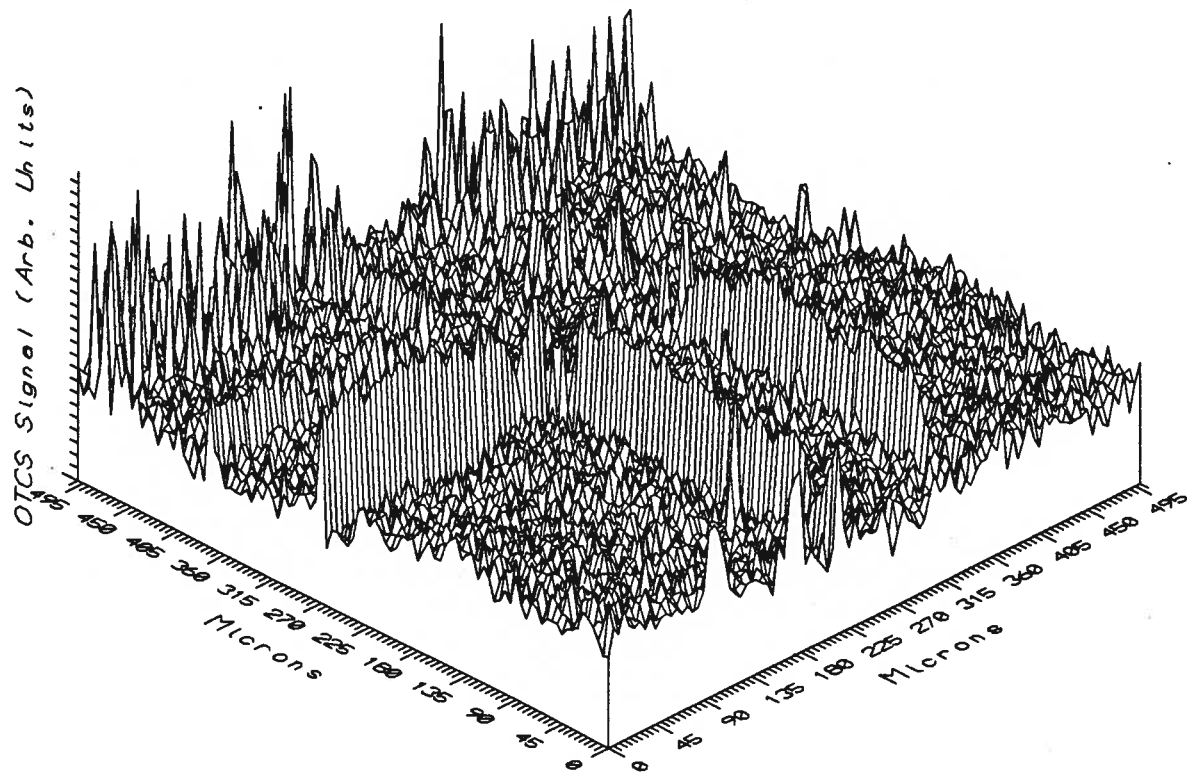


Photo-current Map of 2500 Å Thick Al Test Grid

Fig. 3-2 (a)

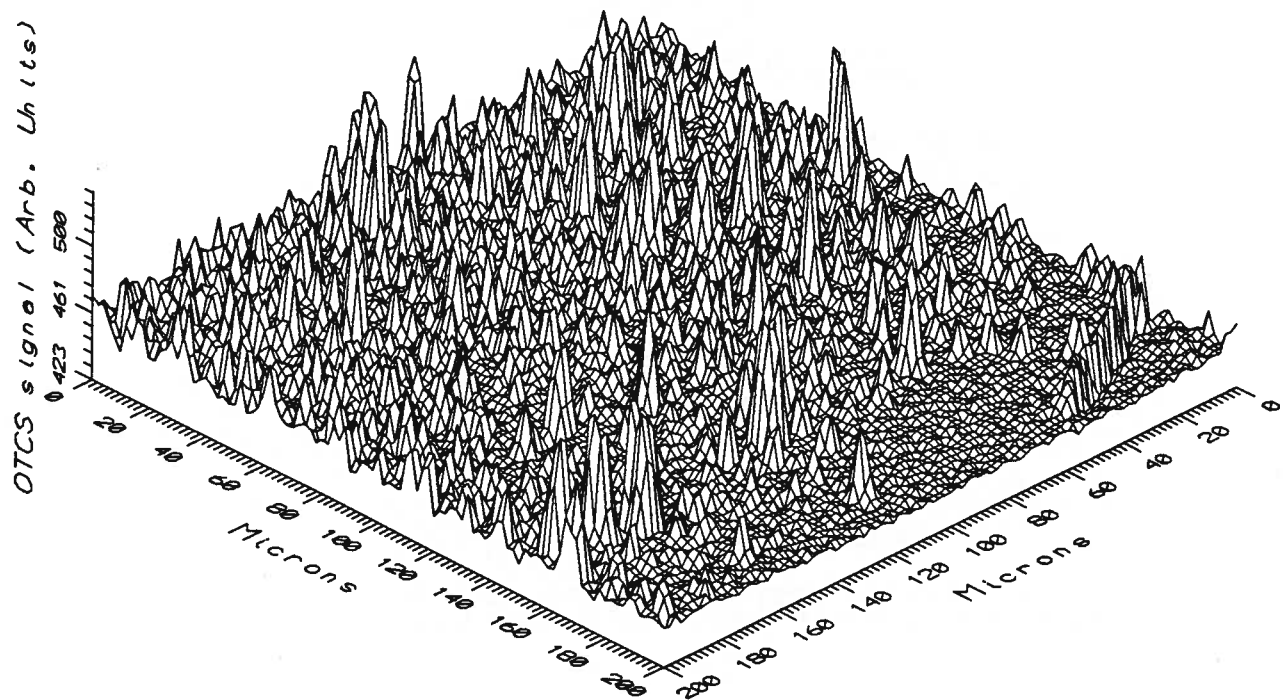


OTCS Signal Map of 2500 Å Thick Al Test Grid

Fig. 3-2 (b)

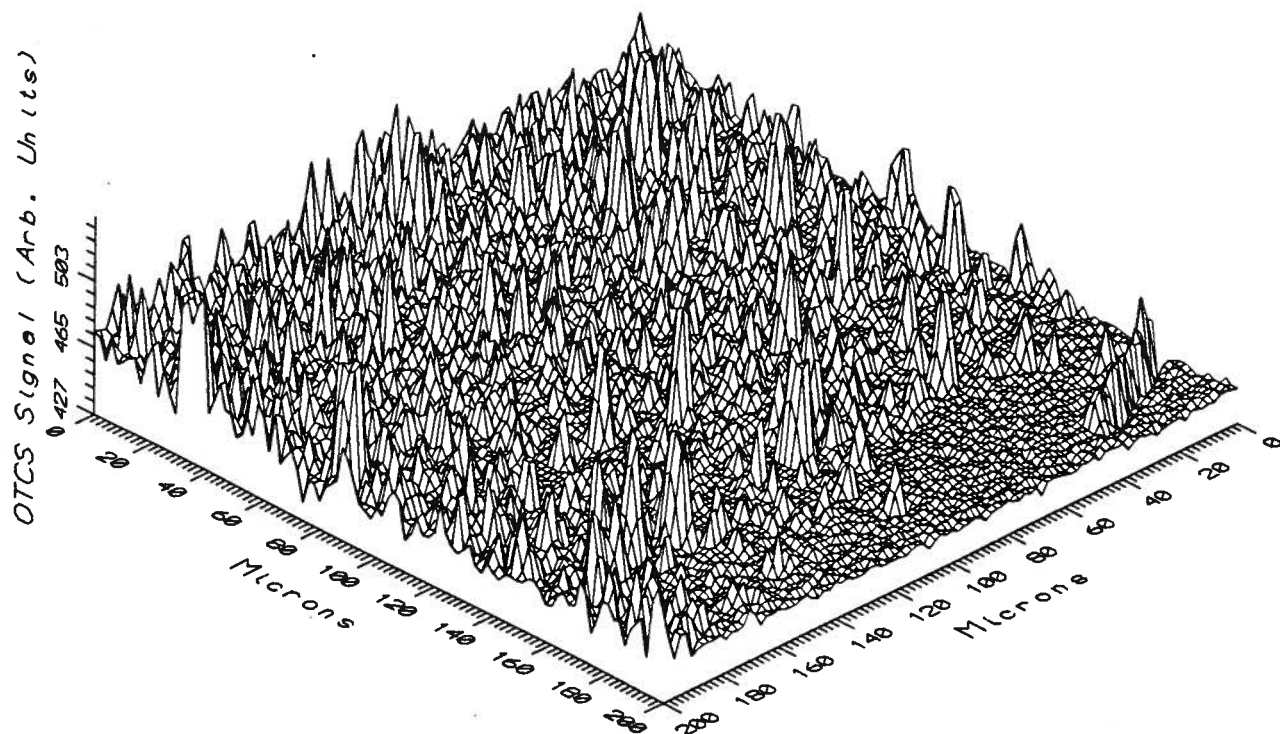
In Figure 3-2(b) the OTCS signal from the same scan is given. It is apparent that although the scanning system is capable of resolving features sizes which are a few tens of microns, the sensitivity of the OTCS signal may not be adequate for resolving small changes in the concentration of deep levels. Moreover it is apparent that there is still a photocurrent signal when the light spot is striking the Al grid. Much of this signal is caused by the reflected light from the Al surface being scattered off the objective lens used to focus the light. This light would impinge on the specimen causing photocurrent to be generated in other areas of the specimen. On the above scans as much of the reflective surfaces near the sample were shielded with "flocked" paper to absorb as much of the light reflected from the surface as possible. In some of the scans without the shielding it was found that the photo generated signals were larger when the light was focussed on the thick aluminium grid.

Scans were also done on specimens with a uniformly thin Al top electrode and a AuGe back electrode. Two separate scans were performed to test the repeatability of the measurements and these are given in Figures 3-3(a) and 3-3(b). The sampling times  $t_1$  and  $t_2$  were chosen to obtain a maximum OTCS signal. The same data is displayed in Figures 3-4(a) and 3-4(b) as a topographical map which displays regions which had the highest signal. Corresponding features are numbered on each map. The two scans demonstrate the repeatability of the system but the absolute coordinates were found to not always be the same. For example there is a shift of roughly 20  $\mu\text{m}$  between the two scans although the starting points were intended to be the same. This error was due to the backlash in the positioning mechanism and differences in the position -



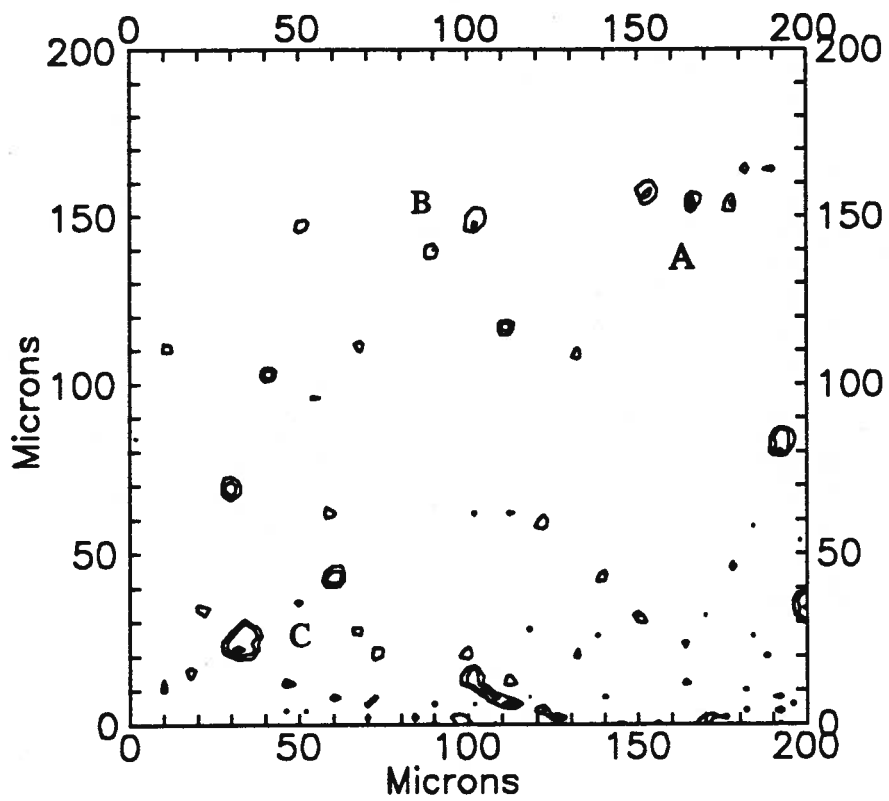
OTCS Scan of 200  $\mu\text{m}$  x 200  $\mu\text{m}$  Area,  $t_1=2$  ms and  $t_2=10$  ms, 10 x Averaging

Fig. 3-3 (a)



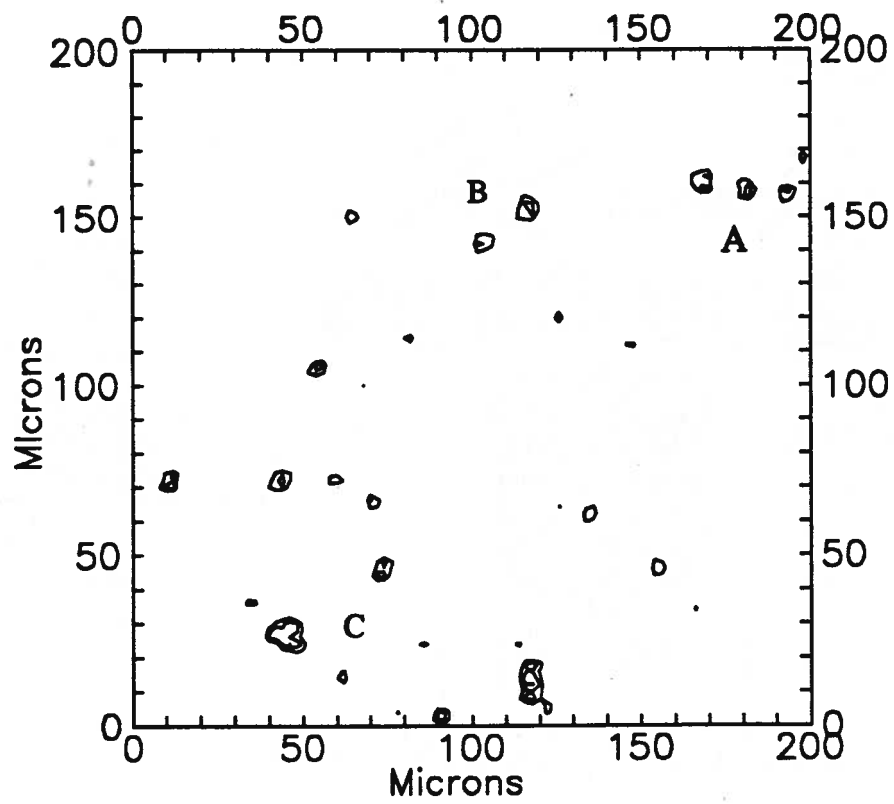
Repeat Scan of Same Area as Fig. 3-3(a) using the same parameters

**Fig. 3-3 (b)**



Topographical Map of Regions with the Largest Signal in Fig. 3-3(a)

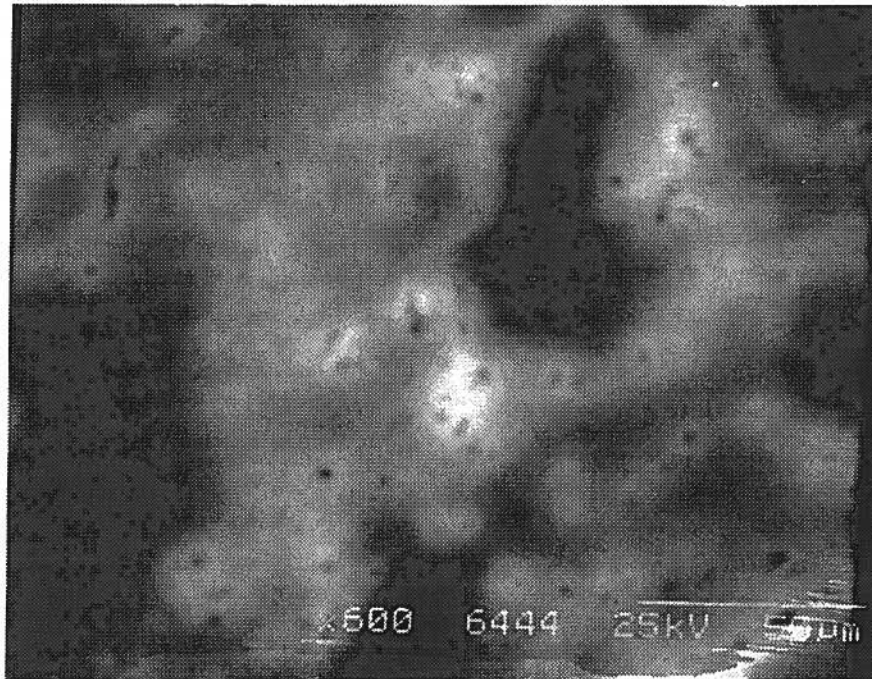
Fig. 3-4 (a)



Topographical Map of Regions with the Largest Signal in Fig. 3-3 (b)

Fig. 3-4 (b)

of the stepping motors at the end of one scan and the start of a subsequent scan. The size of the features observed in the OTCS maps are similar to the size of patterns due to dislocation networks in cathodoluminescence images. An example of this type of image is illustrated in Figure 3-5. The pattern typically consists of a light region often referred to as a "halo" surrounding a darker central spot.



An Example of a Cathodoluminescence Contrast Image

Fig. 3-5

The OTCS signal was measured over a range of temperatures starting at 383 K and ending at 315 K but, was found not to correspond to spectra reported in previous

work. A monotonic increase in both the photocurrent and the amplitude of the OTCS signal was observed. It was not clear which levels were attributable to the transient signal. In the literature OTCS signals have been reported to be dependent on electrode geometries, wavelength of light causing the photocurrent, applied voltage and of course differences in the specimens[Young et. al., 1986],[Mares,1988],[Hui et. al. 1992]. To examine these factors, copper was intentionally diffused into the wafers and examined using different electrode geometries, applied voltages, illumination using sub-band gap and above band gap wavelengths. These experiments were done with a non-scanning system which is similar to those reported in the literature[Young et. al., 1986][Look, 1989][Blood and Orton, 1992]. The diffusion of copper was not as simple as was initially thought and considerable effort was made to develop a method of introducing an appropriate amount of copper.

The diffusion of copper was monitored using cathodoluminescence contrast imaging and examining the current-voltage (I-V) dependencies. This work is reported in the next two chapters. The results of OTCS measurements are reported in Chapter 6.

## Chapter 4

### Preparation of Copper Diffused GaAs Samples

#### 4-1 Introduction

In this portion of the work, the diffusion of copper from the surface of a GaAs wafer into the bulk crystal was examined using cathodoluminescence contrast. The diffusion is driven by a concentration gradient between the surface-deposited copper and the high purity crystal and the process can be roughly modeled using Fick's law given by:

$$J = -D\Delta C$$

where  $\Delta C$  is the concentration gradient,  $J$  is the flux of atoms and  $D$  is a proportionality constant frequently referred to as the diffusion constant. The diffusion coefficient is dependent on factors such as the temperature and the ionization state of the atoms involved. In this work the temperature was varied to control the diffusion rate.

The diffusion constant can be expressed as a function of temperature by:

$$D = D_0 \exp\left(-\frac{Q}{kT}\right)$$

where  $Q$  is related to the free energy required to move a diffusing atom from one stable position to the next,  $k$  is Boltzman's constant and  $T$  the temperature. Although, in practice, these relations are too simplified to accurately model the movement of atoms in

semiconductors, they have nevertheless been used as a starting point in many reported works[Tuck, 1988].

#### **4-2 Literature Review of Diffusion of Copper in GaAs**

The study of diffusion of copper in GaAs is reported to be complicated by both the complex nature of the diffusion mechanisms as well as the difficulty in detecting trace amounts of copper in the GaAs matrix. Factors reported in literature as influencing the movement of copper include: the concentration and type of free electrical charge carriers, the concentration of arsenic vacancies, the concentration of dislocations, the presence of other impurities, electric fields, temperature and pressure.

The diffusion of copper in GaAs was reported to be "complex and confusing" by Blakemore, 1984 and "not significantly clearer today" by Moore, 1992. This difficulty is reflected in the variation in results reported in the literature.

Nevertheless, the results reported in the literature were used as a guide to finding a method of diffusing the required amounts of copper. A sampling of previously reported work on diffusion of copper in GaAs is given in the following section.

Initial studies of the diffusion of copper in GaAs were done in the late 1950's to 1960's by three groups: Hall and Racette, 1964, and Larrabee and Osborne, 1966, and Fuller et. al.[Fuller, 1958],[Quisser, 1966],[Fuller, 1967].

A number of studies have been reported where trace amounts of copper were introduced into GaAs. Some studies have examined diffusion from sources such as copper incidentally adsorbed on free surfaces of substrates during processing steps in

device fabrication[Kang, 1992]. The adsorbed copper is believed to originate from solvents, chemicals and quartz-ware used during the manufacture of both the crystal and electrical devices. However the majority of studies report on results from intentionally putting copper on the surface of a GaAs sample and then subjecting the material to a heat treatment. A summary of some studies are given in Table 4-1.

Copper has been reported to diffuse into crystalline GaAs by means of two main mechanisms[Hall, 1964]. In one the copper moves through the lattice by occupying spaces between Ga and As lattice atoms. This is referred to as interstitial diffusion. In the other, known as substitutional diffusion, the copper displaces either a Ga or As lattice atom. The interstitial mechanism is reported to be much more rapid than the substitutional.

Hall and Racette reported that there were orders of magnitude differences in diffusion rates for p-type and n-type GaAs. Copper is believed to act as an acceptor type dopant. As more copper is included in the GaAs matrix, the free hole concentration increases and this is also reported to increase the diffusion rate. Moreover, in p-type material the solubility of the interstitial species has been reported to increase by factors ranging from  $10^6$  to  $10^{10}$  when compared to undoped material[Hall, 1964].

Additional variables which can affect diffusion processes include: the complexing of the diffused copper with other defects such as vacancies or other impurities, alloying with GaAs at sufficiently high temperatures, and oxidizing effects. From this it would seem that the diffusion rate will depend strongly on experimental conditions which are difficult to control. The literature seems to support this notion in that there is a relatively

large scatter in diffusion constants reported by various laboratories. A sampling of diffusion constants and

Group	Method	Encapsulation	Temperature Range, Time	Method of analysis	Solubility Maximum
Fuller, Whelan, 1957	Electroplated films	Evacuated quartz ampoules	700-1200° C	Auto-radiographs	$5 \times 10^{15}$ - $1 \times 10^{19}/\text{cm}^3$
Hall, Racette, 1963	Electroplated films	Hydrogen for lower temperatures Quartz Ampoule with excess arsenic	500-1100° C 48-.5 hrs	Auto-radiographs	$1.5 \times 10^{16}$ - $7 \times 10^{18}/\text{cm}^3$
Tin, Teh, Weichman, 1987	Residual copper from quartz tubing 1.4ppm	Quartz ampoule with 1 torr excess arsenic pressure	850° C, 24 hrs	PICTS <sup>1</sup> (OTCS <sup>2</sup> )	
Tin, Teh, Weichman, 1988	Vacuum evaporation	Quartz ampoule with excess arsenic pressure	550° C, 12hrs		
Jahn, Menninger, 1991	Residual copper on the surface	Capless sample supported on quartz points	850° & 950° C 10-20s	Cathodo-luminescence	
Zirkle et al, 1990	evaporated and spin on glass for lower concentrations		550° C 12hrs source etched off and backside damaged to getter impurities.	Cathodo-luminescence TDTC <sup>3</sup>	
Macquistan, 1989	0.3-0.5 $\mu\text{m}$ copper thermally evaporated at $6 \times 10^{-5}$ Torr	Capless	600° -1000° C	Auto-radiographs, SIMS <sup>4</sup> , Cathodo-luminescence	< 0.1ppm

<sup>1</sup> Photo-Induced Current Transient Spectroscopy

<sup>2</sup> Optical Current Transient Spectroscopy

<sup>3</sup> Temperature-Dependent Photo-Conductivity

<sup>4</sup> Secondary Ion Mass Spectroscopy

#### Studies of copper in undoped GaAs

Table 4-1

Group, Date	Temperature	Diffusion Constant cm <sup>2</sup> /s	Solubility Limit atoms/cm <sup>3</sup>
Hall, Racette, 1963	197°-210°C	4.2-12x10 <sup>-8</sup>	1.5x10 <sup>16</sup>
Zirkle et al, 1990	500°C	1x10 <sup>-5</sup>	1x10 <sup>16</sup>
Maquistan, 1989	600°C	1x10 <sup>-15</sup>	
Kendall, Devries, 1969	840°C	3.6x10 <sup>-6</sup>	
Larrabee, Osborne, 1966	850°C	2-5x10 <sup>-11</sup> 1-5x10 <sup>-7</sup>	
Tin, Teh, Weichman, 1987	850°C	4.7x10 <sup>-10</sup>	
Third, 1990	850°C	8x10 <sup>-7</sup> - 4.6x10 <sup>-6</sup>	
Jahn, Menniger, 1991	850°C	10 <sup>-5</sup> -10 <sup>-7</sup>	
Fuller, Whelan, 1957	1003°C	0.83-1.4x10 <sup>-5</sup>	2x10 <sup>19</sup>
Fuller, Whelan, 1957	1110°C	2.1-3.1x10 <sup>-5</sup>	8x10 <sup>19</sup>
Fuller et al, 1967	1050°C		1.1x10 <sup>17</sup>

Reported diffusion constants and solubilities of copper in undoped GaAs

Table 4-2

are shown in Table 4-2.

In the reported diffusion parameters, there is considerable variability. For example at temperatures of 850°C the reported range in diffusion constants is from 4x10<sup>-10</sup> to 4.6x10<sup>-6</sup> cm<sup>2</sup>/s. Some of this variation may be due to difficulties in detecting the diffused copper since solubility limits are in the 10<sup>16</sup> - 10<sup>17</sup> atoms/cm<sup>3</sup> range and the background concentrations are suspected to be in the 10<sup>15</sup> atoms/cm<sup>3</sup> range, even for recently manufactured material, made using refined crystal growing techniques. The background concentrations of copper and other impurities may have been higher in material used in

earlier work when crystal manufacturing was less refined.

The ratio of substitutional to interstitial atoms has been reported as approximately 30:1 at temperatures near 700°C [Hall, 1964]. However, information on what the ratio would be at other temperatures was not found. The diffusion mechanisms of copper in GaAs may be further complicated by changes in the ionization state of the copper, which is not believed to be fixed, and the intrinsic carrier concentration in the semiconductor which also varies with temperature. Since the energy of the diffusing copper atom is dependent on the electronic interaction with the lattice this variation in the intrinsic carrier concentration is believed to affect the rate of movement of the copper atoms.

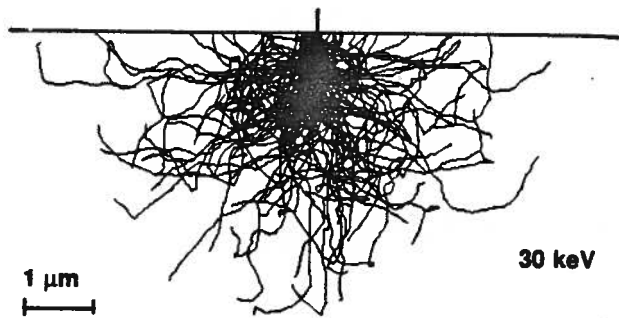
In summary, much of the study of diffusion of copper in GaAs by thermal means has been concentrated on heat treatments in excess of 700°C. As shown in Table 4-1, a number of techniques have been used to study copper incorporation into the GaAs lattice including cathodoluminescence, photoluminescence, secondary ion mass spectrometry and variations of deep level transient spectroscopy (DLTS) methods. A brief overview of literature reporting on methods of detecting copper in GaAs is presented in the following sections.

#### **4-2.1 Cathodoluminescence Studies of Copper in GaAs**

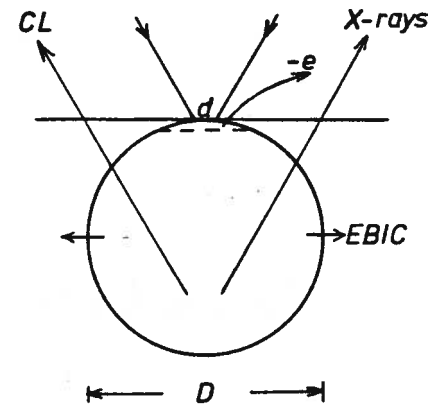
Cathodoluminescence (CL) is the phenomenon of light emission when a material is irradiated by an electron beam. The basic mechanism involves the creation of electron hole pairs when the material is stimulated by an electron beam. These pairs recombine, in some cases by radiative recombination resulting in the emission of light. - In many CL

instruments a modification is made to a scanning electron microscope such that the detected signal is the emission of light from a particular region as opposed to secondary or backscattered electrons. Spatial variation in the efficiency of radiative recombination results in a contrast image and is commonly referred to as spatially resolved CL contrast imaging. In some instruments, the light is spectrally resolved with respect to the wavelength of the light emission to determine the magnitude of the transition energies involved [Jahn, 1991]. Numerous designs optimizing the collection or resolving the light emission are commercially available.

Since more light is of course emitted in material in which the recombination lifetime of radiative recombination is shorter than the recombination lifetime of non-radiative processes, regions containing higher concentrations of non-radiative recombination sites such as impurities and crystal defects will generally appear darker. However, several additional factors should be taken into consideration for correctly interpreting CL images. One is that because the origin of light emission is below the sample surface, the differences in brightness may also depend on variation in the absorption of light by the surrounding material. The source of the light emission can be estimated as being the same as the volume of the scattering range of the primary electrons. This region can be roughly described as a spherical region with a diameter of several microns and tangent to the surface of the specimen. A Monte Carlo simulation of scattering of 30 keV electrons in GaAs along with a schematic representation of the electron semiconductor interaction are illustrated in Figures 4-1 (a) and (b) respectively.



(a)[Yacobi, 1990:p. 64]



(b)[Holt, 1989:p. 11]

**Fig. 4-1**

Thus if crystal non-uniformities affect the absorption of light it can be expected that this will show up in CL contrast images even if the emission intensity may be the same. In addition it is reported that contrast is sometimes dependent on the temperature of the sample[Eckstein, 1990]. Due to these effects CL images may be open to interpretation and may require additional information to determine mechanisms involved in the formation of the contrast image.

A few studies of cathodoluminescence of copper-contaminated GaAs were found. Third et. al., 1989 and Jahn et. al., 1991 reported on the effect of copper on the contrast in CL images. In these studies the effects of copper contamination from copper adsorbed on the surface of GaAs crystals during short heating cycles were investigated. Both studies report results from heating samples of SI LEC GaAs to 850-950°C for very short time periods of 5 to 20 seconds. This type of thermal cycling is not uncommon in the

fabrication of GaAs electrical devices using ion implantation techniques. The function of these heat treatments is to anneal out damage induced in the crystal lattice by the bombardment of ions and to preferentially shift a significant portion of the implanted dopant ions into electrically active sites. The short time periods are used to minimize the lateral diffusion of dopant ions thereby allowing greater control in defining electrically active areas. Additionally, with such short heating cycles the out diffusing of arsenic can be minimized and steps to apply encapsulation layers may be eliminated simplifying manufacturing processes.

Third found that luminescence from the regions adjacent to free surfaces increased relative to the central portion of the wafer after the heat treatments. This was attributed to the inward diffusion of copper adsorbed on the surface of the wafers prior to annealing. The source of the copper was suspected to be residual amounts present in processing chemicals and apparatus used to handle the wafers.

The studies of Jahn spectrally resolved the luminescence into two main wavelengths. Peaks for the radiation were found for energies corresponding to a 1.36eV and 1.51eV transition. They too observed band structures adjacent to the free surfaces after heating SI LEC GaAs at 850°C and 950°C for 10 and 20 seconds. However two possible states for the copper impurity were found, one which increases the luminescence and another in which the luminescence in the bands decreased. The increases and decreases are with respect to the light emission from the central bulk region. In some cases the luminescence corresponding to an energy shift of 1.51eV decreased, while the luminescence at the 1.36eV wavelength increased.

Although in these works the change in luminescence was attributed to the migration of copper into the GaAs lattice from the surface, Chin et. al., 1985 reported increases in luminescence due to diffusion processes involving As vacancies and not the indiffusion of copper. The increase of the luminescence intensity in this case was also adjacent to the surface of the samples. Chin also reported that for heat treatments at 550°C for 4 hrs, the increase in luminescence occurred in regions 100-200 $\mu\text{m}$  from the surfaces of the crystal. When samples were capped with plasma-deposited SiN<sub>x</sub> or annealed with an arsenic over-pressure, the changes in luminescence were much reduced.

In conclusion, it seems that there are a number of mechanisms which may cause an increase in luminescence. Furthermore, depending on which site the copper occupies in the GaAs lattice, there may be either an increase or decrease in luminescence. It has also been reported that CL contrast images are sensitive to the particular instruments which are used [Fillard et. al. 1988]. Therefore additional information may be required to verify the incorporation of copper impurities in GaAs.

#### 4-3 Experimental Work

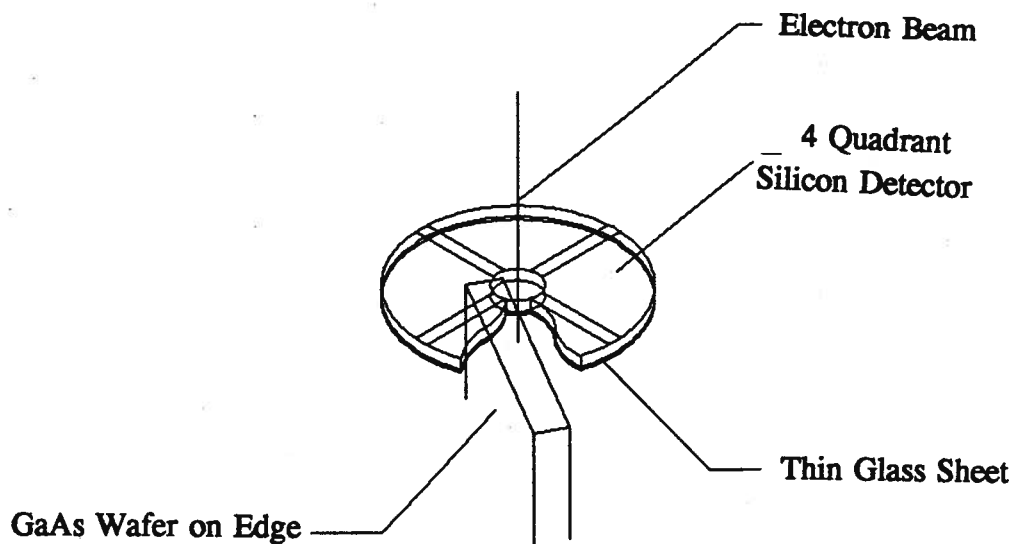
The goal of this portion of the work was to develop a procedure to reproducibly introduce an amount of copper into SI GaAs wafers so that the presence of copper could be easily detected yet not compromise the semi-insulating nature of the material. A variety of methods have been used to incorporate copper into GaAs. Some of these involve the growth of epitaxial layers with a controlled introduction of copper. These methods, although more well controlled than those used in this work were not used in this

work for a number of reasons. One was that the behaviour of copper during device fabrication was of interest. Moreover, the epitaxial growth methods were both expensive and not readily available in this laboratory. For this work, a quantity of copper was deposited onto a free surface of a GaAs wafer and then diffused in at elevated temperatures. In initial studies, segments of GaAs wafers were partially immersed in a dilute  $\text{CuSO}_4$  solution followed by heat treatments. A comparative examination was made between regions of the sample which had been immersed from areas which were not exposed to the  $\text{CuSO}_4$ . These methods were similar to those used in the work reported by Third, 1989.

The heating cycles which were initially used are similar to those used in fabrication of electrical devices using ion-implantation techniques. With this method, it was found that it was difficult to control the amount of copper being diffused in. There were relatively small changes in the CL contrast in the areas which were immersed in copper sulphate solution. However in conductivity measurements which were carried out concurrently, the specimens displayed no change or a drastic change in the conductivity. It seems likely that using this method the amount of copper which is diffused in is controlled by how much material is deposited on the surface. Thus the amount of copper which is incorporated into the GaAs was largely determined by how much copper was left on the surface after immersion in the  $\text{CuSO}_4$  solution. The amount of adsorbed copper is likely to depend on surface conditions of the polished wafer such as the thickness of native oxide and surface roughness. Since these qualities are difficult to reproduce, different amounts of copper may have been adsorbed.

Another method was used in order to improve the control over the amount of copper which was introduced. This was to vacuum evaporate a thin, 200-400Å, layer of copper and control the amount being diffused in by varying the temperature of the heating cycle.

A diagram illustrating the instrument used to obtain CL contrast images is given in Figure 4-2.



Schematic Diagram of the Apparatus Used to Obtain CL Images

Fig. 4-2

A modified scanning electron microscope (SEM) was used to obtain CL contrast images. A CL detector manufactured by GW Electronics was installed through a port in the vacuum specimen chamber. In this case a silicon radiation sensor which is normally

used to detect backscattered electrons had been altered by installing an optically transparent electron barrier in front of the silicon detector.

In the initial stages of this work an ETEC SEM was used. However part way through the work the ETEC unit was replaced with a Hitachi model 5400 but the same photodetector and amplifier were used. The energy of the electron beam was typically set at 30keV. Beam energies of this magnitude are not uncommon in the literature to obtain contrast CL images [Third, 1989],[Chin et. al., 1985].

#### 4-3.1 Introduction of Copper by Immersing in CuSO<sub>4</sub> Solution.

Work by Third, a portion of which was done in this laboratory, was used as a starting point for this study.

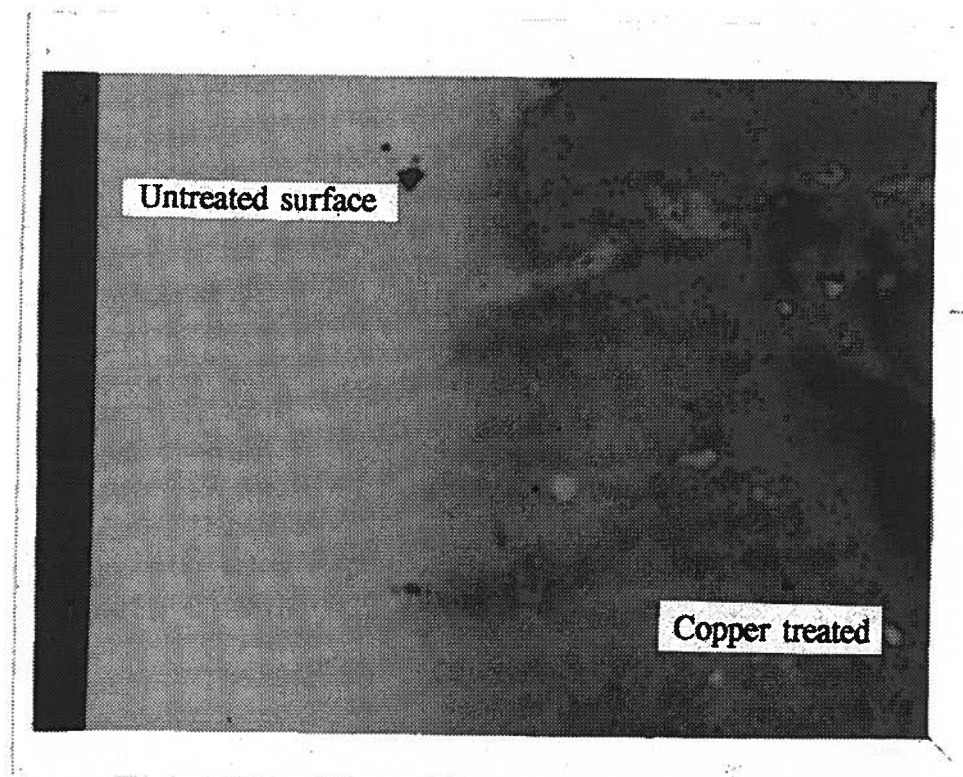
Sections of SI LEC GaAs wafers were partially immersed in 0.1M copper sulphate solution. These were then subsequently rinsed in flowing de-ionized (DI) water and then annealed in an AG Associates 210T Rapid Thermal Annealing (RTA) oven for 5-10 seconds at temperatures of 850 and 950°C. No encapsulation to prevent the out diffusion of arsenic was used at this point but the annealing chamber was purged with nitrogen.

The primary reason for not encapsulating the wafer prior to heat treatments was to minimize the number of processing steps to reduce the probability of contaminating portions not immersed in the copper sulphate solution. In addition, Third found no discernible differences between encapsulated and unencapsulated samples by CL contrast imaging using similar RTA heating cycles. One of the advantages of heating a specimen using an RTA method is that the heating cycle is sufficiently short that there should not

be appreciable amounts of arsenic out-diffusion from the free surfaces of the GaAs wafers.

In these particular experiments, it was intended that the portion which was not exposed to the copper sulphate solution would act as a "control" for the region which was immersed. Since both halves received the identical rinse and heat treatments, differences between the two should be attributable to differences in amounts of copper present in the crystal lattice.

Photographs of the CL contrast images of these samples are given in Figure 4-3.



CL Image of Surface of GaAs Partially Immersed in  $\text{CuSO}_4$  and Heated at  $850^\circ\text{C}$

**Fig. 4-3**

It was found that areas exposed to  $\text{CuSO}_4$  solution appeared darker in comparison with unexposed regions in the CL contrast images. The faint outline of a polygonal shape which can be seen in the photograph is a etched mark which was intentionally placed on the surface to indicate the position to which the sample was immersed in the copper sulphate solution.

These results are in contrast to results obtained by Third in which regions suspected to contain a higher concentration of copper appeared relatively brighter. There are several reasons why the results obtained in these experiments were different. In particular, using this method, it was difficult to control the amount of copper being introduced. In some cases in which the samples were rinsed thoroughly in DI water after immersion in the  $\text{CuSO}_4$  solution, there appeared to be no discernible differences between the copper treated and untreated regions. This was the case in the CL images as well as in conductivity measurements which are detailed in Chapter 5. In other cases, when the samples were insufficiently rinsed, the samples were electrically conductive to the point where the samples could no longer be considered to be undoped. The sample in Figure 4-3 was only lightly rinsed and would most likely have been conductive.

Electrical and CL experiments were done on separate samples since the samples subjected to electron beam irradiation displayed deposits of carbon. This problem is not uncommon in SEM examinations.

It is possible that in some samples, sufficiently large quantities of copper were introduced which resulted in a reversal of the CL contrast image. In other samples virtually all of the copper sulphate may have been rinsed off resulting in no appreciable

increase in copper contamination on the immersed portion. Another experimental difficulty was to ensure that only certain regions of a wafer were exposed to the copper sulphate solution. Using a method of dipping in solution followed by rinsing in DI water, it is possible that traces of copper sulphate solution adsorbed on one section would be redissolved into the rinsing bath and partially redeposited on other portions of the wafer.

Another factor which should be taken into consideration is that there may have been differences in the GaAs wafers which were used. As discussed earlier, the diffusion process is believed to be sensitive to experimental conditions and it is possible that the characteristics of the GaAs material used in this experiment were markedly different than in the material examined by Third.

Following a device fabrication procedure often used in this laboratory, the surfaces of the GaAs wafers were initially etched using a sulphuric acid/hydrogen peroxide solution. This step serves to remove surface damage and contamination which may be present from the manufacturing process. This step may also have contributed to the differences which were found. In addition, the wafers used in this experiment were among the last produced by Johnson-Matthey in Trail, B.C. The wafers used by Third were from earlier production runs. During this time, changes in manufacturing were continuously being made to improve suitability for use in electrical device fabrication.

In conclusion the method of introducing copper by dipping GaAs in a copper sulphate solution was found to be difficult to reproduce. The regions which were exposed to the copper sulphate appeared darker in CL contrast images. After several attempts at introducing an appropriate amount of copper, this method was abandoned.

## **4-3.2 Deposition of copper using vacuum thermal evaporation**

### **4-3.2.1 Heat Treatments in a Tube Furnace**

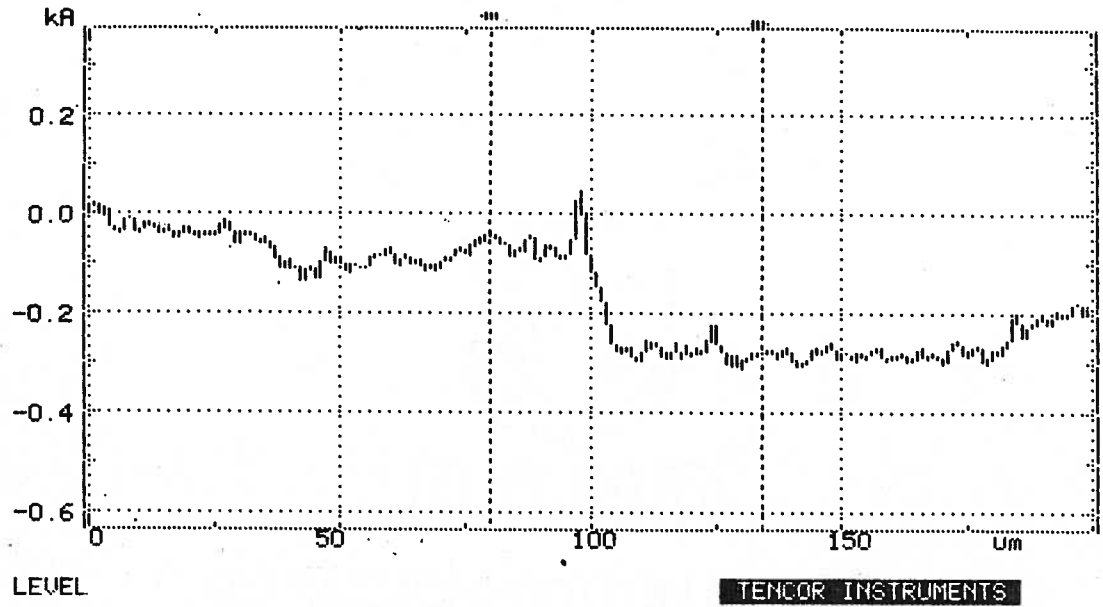
In the next series of experiments, 100-200 Å of copper were thermally evaporated onto the surface of the GaAs in vacuum. These samples were subsequently encapsulated using plasma enhanced chemical vapour deposited (PECVD) silicon nitride to prevent the out diffusion of arsenic during heat treatments. In conventional furnace heating cycles the samples were heated for periods ranging from 30 minutes to several hours. Initially the samples were heated at temperatures and times commonly used in annealing ion implanted wafers. For this the samples were heated to 850°C for roughly half an hour. These heating cycles were used for two reasons. One was to observe a distinct change in the CL contrast due to copper. Secondly, since these cycles are used routinely in device fabrication it would verify the fast indiffusion of copper reported by device manufacturers.

In these experiments, it was found that regions which were covered with copper were roughened considerably by heat treatment. These can be seen in the profilometer measurements made using a Tencor Alpha-step 200 profilometer. Figure 4-4(a) is the boundary between the copper film and the bare GaAs surface prior to heating. Figure 4-4(b) is the same boundary after heating and removal of the silicon nitride and copper film. The silicon nitride and copper were removed by sequentially immersing in solutions of buffered HF, 10% NH<sub>4</sub>OH and 10% KCN.

```

12/09 14:43
ID #
VERT. 1kA
L - 45. A
R - 285. A
- 240. A
Avg 100. A
TIR 355. A
Ra 95. A
HORIZ. 200um
L - 80.00um
R 134.0um
54.00um
Area 0.0667
SCAN MENU 3
um s/um
2000 .2 1
200 1 5
80 5 25
SCAN t=20sec
DIR. ->
STYLUS 11mg
116 165um LEVEL

```



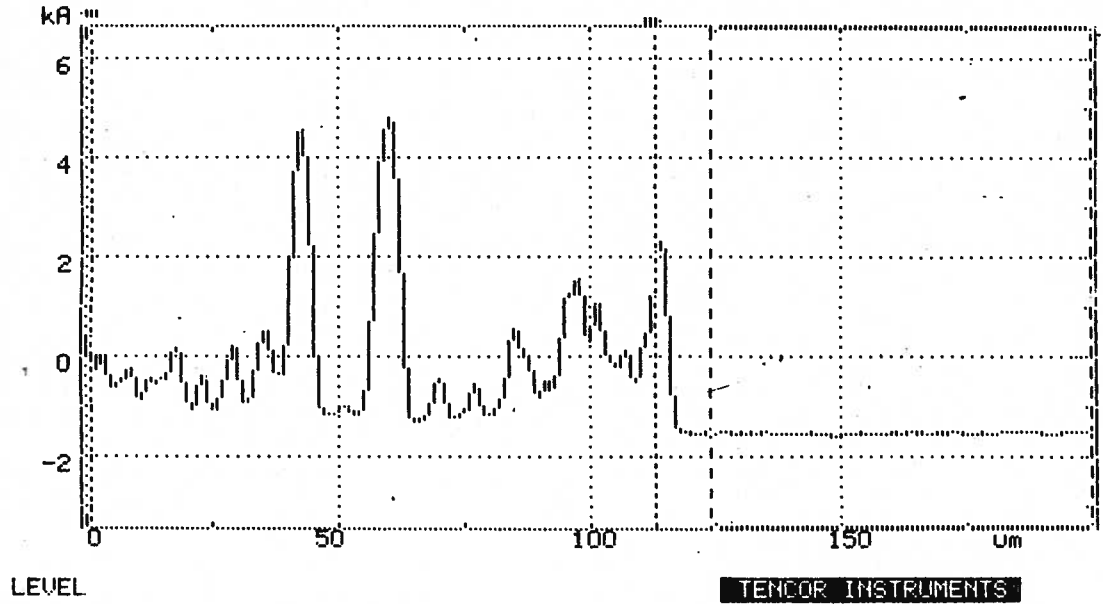
Profilometer Scan of Copper Film-GaAs Boundary Prior to Heat Treatment

Fig. 4-4(a)

```

12/11 18:32
ID #
VERT. 10kA
L 420. A
R 1.360kA
dAV 1.520kA
Avg 1.510kA
TIR 6.100kA
Ra 905. A
HORIZ. 200um
L 1.00um
R 113.0um
112.0um
Area 2.8665
SCAN MENU 3
um s/um
2000 .2 1
200 1 5
80 5 25
SCAN t=20sec
DIR. ->
STYLUS 11mg
126 195um LEVEL

```



Profilometer Scan of Copper Film-GaAs Boundary After Heat Treatment

Fig. 4-4(b)

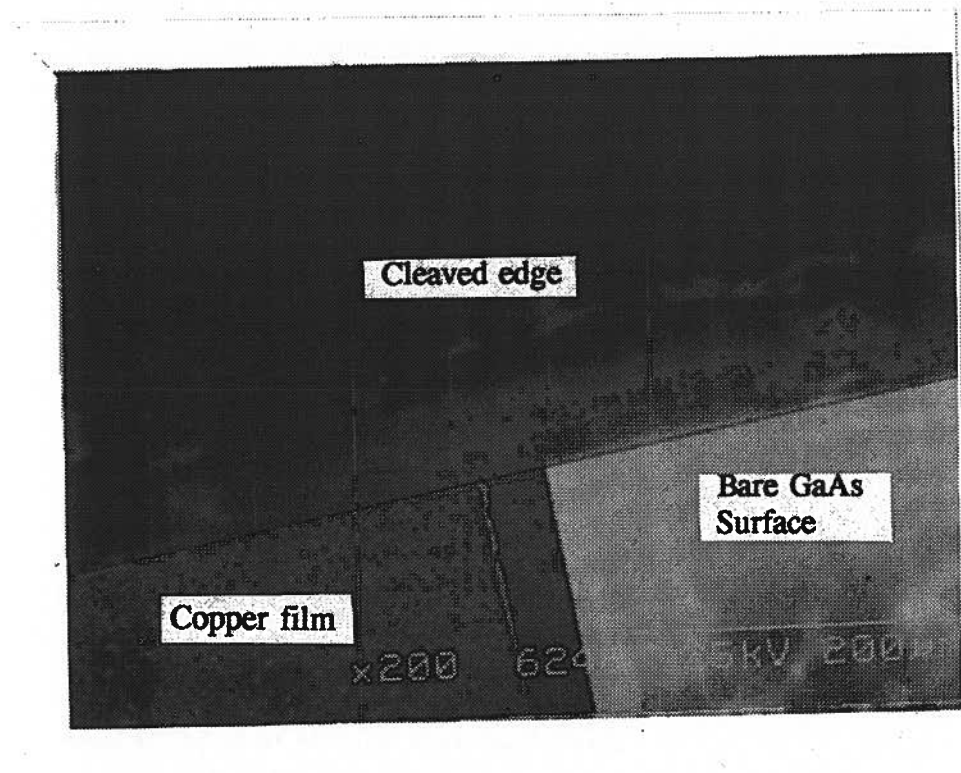
Attempts to restore the surface to a mirror like condition by chemically etching were unsuccessful. To restore the surface so that the copper treated side was visibly identical to the untreated portions required first grinding with 800 grit silicon carbide paper followed by polishing using 5 $\mu$ m and 0.3 $\mu$ m alumina slurry. To ensure that effects due to polishing damage would not be present, approximately 4 $\mu$ m of the surface was removed using a 8:1:1 H<sub>2</sub>SO<sub>4</sub>:H<sub>2</sub>O:H<sub>2</sub>O solution.

Similar roughening of GaAs wafer surfaces were reported by Maquistan, 1988, and were believed to be due to the formation of liquid phases and the alloying of copper with GaAs during comparable heating cycles.

Although there were changes in the CL contrast images in both copper covered and uncovered regions after heat treatment, there were no visibly apparent differences between the areas which were covered with copper during the heat treatment and regions which were left uncovered. It was suspected that at these temperatures the copper was diffused almost uniformly throughout the sample.

Temperatures ranging from 500 to 950°C in 150°C increments were used. A marked change in CL contrast images were found between heated and unheated material for temperatures above 800°C. The change consisted of reversal in contrast between the dislocation networks and the background. Prior to heat treatments the dislocation networks have a dark core surrounded by a brighter region. This region is also brighter than the surrounding background. Upon heating this area becomes darker with respect to the surrounding background. These results are similar to those reported by Third, 1989 and Jahn et. al, 1991.

For temperatures of 650°C or less there were no clearly visible differences in the CL contrast images of heated and unheated samples. Again there was no visible evidence of copper diffusion from the copper treated areas. Figure 4-5 is a CL contrast image of a cleaved edge in which the copper film can be seen. This sample was heated to 500°C for 4 hours. No apparent difference can be seen in the CL pattern on the cross sectional edge for copper treated and untreated areas. The bright region next to the copper film on the front face was related to the surface charging effects due to the scanning electron beam.



CL Image of Cleaved Edge of a GaAs Wafer Heated at 500°C for 4 hrs.  
at the Boundary of the Copper Film

Fig. 4-5

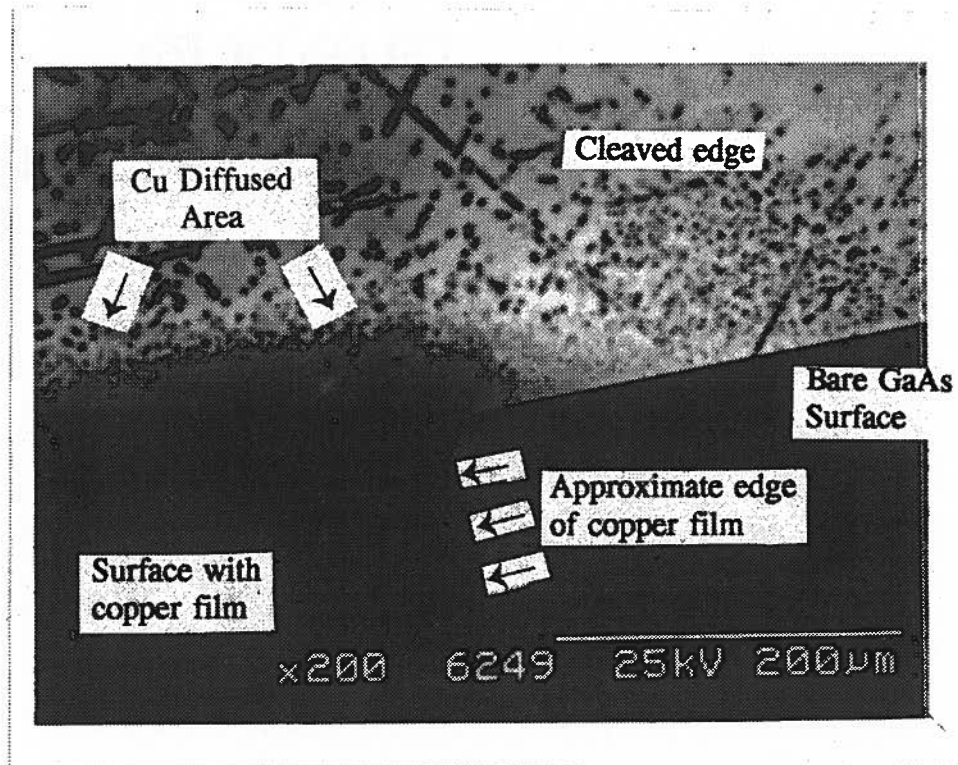
This brightening was also visible in the secondary electron images. Although it is difficult to explain the increase in light from this region, since it occurred only along the edge of areas not covered by copper, it is not believed to be related to the indiffusion of copper. The bright regularly spaced lines which are visible are an artifact of the amplifier used to increase the signal from the silicon photo-detector. The appearance of the bright lines was related to specific gain contrast settings on the amplifier unit. To obtain sufficient contrast required to image dislocation networks, the amplifier gain was close to maximum. The bright lines are likely to be due to non-linearities in the electronics. It was suspected from these results that heating cycles of 30 min were sufficiently long to diffuse the copper to such an extent that the sample appeared uniform under CL examination.

#### **4-3.2.2      Heat Treatments Using Rapid Thermal Annealing Methods**

RTA anneals at 950°C for 5-10 seconds have also been used in this laboratory to electrically activate implanted dopants. Heating the copper at these temperatures results in a drastic change in the cathodoluminescence image. This can be seen in figure 4-6(a). In this photograph the area that the copper has diffused into can be seen as a dark region, suggesting that the presence of copper somehow had introduced non-radiative recombination sites. The luminescence would then be expected to be lower from these regions. Another feature of the darker region was that it appeared to be rather granular and formed from a collection of dark spots. This suggests that the copper may complex with other defects such as dislocations. Moreover, the dark spots appeared to align with

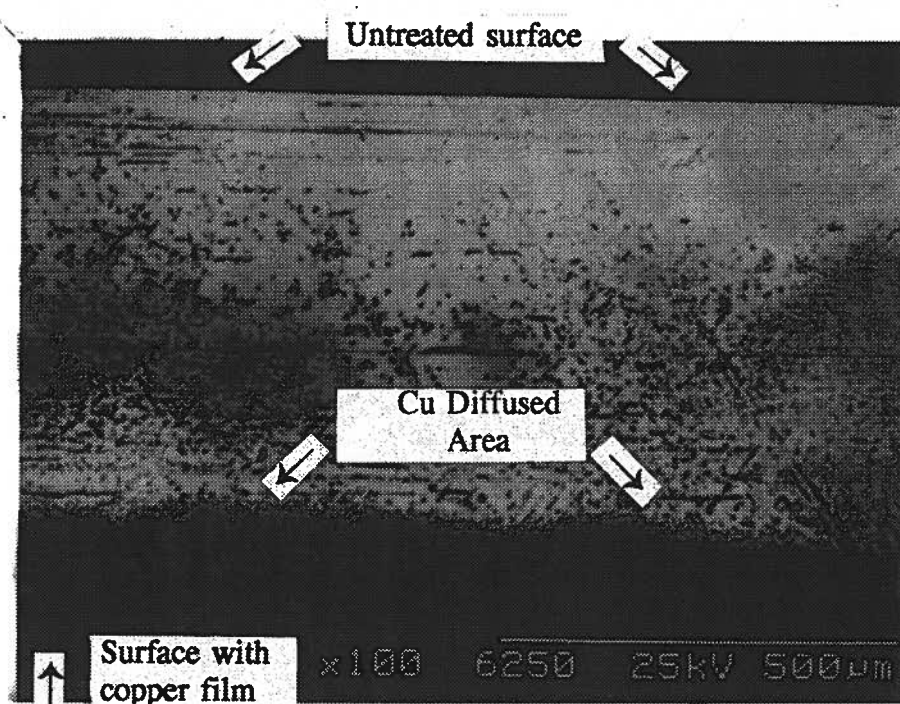
the  $\langle 1,1,1 \rangle$  planes in the crystal. This alignment could also be seen in dark spots which were in the bright regions away from the copper. This can be seen in figure 4-6(b) which is another view of the sample seen in figure 4-6(a) from a different perspective.

It is apparent that the darkening in the CL contrast image is due to presence of copper since there are no changes to the opposing face of the wafer or areas removed from the copper film.



CL Image of Cleaved Edge of a GaAs Wafer Heated at 950°C for 5 s.  
at the Boundary of the Copper Film

Fig. 4-6 (a)



CL Image of Cleaved Edge of a GaAs Wafer Heated at 950°C for 5 s.

Fig. 4-6 (b)

Although the copper diffusion was clearly visible in these photos, the areas where the copper was diffused were no longer semi-insulating. Since the samples were heavily contaminated from a microelectronics perspective, the conditions would not be representative of device quality substrate material. For these reasons, heat treatments at lower temperatures were pursued to reduce the amount of copper indiffusion.

The next set of heat treatments ranged from 450 to 750°C for periods of 50

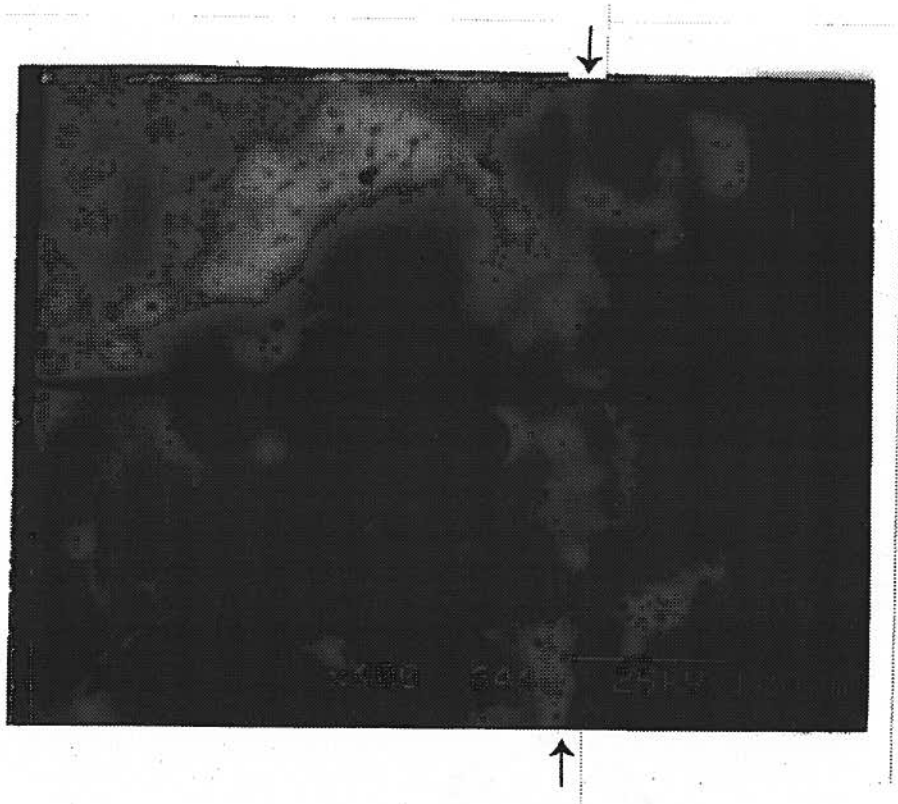
seconds. For these RTA treatments, the differences in luminescence between regions exposed to copper and untreated areas were much smaller than in the samples heated at much higher temperatures. From electrical measurements it was evident that copper treated regions were being modified by the heat treatments. A faint band, adjacent to the copper-treated surface which was darker relative to the bulk, could be seen in most of the CL contrast images. In some areas of the sample, the contrast would disappear and in most cases the differences were sufficiently small to make the estimation of diffusion depth difficult. Photographs with the largest contrast are presented in Figures 4-7 (a), (b), and (c). These are of samples which were heated at 500°C, 550°C and 600°C for 50 s respectively. The approximate positions of the band edges are marked with an arrow. The estimated depths are 58  $\mu\text{m}$ , 120  $\mu\text{m}$ , and 250  $\mu\text{m}$  for the 500°C, 550°C and 600°C samples. In areas unexposed to copper no band structures were observed.

The diffusion constants estimated from the band structures observed in these CL images are given in Table 4-3.

Temperature, Time	Estimate of Diffusion Depth	Calculated Diffusion Constant
500°C, 50 s	57.5 $\mu\text{m}$	$1.7 \times 10^{-7} \text{ cm}^2/\text{s}$
550°C, 50 s	120 $\mu\text{m}$	$3.0 \times 10^{-6} \text{ cm}^2/\text{s}$
600°C, 50 s	246 $\mu\text{m}$	$7.2 \times 10^{-6} \text{ cm}^2/\text{s}$

Estimates of Diffusion Constants of Samples Heated at 500°, 550° and 600° C

**Table 4-3**



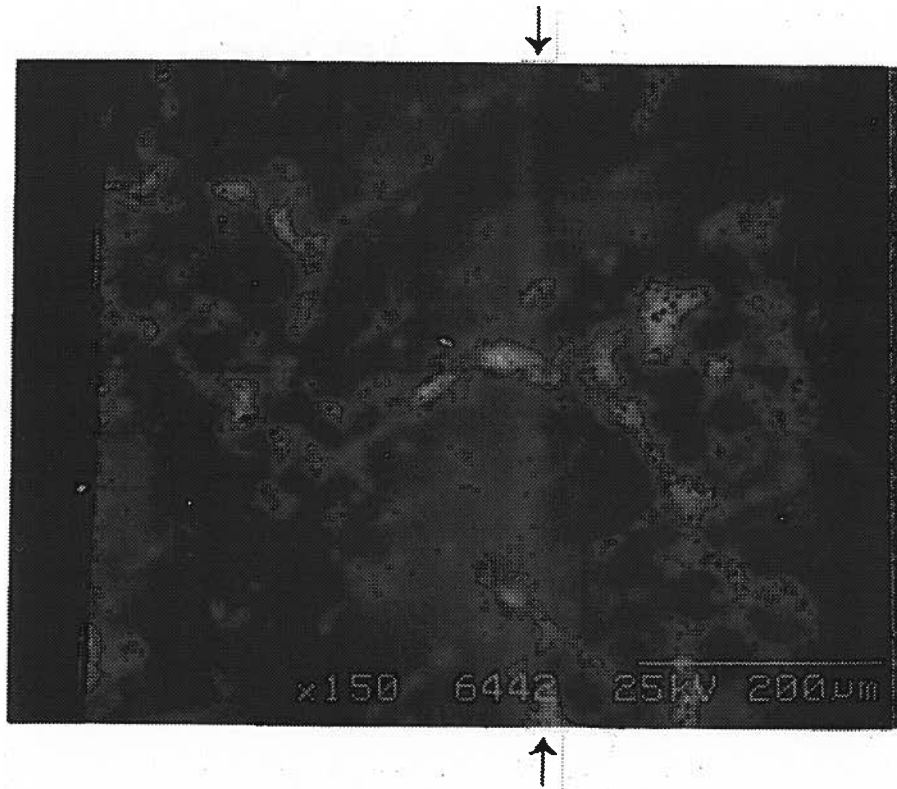
CL Image of a Cleaved Edge of a GaAs Wafer Heated at 500°C for 50 s  
With a Copper Film on One face

Fig. 4-7 (a)



CL Image of a Cleaved Edge of a GaAs Wafer Heated at 550°C for 50 s  
With a Copper Film on One Face.

Fig. 4-7(b)



CL Image of a Cleaved Edge of a GaAs Wafer Heated at 600°C for 50 s  
With a Copper Film on One Face

Fig. 4-7(c)

One apparent feature is that the gettering to dislocations seems to occur only in samples heated at temperatures above 800°C. The main heating process in RTA is due to free carrier absorption since the bulk of the energy output from the heated tungsten filaments of the quartz halogen lamps that are used as the heat source in RTA ovens are

in the infra-red wavelengths, for which GaAs is transparent. In infra-red images of GaAs crystals, the defects and impurities appear as dark spots[Fillard et. al., 1988]. Localized regions where the free carrier absorption is higher may heat at a faster rate which may cause localized temperature gradients.

#### 4-4 Conclusion

Cathodoluminescence images clearly resolved the diffusion from copper which was deposited on a surface of a GaAs wafer and subsequently heated to 950°C for 5 s. The copper seems to have precipitated or complexed with other defects such that the image of the diffused copper appeared granular. In addition, less luminescence was detected in copper diffused regions. In the literature, direct correlation of the effects of copper to features in CL contrast images was not found. However in the samples in which diffused copper was visible in the CL images, the samples were no longer semi-insulating. Presumably this was due to the slightly n-type SI GaAs being converted to p-type material due to the heavy acceptor doping. The CL contrast images indicated a marked change in the luminescence due to structural changes after annealing at temperatures in the 800° to 950° C range, even in areas which were not exposed to copper. These changes where the relative contrast of the dislocation networks and the background reverses after heat treatment have also been reported by a number of groups[Third et. al., 1989],[Jahn et. al.,1991],[Kang et. al., 1992]. Moreover dark regions indicating a presence of non-radiative recombination centres were concentrated along <111> lattice planes.

The changes in the CL contrast images for samples annealed at lower temperatures

were found to be quite small making the measurement of diffusion depths very difficult. Some measurements of the diffusion depth were made using these images giving diffusion constants which ranged from  $1.7 \times 10^{-7}$  to  $7.2 \times 10^{-6}$   $\text{cm}^2/\text{s}$  for temperatures ranging from  $500^\circ$  to  $600^\circ\text{C}$ .

RTA anneals of less than 1 minute at temperatures ranging from  $450^\circ\text{C}$  to  $650^\circ\text{C}$  were found to introduce sufficient copper to alter the electrical conductivity of samples. The electrical characterization of copper diffusion is detailed in the next section. Although there were clear differences in electrical behaviour between areas which were exposed and unexposed to copper, the CL contrast between these areas was low.

In all cases, the copper diffused regions appeared darker in the CL contrast images. Therefore at low contamination levels of interest in electrical devices, the copper could not be imaged clearly using CL methods. Altering the sample temperature during CL examination, using different beam energies or currents, and spectrally resolving the light emission may improve the level of CL contrast but these options were not readily available and were not pursued.

## Chapter 5

### The Effect of Copper on Current-Voltage Characteristics

#### 5-1 Introduction

In this section, studies are reported of the dependence of current as a function of applied voltage in samples used in OTCS experiments. The dependence of the current-voltage (I-V) characteristics on the electrode material and the method of fabrication, the amount of diffused copper, the illumination and the temperature was investigated. This portion of the work had several goals. One was to examine the behaviour of electrical contacts made with the semi-insulating material to be investigated using OTCS. Most well established techniques for making electrical contacts to GaAs have been developed for application on doped, electrically conductive GaAs. In reported OTCS studies of semi-insulating "as grown" material, similar methods of electrode fabrication are used with the intention of forming electrodes with electrical characteristics comparable to those found on electrical devices. The behaviour of electrodes fabricated using these techniques on high resistivity material can be expected to be different. Furthermore, the temperature range in which most devices operate are not as extreme as those which can be found in OTCS experiments and again it is possible that the contact characteristics are different at these temperatures. Another motivation for examining the I-V characteristics was to monitor the diffusion of copper by measuring electrical changes in the material without performing time-consuming and moderately expensive OTCS studies. The goal was to

find a method of introducing sufficiently small amounts of copper into GaAs so that a barely detectable change in electrical characteristics would occur. The appropriate specimens would then be investigated using OTCS and compared with control samples which were not intentionally exposed to copper. The effect of different electrode materials and geometry in enhancing differences in the behaviour of electrical contacts made to copper-treated and untreated samples was also examined.

In interpreting data from OTCS experiments it is important to ensure that the characteristics of the electrical contacts are not inadvertently manifested in the collected data. Moreover, during typical OTCS temperature scans, the free carrier concentration may change by several orders of magnitude. This too may lead to differences from the expected electrical behaviour of the electrodes. Therefore, a detailed knowledge of the behaviour of the contact under a variety of conditions is important in deducing trap parameters accurately from transient current data.

Electrical contacts to semiconductors are frequently classified into three main types: ohmic, blocking and injecting[Bube,1992]. In practice, contacts are not purely one type or the other and display characteristics found in other types to some degree. For example, at sufficiently low voltages most contacts have a linear current voltage relation typical of ohmic type contacts. In other cases such as ohmic contacts to high resistivity GaAs, it has been reported that at sufficiently high applied voltages, ohmic contacts reach a space charge limited regime resulting in a drastic increase in the current. The choice of contact for a particular OTCS application often depends on factors such as whether minority or majority carriers are being examined, and whether these carriers are

*n* or *p* type. Other considerations in the selection of contacts include maximizing the signal to noise ratio by maximizing the photocurrent and minimizing the current in the dark. Furthermore, choosing electrodes which require the least amount of processing reduces the chance of altering the sample. For example, forming ohmic contacts usually requires a sintering process to diffuse dopant atoms into the semiconducting material under the contact metallization. The heat treatment as well as the introduction of dopant atoms under the electrode metal may induce changes in the substrate material being examined.

## **5-2 Methods Reported in Literature**

In the literature, a variety of methods has been used to create electrical contacts to SI GaAs for OTCS studies. Some of the reason for this may be due to the assumption that since the resistivity of the GaAs is high, the impedance due to the contacts is likely to be small in comparison with that of the semiconductor. It has been suggested that for SI GaAs "it is sometimes possible to get by with crude contacts" and contacts formed by "unalloyed In, silver paste and even a conductive rubber have been used"[Look, 1989]. Some examples from OTCS studies which were used as comparisons with this work are listed in Table 5-1.

This may be one of the sources of inconsistencies of OTCS experiments. It is widely reported that the determination of trap parameters of levels which are detected using OTCS methods are dependent on the electrode material and geometry[Young, 1989][Blight, 1986]. In the literature which was referenced for this work, there were no

studies found which examined the resistance or I-V characteristics of the contacts.

Work	Electrode metal	Type	Geometry
Tin, et. al., 1988	Sintered Indium	Ohmic	Planar
D. Hui, 1989	Au, AuGe, Al	Ohmic, Schottky	Planar, sandwich
Blight et al., 1988	Not Reported	Ohmic	Planar
Fang et al., 1989	AuGe	Ohmic, Schottky	Planar, sandwich
Yoshie et al., 1985	AuGe	Ohmic	Sandwich

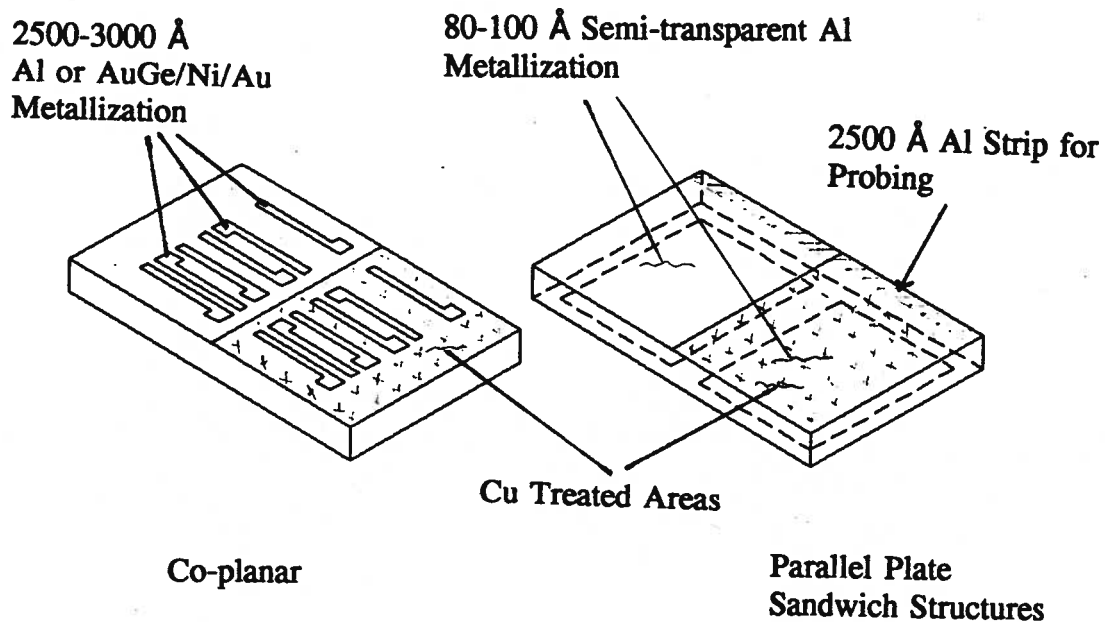
### Types of Electrodes Used in Reported OTCS Work

**Table 5-1**

#### **5-3 Fabrication of Samples**

Many of the samples used in this section were prepared in parallel with samples used in the CL contrast studies. For these experiments a 100 to 200Å thick copper film was deposited on approximately half of one side of the specimens. The specimens were 2 cm by 2.3 cm segments cleaved from 3 inch GaAs wafers approximately 625 μm in thickness. These were then encapsulated with PECVD silicon nitride and heated using either a Mini-Brute tube furnace or an AG Associates RTA. After removal of silicon nitride and undiffused copper, the samples were restored back to a mirror-like finish. Samples which were annealed at temperatures much higher than 500° C in the furnace and 700° C in the RTA required grinding and mechanical polishing steps to renew the surface. Similar findings were reported by Maquistan, 1989, and were believed to be caused by the formation of liquid phases at the copper GaAs boundary at elevated temperatures. The specimens which were used in OTCS studies were RTA heated at temperatures lower

600° C and the surfaces of the samples were not badly damaged by the presence of copper and required only the removal of remaining copper followed by a chemical etch to restore the surface. To ensure removal of damage which was not visibly apparent, several microns of the surface were removed from all samples using a 8:1:1/H<sub>2</sub>SO<sub>4</sub>:H<sub>2</sub>O<sub>2</sub>:H<sub>2</sub>O etch. This etch has been used in preparing wafers for device fabrication. Following this step, electrode metal was thermally evaporated in a vacuum system and shaped using a "lift-off" technique. Three different electrode structures were used. These are co-planar ohmic, co-planar Schottky and a parallel plate "sandwich" structure with a semi-transparent Schottky contact as one plate and an ohmic contact as the other. Figure 5-1 illustrates the different contacts.



Electrode Geometry of Specimens

Fig. 5-1

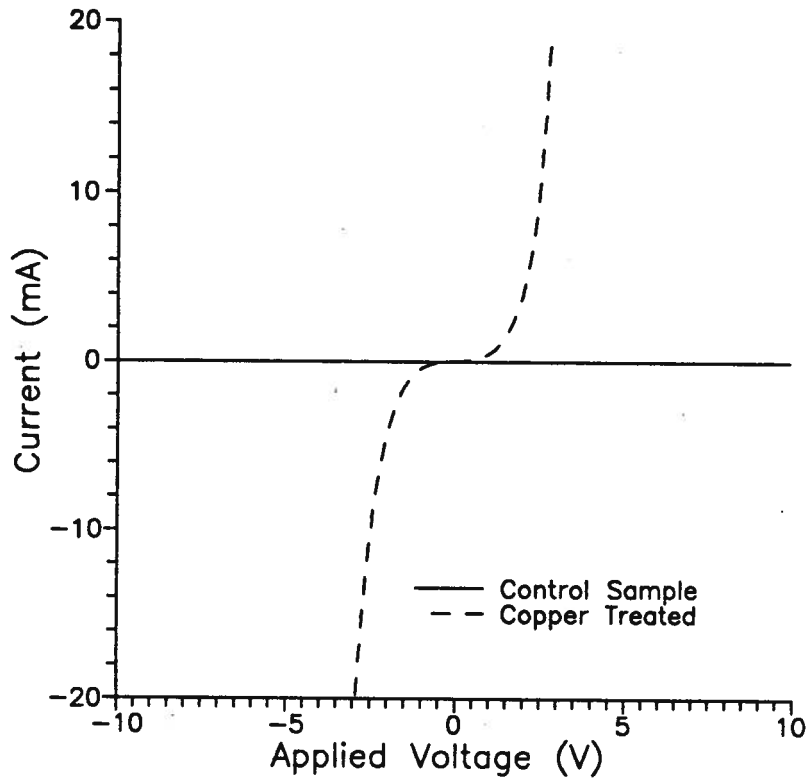
AuGe\Ni\Au electrodes were heated at 435° C to diffuse in Ge to create an ohmic contact. A detailed description of the fabrication procedure is included in Appendix A. The electrical conductivity of these samples was measured using a Hewlett Packard(HP) 4145A semiconductor parameter analyzer in conjunction with a Wentworth probe station to make electrical contacts to the electrodes. In the studies where the temperature of the dependence of the contacts was examined, the samples were placed in a MMR low temperature micro-positioner (model LTMP-3) chamber. In initial work, the data was graphically recorded by plotting using a HP 4745 plotter. In later studies the data was transferred to a personal computer to speed data collection and for convenience.

### 5-3.1 Heat Treatments in a Tube Furnace

The first samples were subjected to temperature cycles typically used for annealing out damage due to ion-implantation of dopant during device fabrication. These specimens were found to be sufficiently electrically conductive that they could no longer be considered semi-insulating. This was presumably due to relatively large quantities of copper being diffused into the GaAs lattice from the copper film deposited on the surface, resulting in the material being doped *p*-type. Moreover, both the control side as well as the side covered with a copper film was conductive. Similar results were found by Tin et. al. 1988 using comparable methods where the copper was found to diffuse throughout samples.

#### 5-4 Heat Treatments Using Rapid Thermal Annealing Methods

I-V plots of Al electrodes formed on GaAs heated at 950°C for 5 seconds with and without copper on the surface are given in Figure 5-2.



I-V Plots of Copper Treated and Untreated Specimens heated at 950°C for 5 s

**Fig. 5-2**

The current in the copper treated sample, represented by a dashed line, resembles the characteristics of blocking contacts with a breakdown voltage of about 2.5 V. The magnitude of the sample current on the control side was in the range of nano-amperes indicating that the diffusion of copper was well confined to the region which was covered by the copper film during the heat treatment unlike the samples which were furnace

heated for 30 minutes or more. However, the copper treated samples which were heated at temperatures commonly used for post implantation anneals were not suitable for investigation using OTCS due to the small relative increase in conductivity under illumination in comparison with the conductivity in the dark.

### 5-3.2.1 Planar Ohmic electrodes

A contact would logically be considered to be ohmic if the magnitude of current passing through the contact is linearly proportional to the applied field, but in many applications the term is also used to mean that the series resistance due to the contact is small. Thus, in some cases, ohmic contacts are assumed to be of sufficiently high conductance that resistance of the contacts can be considered negligible in comparison with other circuit elements. Although it would seem that this would be the case with SI material where the resistivity of the GaAs between the electrodes is very high, it was found in this work that the resistance related to the contact was considerable.

There are two possible methods of forming ohmic contacts to semiconducting materials. In one, a metal is chosen with a work function,  $\phi_m$ , which is lower than the electron affinity,  $\chi_{sc}$  of the semiconductor so that the electron barrier height given by:

$$\phi_{bn} = \phi_m - \chi_{sc}$$

is small. However with GaAs, the barrier height is largely independent of the metal work function. A high density of surface states is believed to fix the barrier height at about 0.8 eV[Sze, 1981]. In practice the method generally used to form ohmic contacts is to create a heavily doped region below the electrode metal. This reduces the thickness of the

barrier height allowing for a greater amount of tunnelling current. In order to increase the tunnelling current sufficiently, dopant concentrations close to  $5 \times 10^{19}$  atoms/cm<sup>3</sup> are typically used[Palmstrøm, 1985]. A number of methods are used to introduce dopants into the GaAs matrix such as ion-implantation, epitaxial growth and diffusion. Creating an amorphous disordered layer with a large number of states near the surface below the electrode metal has also been proposed as a method of creating low resistance contacts[Palmstrøm, 1985].

The method used in this work, was to thermally evaporate and sinter a commercially available alloy of 88% Au and 12% Ge. This is a common technique in device fabrication

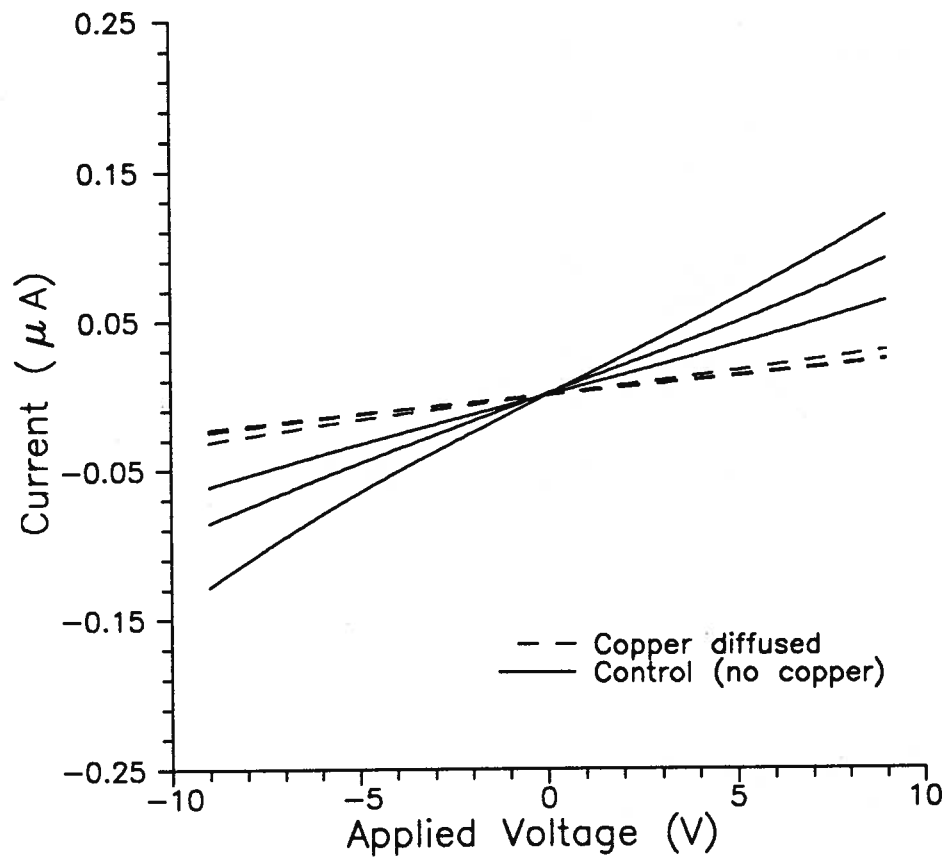
Although the main motivation for the use of ohmic contacts in OTCS studies is to reduce the resistance of the contacts, there are other advantages such as reduced dependence of the contact behaviour on surface conditions of the crystal compared to other contact techniques such as Schottky metallizations. In processing GaAs, it is difficult to control surface conditions. A thin native oxide is known to form within a few minutes of exposure of free GaAs surfaces to the atmosphere and the composition of this oxide is suspected to depend on prior processing steps. For example, sulphuric acid based etches have been found to preferentially etch gallium leaving an arsenic-rich surface and the oxide growing on such a surface would be expected to reflect these conditions. In a sintering process, the dopant diffuses through the thin oxide, into the underlying bulk. Thus the electrical behaviour of contacts formed using these methods is believed to be relatively independent of the characteristics of oxide layers. One disadvantage of using

sintered AuGe electrodes is that a heating step is required which may alter the sample due to the unintentional diffusion of material either in or out of the crystal. It has been reported that the germanium can diffuse into the GaAs in the range of microns and form complexes with other impurities. Moreover the spatial distribution of the amount of dopant which diffuses into the GaAs is not uniform. Spikes of germanium have been reported to form where the dopant diffuses in a greater distance. This could occur as a result of dislocations, other impurities in the crystal or the formation of different phases at the electrode metal-substrate interface during alloying[Palmstrøm, 1985].

In conclusion, various methods have been developed to create well behaved ohmic contacts with low resistance to doped GaAs, however, none of the methods were developed specifically for use with high resistivity material. Moreover, the mechanisms of contact formation, and the metal-GaAs interface does not appear to be fully understood. For example Lehovc and Pao, 1988, reported on work which demonstrated the formation of space charge layers at interfaces between heavily doped  $n^+$  and  $p^+$  layers and SI material. This would presumably be the situation for an ohmic contact which included a heavily Ge doped layer. In this work effort was made to examine the behaviour of electrodes made using these techniques on semi-insulating material.

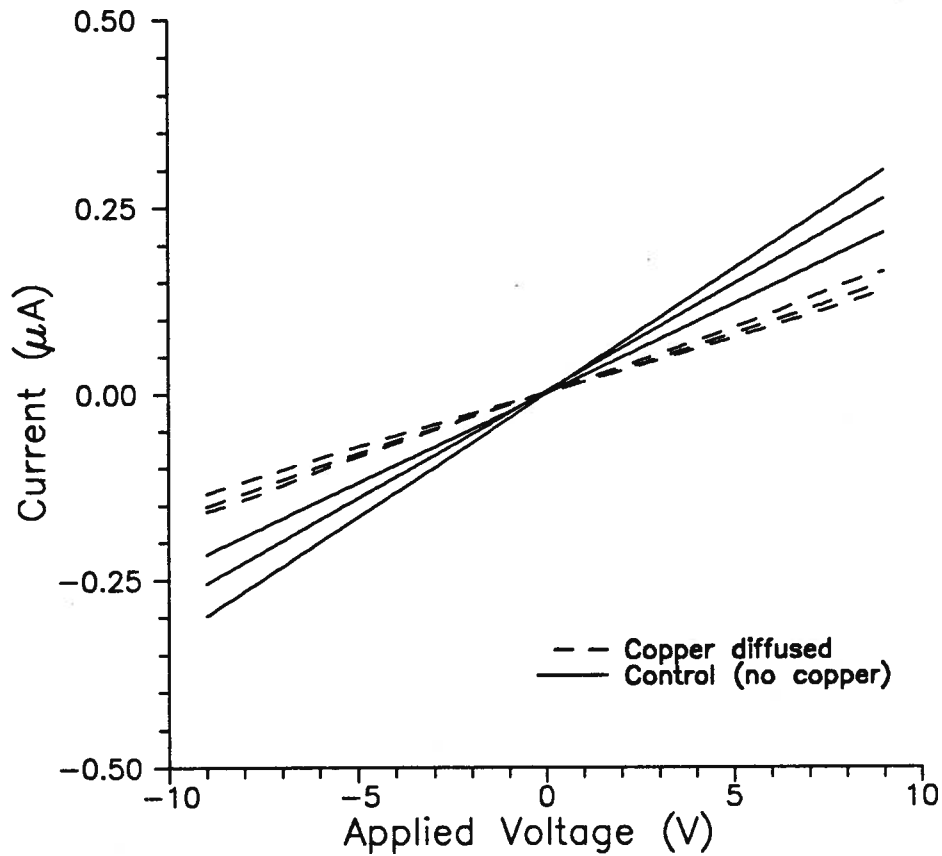
### **5-3.2.2      Results of Measurements**

The conductivity of samples treated with copper decreased for samples heated in the range of 500°C to 600°C. AuGe\Ni\Au electrodes placed on both copper treated and control samples displayed linear current voltage behaviour. This is illustrated in Figure 5-4(a) and (b). Each sample had electrodes with three different spacings.



I-V Plot of AuGe/Ni/Au Electrodes, Specimen Heated at 550°C for 50 s

Fig. 5-3 (a)



I-V Plots of AuGe\Ni\Au Electrodes, Specimen Heated at 600°C for 50s.

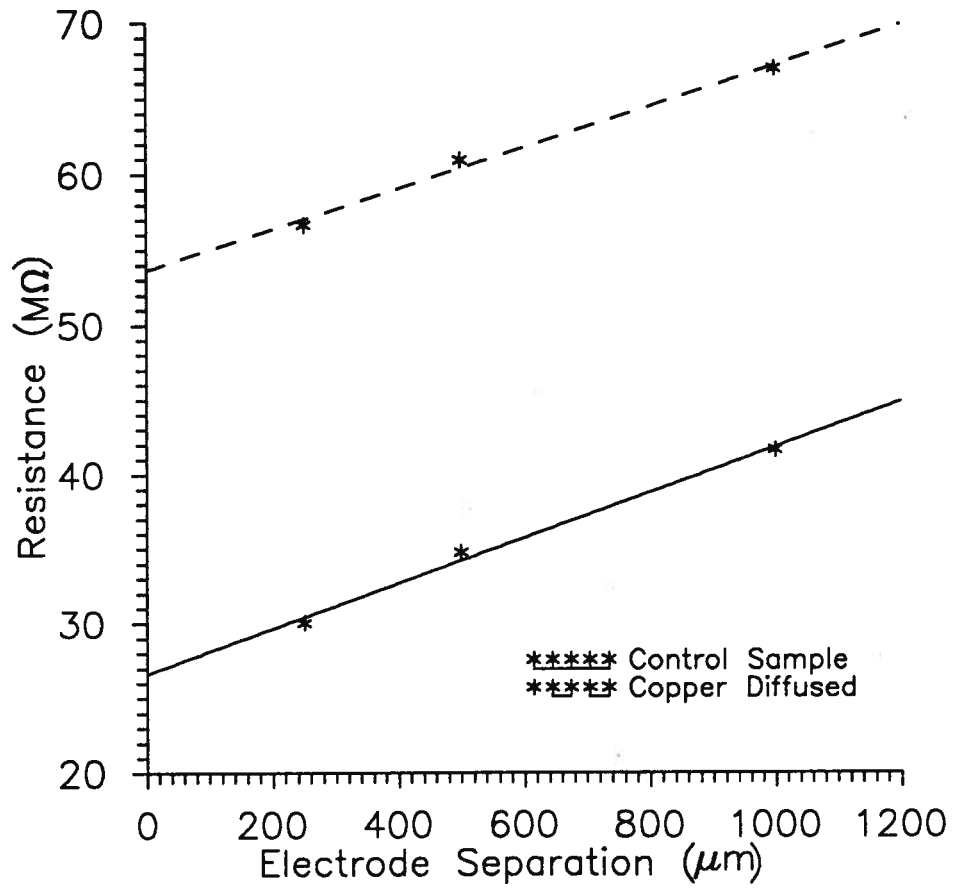
Fig. 5-3 (b)

Although an increase in the conductivity for copper diffused samples can be explained by the formation of acceptor levels, the causes for the decrease in conductivity is not as clear. One cause may be an increase in contact resistance rather than an increase in the resistivity of the bulk semiconductor. Using transmission line model (TLM)

measurements, the contact resistance and the sheet resistivity of the substrate may be determined[Look, 1989]. The TLM method was originally proposed by Shockley, and is so named because an analogy was made with a lossy transmission line. In this method the resistance between similar electrodes spaced varying distances apart are measured. The total resistance between the electrodes is expressed as:

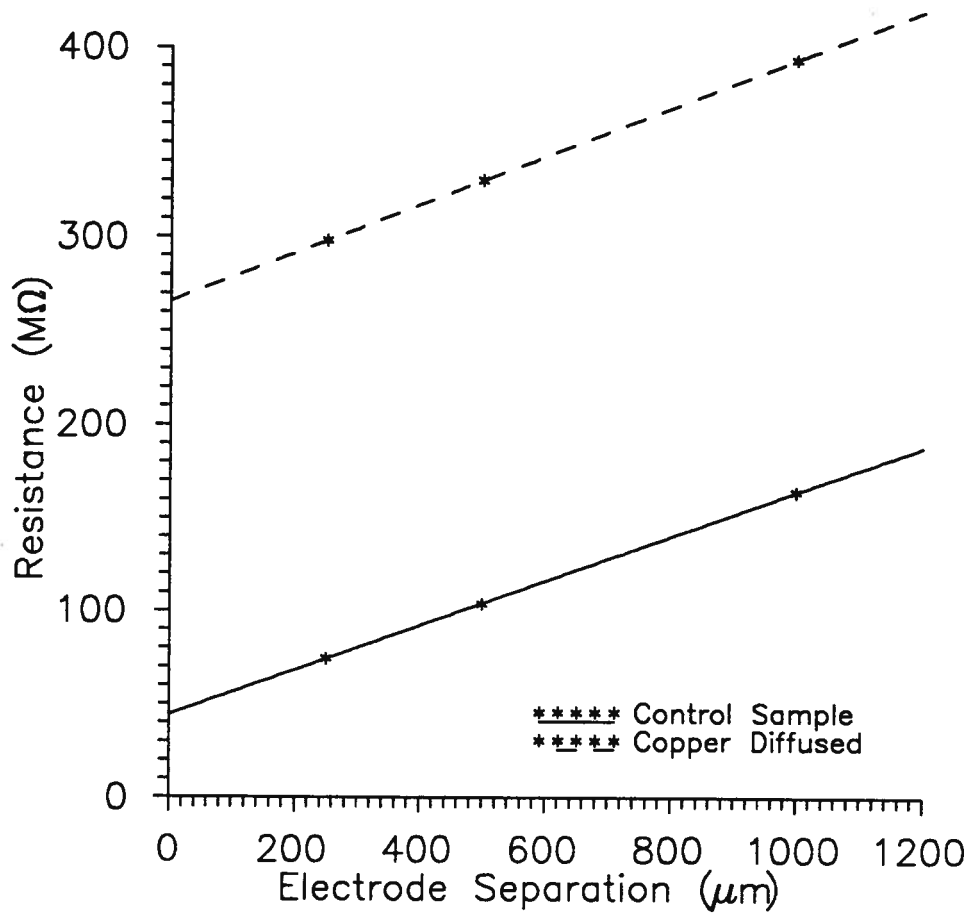
$$R = 2R_c + r_s(l/w)$$

where  $R_c$  is the resistance of one contact,  $r_s$ , is the sheet resistivity of the material between the electrodes,  $l$  is the spacing between the electrodes, and  $w$  is the width of the electrodes. In the TLM method the resistance of the specimens are plotted as a function of the spacing between electrodes. The slope of this plot gives  $r_s/w$  and the y-intercept gives a value for  $2R_c$ . In the usual case, the method is applied to a conductive layer shaped in a fashion such that the path of conduction is well defined. In this case, it is applied to a wafer approximately 625  $\mu\text{m}$  thick which is assumed to be homogeneous, and the current path is not well defined due to effects such as surface conduction, fringing fields, and differences in resistivity of material below the electrodes. This makes it difficult to accurately determine values for the resistivity of the material and the contact resistivity. However in this study, the measurement was used to determine the respective contribution of the SI bulk and the contacts to the total resistance measured across adjacent electrodes. Plots of the resistance versus the electrode spacing for sample heated at 500° and 600°C with and without copper are given in Figures 5-4(a) and (b) respectively.



Resistance as a Function of Electrode Separation for Specimens  
Heated at 500°C for 50 s

Fig. 5-4 (a)



Resistance as a Function of Electrode Separation for Specimens Heated at 600°C for 50 s

Fig. 5-4 (b)

Estimates of sheet resistivity of the GaAs between the electrodes, the contact resistance, and the contact resistivity which were determined for the specimens heated at 500° and 600°C are summarized in Table 5-2. The resistance of samples which were heated at

600°C were observed to have a higher resistance than the samples heated at 500°C. Much of this increase was due to an increase in contact resistance.

Sample	Sheet Resistivity (MΩ/□)	Contact Resistance (MΩ)	Contact Resistivity (KΩcm <sup>2</sup> )
500° C, Control	76.1	26.6	339
500° C, Cu Treated	67.6	53.7	805
600° C, Control	600	44.1	661
600° C, Cu Treated	641.5	266	3990

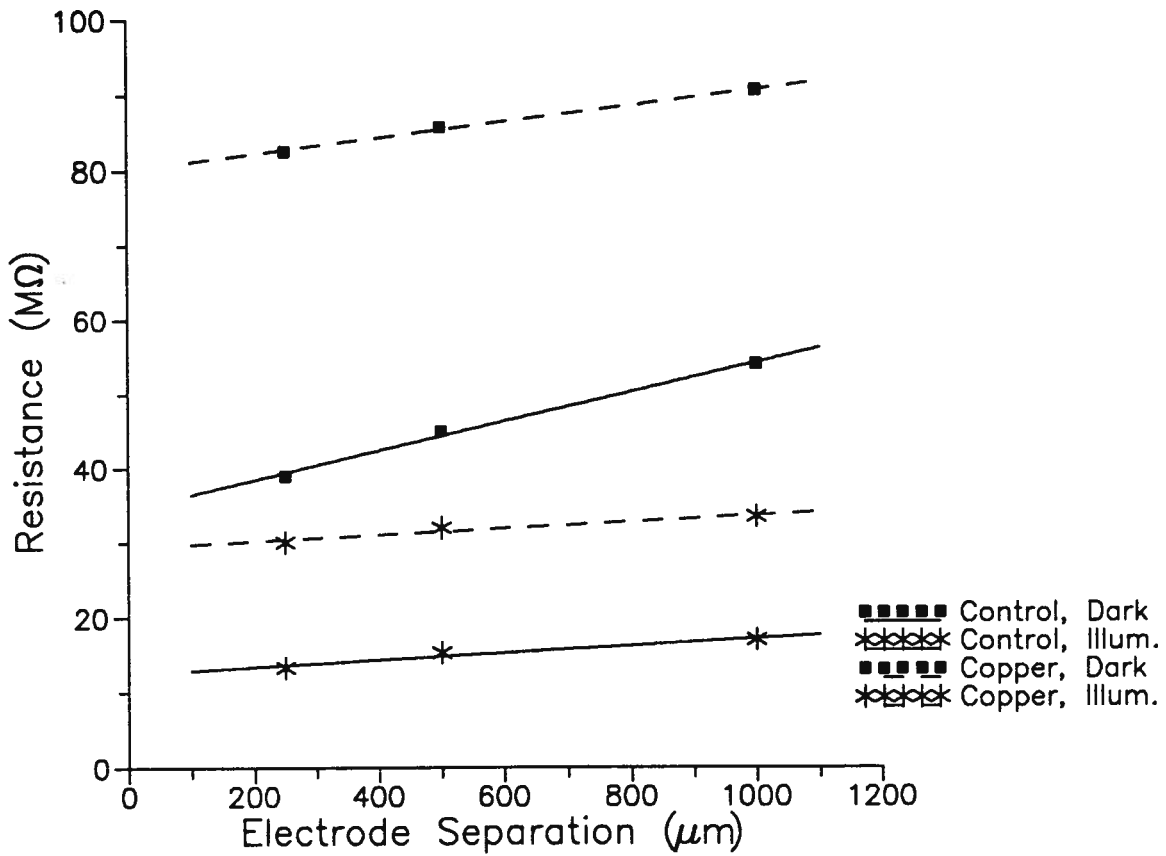
#### Resistance Parameters in Planar Ohmic Contacts

**Table 5-2**

There was also an increase in resistance in samples which were treated with copper in comparison to the control samples. Again much of the increase was due to changes in the contact resistance with the contact resistance constituting a significant portion of the total resistivity. As an example, for a sample heated at 500°C with no copper and electrodes separated 1000 μm apart, the resistance due to the contacts were estimated to be 27 MΩ and the resistance due to the semiconductor would be 15 MΩ. Clearly the contact resistance could be expected to be significant in determining the current.

To investigate the changes in the resistance due to illumination, similar I-V measurements were carried out for a sample heated at 600°C with and without illumination. The source of illumination for these measurements was an incandescent light built into the Bausch and Lomb Microzoom microscope used to view the specimens

during electrical probing. The intensity of the illuminator was set to the lowest setting. The results of these measurements are plotted in figure 5-5. Again it was found that there were large variations in the contact resistance accompanied by smaller changes in the resistance due to the bulk.



Resistance as a Function of Electrode Separation under illumination and in the Dark for Specimens Heated at 600°C for 50 s

Fig. 5-5

Resistance parameters calculated from these measurements are tabulated in Table 5-3.

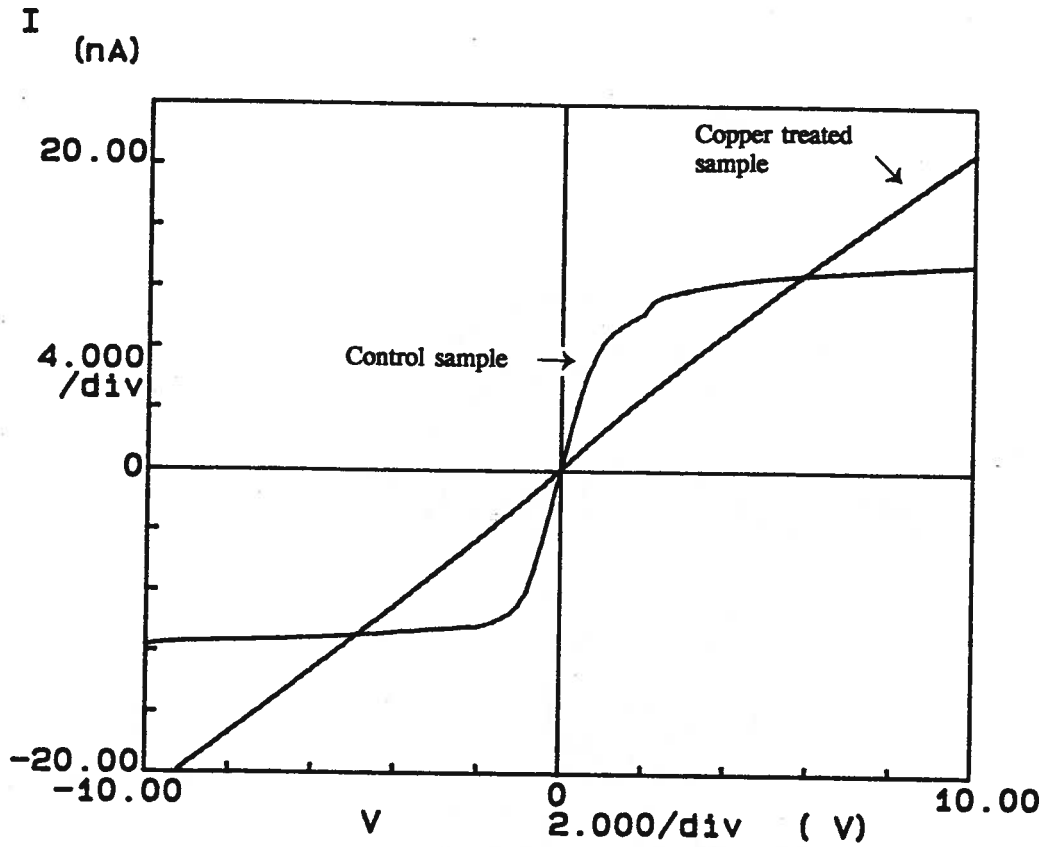
Sample	Sheet Resistivity ( $M\Omega/\square$ )	Contact Resistance ( $M\Omega$ )	Contact Resistivity ( $K\Omega\text{ cm}^2$ )
Control (dark)	98.6	34.5	518
Control (illum.)	23.6	12.5	187
Cu treated(dark)	53.3	80.1	1200
Cu treated(illum.)	21.6	29.4	440

Resistance Parameters in Planar Ohmic Contacts Under Illumination and in the Dark

**Table 5-3**

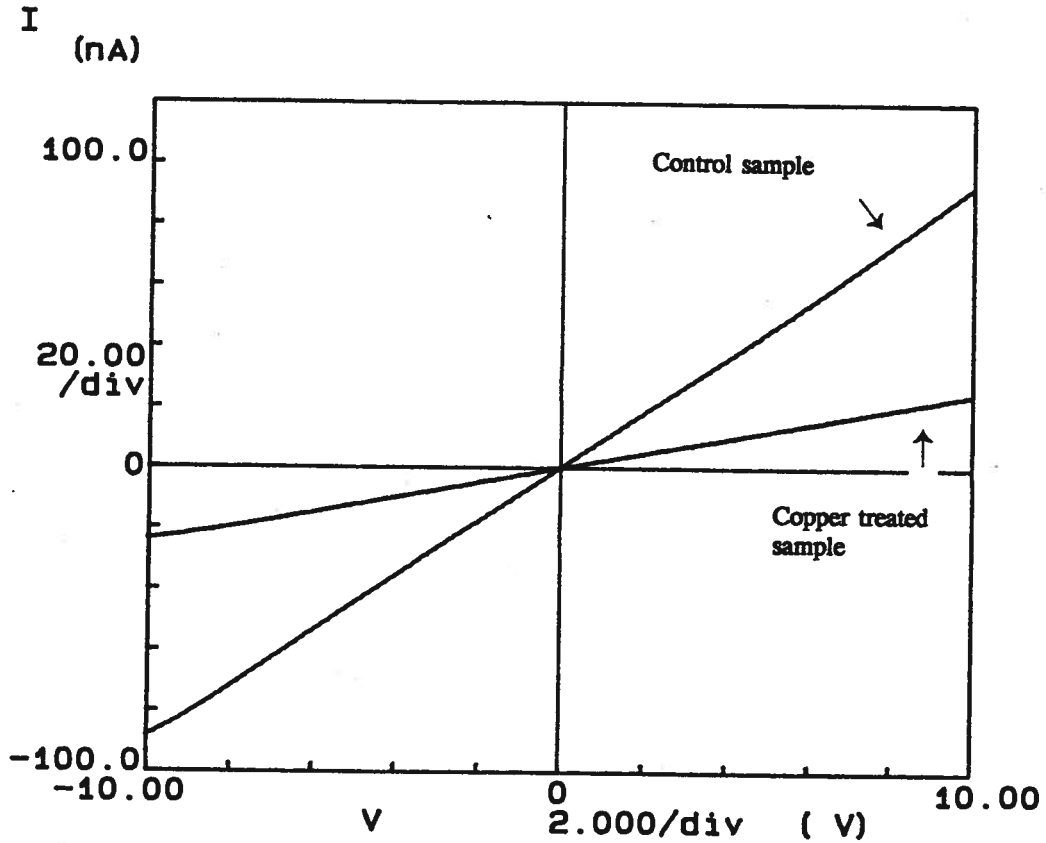
Since the thickness of the electrodes is approximately 2500 Å, it is not expected for the light to perturb the region below the electrodes.

Another interesting feature which was found in copper-diffused samples was that the contacts displayed a linear I-V relation before they were sintered. The control samples which were not exposed to copper displayed Schottky characteristics as typically encountered. Moreover, the resistance of the contacts to the copper-treated regions did not change significantly after sintering whereas on the untreated side the resistance of the contacts was appreciably lower. I-V characteristics of AuGe/Ni/Au electrodes to GaAs samples which are copper-diffused and undiffused before and after a sintering at 435°C for 2 minutes are shown in Figures 5-6(a) and (b) respectively.



I-V Plots for AuGe Metallizations Prior to Sintering for  
Cu Treated and Control Specimens

Fig. 5-6 (a)



I-V Plots for AuGe Metallizations After Sintering, for  
Cu Treated and Control Specimens

Fig. 5-6 (b)

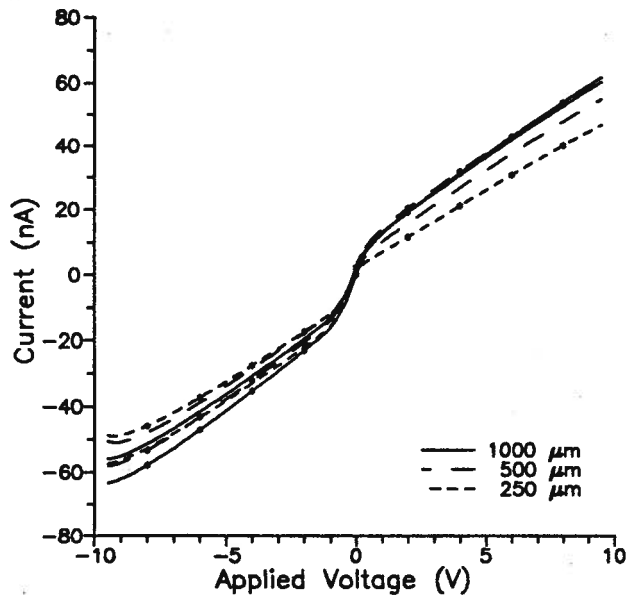
### 5-3.2.2 Planar Schottky Contacts

Schottky contacts are used as rectifying contacts in diodes and gate structures in MESFETs (Metal Semiconductor Field Effect Transistors). From a fabrication point of view Schottky contacts are less complicated than ohmic contacts because they do not

require alloying. Usually the only steps taken are to ensure that the surface on which the metal is to be deposited is free of any contamination. In practice, the barrier height is almost always close to 0.8 eV. A number of metals have been used to form Schottky contacts; some examples are aluminium, chromium, gold, and titanium. In this work aluminium was chosen since it is comparatively easy to shape using a "lift-off" technique and thermal evaporation.

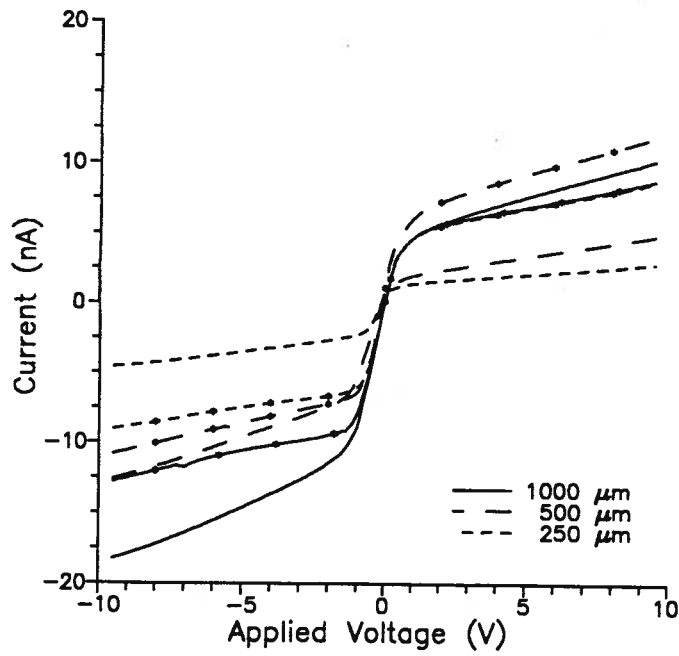
#### **5-3.2.4      Results of Measurements**

For these samples, the electrode shapes were identical to those of the ohmic contacts investigated in the last section. The I-V characteristics of Al electrodes deposited on specimens with copper indiffused at temperatures ranging from 450° to 950° C were examined. For samples heated at temperatures in the 500° to 600° C range, the resistances in the copper-treated samples were consistently higher than in the control specimens. For samples which were heated at temperatures much above 650° C, this effect was reversed with the copper-treated samples becoming increasingly conductive with treatment temperatures. These results seem to be in agreement with data reported by Hall and Racette in which the solubility limit of copper in GaAs starts to increase rapidly at about 625° C. At temperatures below this the solubility limit was reported to levels off near  $1 \times 10^{16}$  atoms/cm<sup>3</sup>. The I-V plots for samples heated with and without copper at a range of temperatures from 450° C to 850° C are given in Figure 5-7.



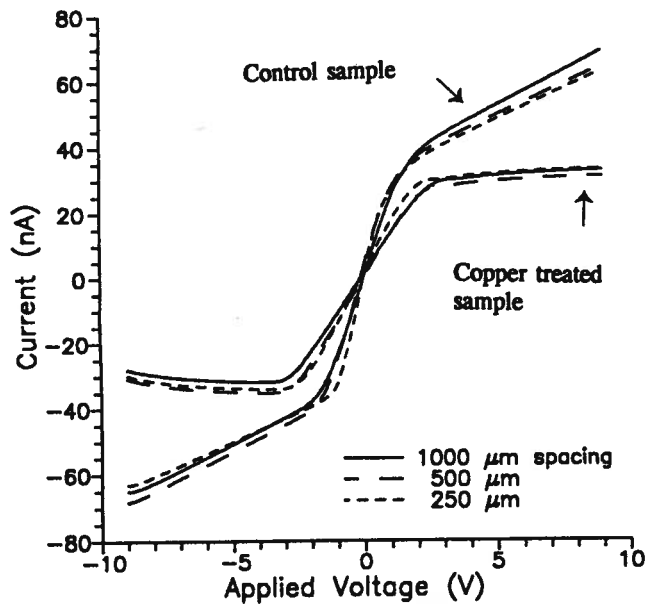
I-V Characteristics of Al Electrodes on GaAs with No Heat Treatment

5-7 (a)



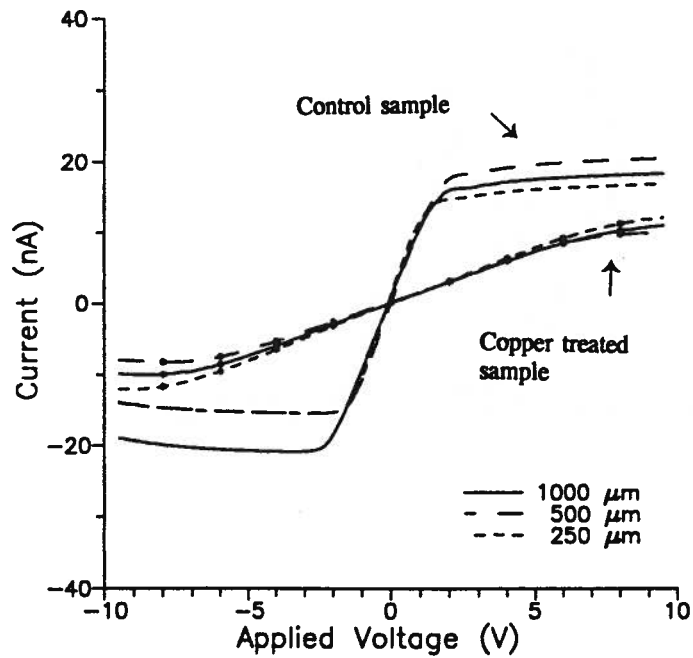
I-V Characteristics of Al Electrodes on GaAs Heated at 450°C for 50 s

5-7 (b)



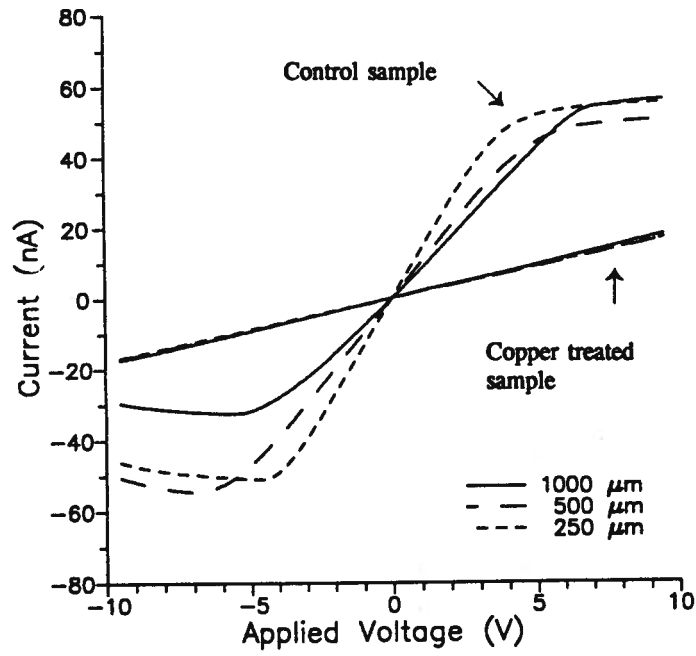
I-V Characteristics of Al Electrodes on GaAs Heated at 500°C for 50 s

5-7 (c)



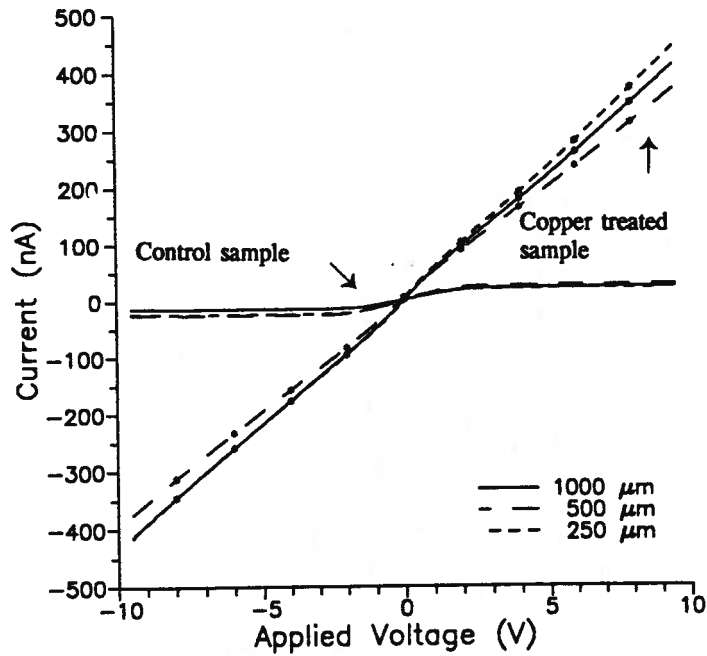
I-V Characteristics of Al Electrodes on GaAs Heated at 550°C for 50 s

5-7 (d)



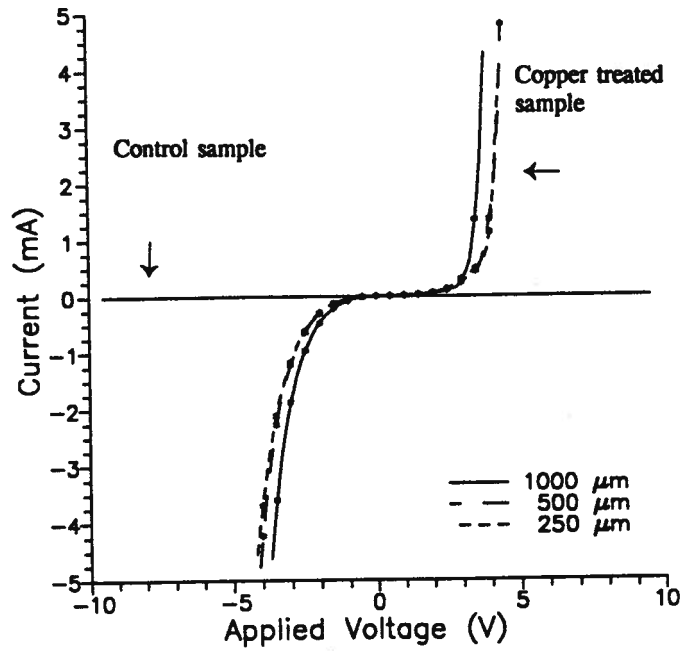
I-V Characteristics of Al Electrodes on GaAs Heated at 600°C for 50 s

5-7 (e)



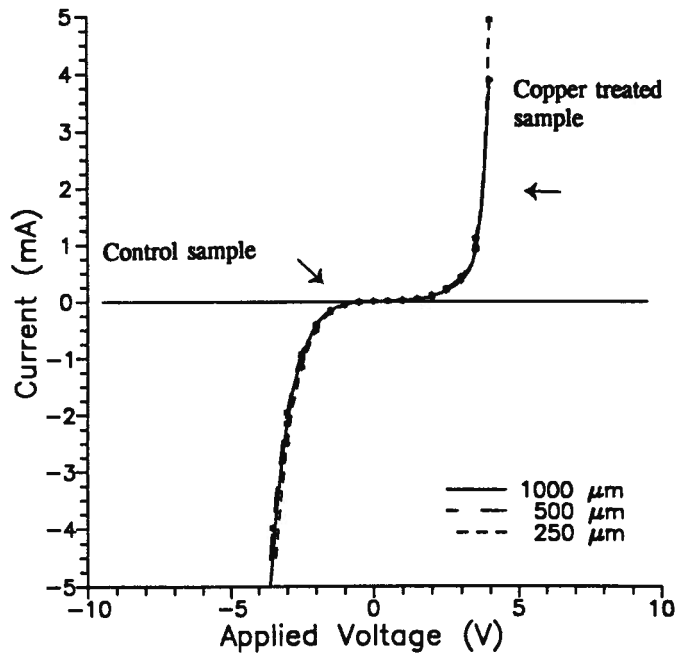
I-V Characteristics of Al Electrodes on GaAs Heated at 650°C for 23 s

5-7 (f)



I-V Characteristics of Al Electrodes on GaAs Heated at 750°C for 13 s

5-7 (g)



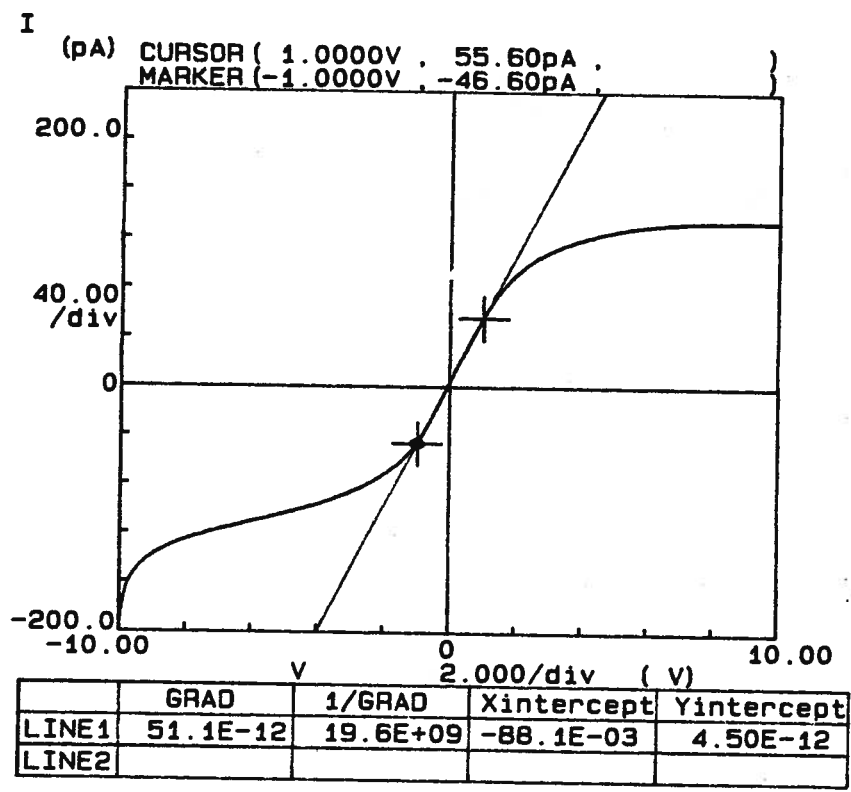
I-V Characteristics of Al Electrodes on GaAs Heated at 850°C for 5 s

5-7 (h)

In the plots given in Figure 5-7, there are three traces each for copper-treated and untreated specimens corresponding to measurements on electrodes separated by gaps of 250, 500 and 1000  $\mu\text{m}$ . It is apparent that, in most cases, the dependence of the conductivity on the separation between the electrodes is not clear. In many samples there are only very small variations in I-V characteristics with electrode spacing while in other samples, changes in the resistance do not reflect the changes in the electrode spacing. Again, this suggests that the contacts play a significant role in determining the current.

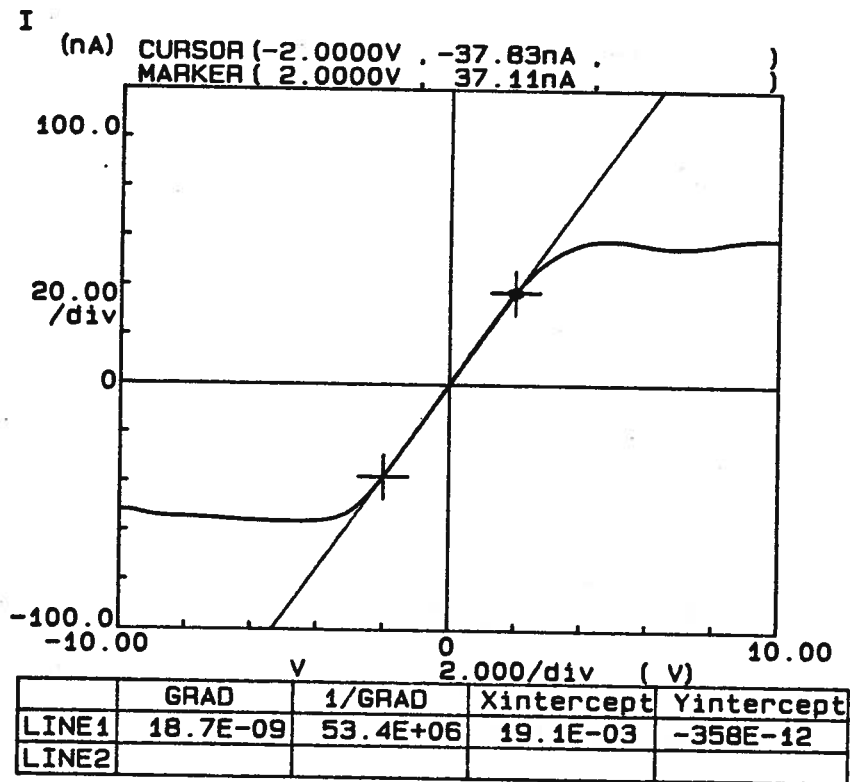
#### **5-3.2.5 Effect of Temperature on I-V behaviour**

The dependence of the I-V characteristics on temperature of the planar Al Schottky contact specimens was also studied. I-V measurements were made at 250, 300 and 350 K under illumination as well as in the dark. Two different LEDs, one with a wavelength of 670nm and the other with 932 nm were used to investigate the effects of using light energies above and below band gap energy. I-V plots of parallel Schottky electrodes on material heated at 550°C for 50 s with copper are given in Figure 5-8 at measurement temperatures of 250, 300, and 350K. The voltages at which the Schottky contact displays a linear I-V behaviour and the voltage where the current becomes less dependent on voltage is clearly affected by temperature. In some OTCS experiments the applied voltages are in this range.



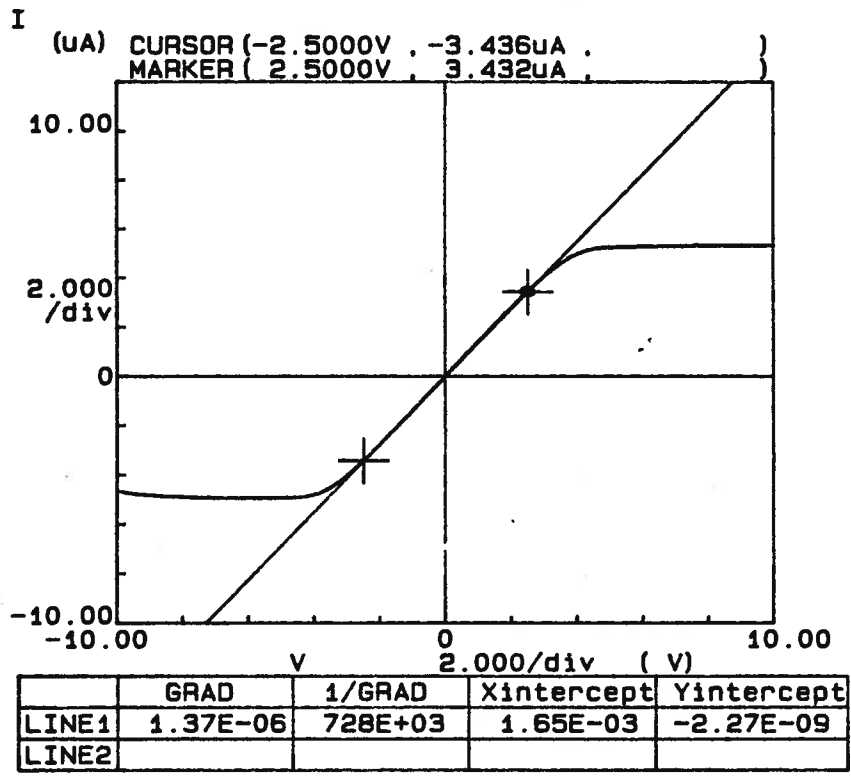
Control Sample Heated at 550°C, I-V Characteristics Measured at 250K

Fig. 5-8 (a)



Control Sample Heated at 550°C, I-V Characteristics Measured at 300K

Fig. 5-8 (b)

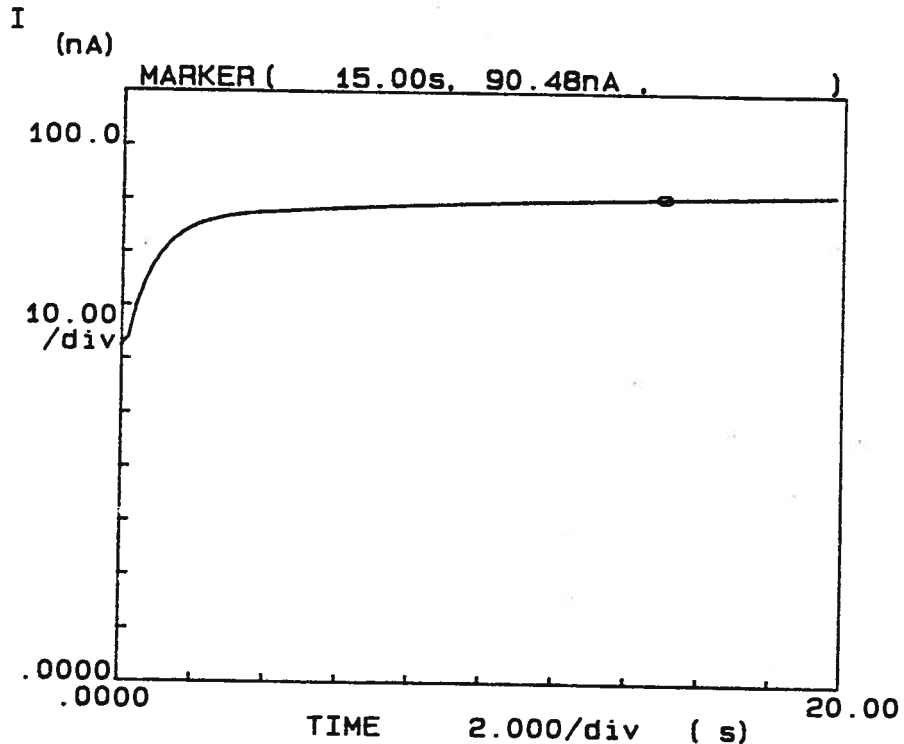


Control Sample Heated at 550°C, I-V, Characteristics Measured at 350K

Fig. 5-8 (c)

### 5-3.2.6 Temporal Variation in Current

In many of the samples which were examined, there was a significant time period required for the current to reach steady state after the application of voltage. In all of the measurements reported in previous sections, the voltages were applied for a sufficient period of time for the current to reach steady-state before collecting data. This suggests the build up of a space charge region. The changes in current after applying voltage were not always the same. In most cases the current increased with time but in some, the current decreased. In addition the magnitude of the increases or decreases varied significantly. Figure 5-9 shows the plot of the current as a function of time for a sample with Al electrodes.



Temporal Variation in the Current with Constant Applied Voltage

Fig. 5-9

#### 5-4.4.1 Parallel plate structures

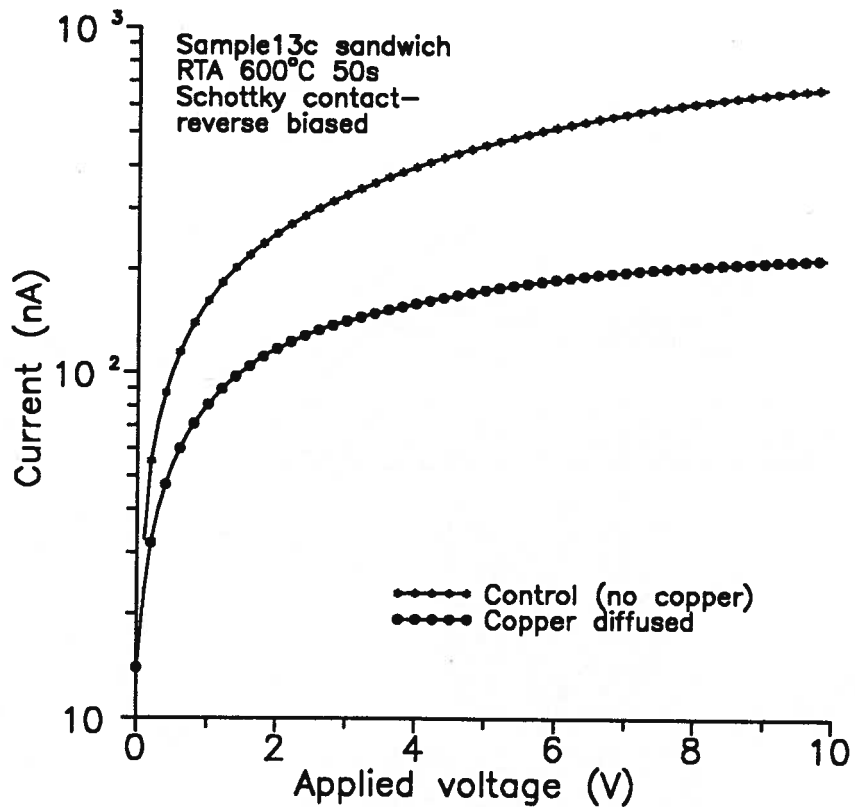
In these structures, the electrodes are on the opposing <100> faces of the wafer segment. One electrode is ohmic and the other Schottky. Both ohmic and Schottky contacts use the sample metal as used for the work on coplanar electrodes. The main differences between the two geometries are that the areas of the electrodes are larger and the direction of current flow is through the wafer rather than across. The Schottky electrode is semi-transparent and made from aluminium 80 to 100 Å thick and normally reverse biased for OTCS measurements. It has been found that biasing the electrodes in this fashion results in larger photocurrent to dark current ratios that are beneficial in increasing the signal to noise ratio in OTCS data[Hui, 1989].

In the OTCS apparatus used for this work the samples are illuminated from above. Due to reflections near the samples, the sides are also illuminated. To prevent a conductive path due to illumination between front and back electrode, the back ohmic contact did not extend to the edges of the sample. There was roughly one millimetre separation between the edges and the electrode. The front contact however covered the entire top surface of the specimen.

One concern, was the thermal stability of the thin semi-transparent Al electrode. During the temperature cycling of the specimen in OTCS measurements it was conceivable that the Schottky contact could degrade due to oxidation of the Al or reactions with the GaAs. It has been suspected that contact behaviour may change with repeated thermal cycling.

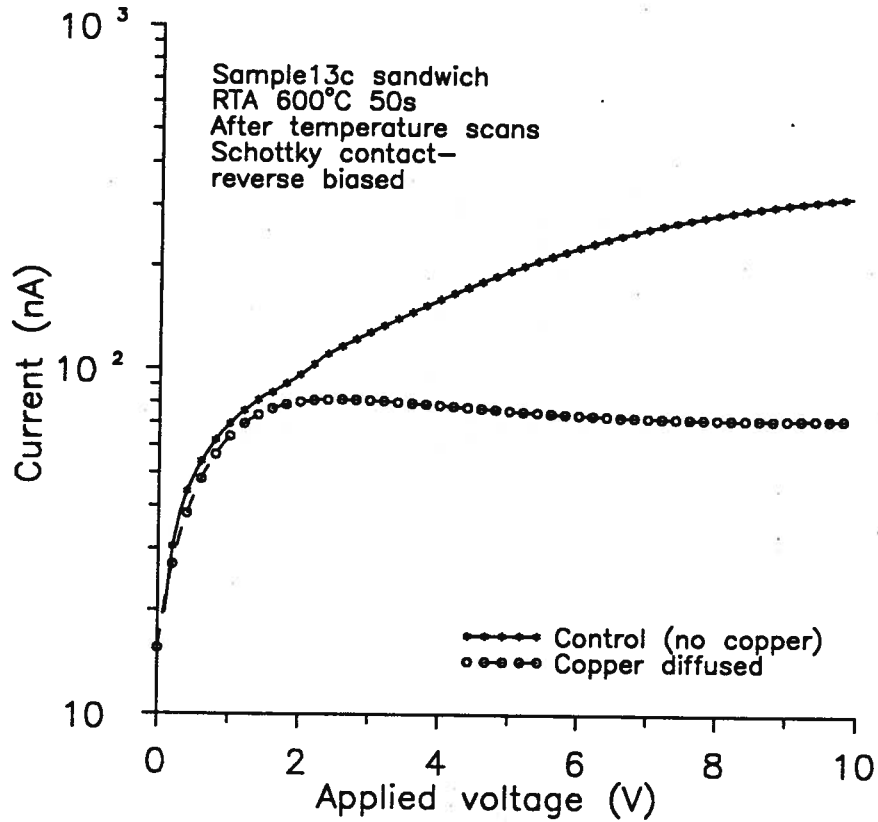
I-V measurements for these structures were made before and after eight

temperature cycles which consisted of cooling the samples to 250°C and then heating to 350°C. Although there were decreases in the current after the heating cycles, the I-V characteristics of the electrodes did not change significantly from cycle to cycle. This can be seen in the plots in Figures 5-10(a) and 5-10(b).



I-V Plot of Parallel Plate Samples Prior to OTCS Measurements

Fig. 5-10 (a)



I-V Plot of Parallel Plate Samples After OTCS Measurements

Fig. 5-10 (b)

**5-7 Conclusion**

The resistivity of the copper-diffused specimens were found to be highest in samples which were heated at temperatures near 550°C. In these samples, the resistivity of the copper-treated samples was higher than in samples not intentionally exposed to

copper during the heat treatment. This was found for all of the electrode geometries and metals which were examined.

In ohmic contacts, the resistance of the contacts was found to be much larger than the resistance due to the bulk material.

Linear I-V behaviour was observed for AuGe/Ni/Au contacts made to copper diffused regions prior to sintering. In the usual case this type of electrode displays rectifying characteristics before sintering and ohmic behaviour after, with an accompanying reduction in the contact resistance. This behaviour was not observed in the control samples. Moreover there was no apparent decrease in the resistance of the contacts on copper-treated material after sintering as is normally found. Similar contacts made to untreated regions were rectifying prior to and ohmic following sintering. In this section it is reported that electrodes routinely used in OTCS studies are not always ideal. In most cases, the change in temperature and the resulting change in the free carrier concentration result in marked changes in the contact characteristics.

In addition it was found that AuGe/Ni/Au ohmic contacts displayed a surprisingly high resistance. In the literature, these contacts are generally regarded as being of low resistance. In TLM studies, it was found that the contact resistance is likely to be a significant portion of the total resistance between the electrodes and the resistance of the bulk material may not be the main factor in determining the current flow. In addition the presence of copper in the GaAs increased the resistance significantly.

Schottky contacts of various spacings were also examined. There was relatively little change in I-V behaviour as electrode spacing increased from 250  $\mu\text{m}$  to 1000  $\mu\text{m}$ .

This too suggests that the contacts play a large role in limiting the current in the samples.

The contact regions would be expected to contain different defects and concentrations of defects than the bulk regions. Thus if the current is controlled largely by regions created due to the presence of electrodes, transients in the current and corresponding OTCS signals would not be due the release of carriers from bulk trapping levels.

Significant increases in sample resistance were found for samples which were diffused with copper at temperatures between 500°C and 650°C. It is suspected that much of this increase is due to a change in the contact resistance. It is probable that changes in the resistance to the bulk are also taking place but these changes were not apparent. Changes in the bulk would be expected to be quite complex. For example, it is well recognized that copper can compensate free n-type carriers by introducing several deep acceptor states[Blanc et. al., 1960],[Roush et. al., 1993]. However, copper has also been reported to complex with EL2 resulting in a decreased concentration of EL2 which could at the same time serve to increase the free electron concentration.

## Chapter 6

### Comparison of Non-scanning Optical Transient Current Spectroscopy Applied to Copper Doped and Undoped GaAs

#### 6-1 Non-scanning OTCS

Non-scanning OTCS experiments were carried out using a system developed by Hui, Backhouse and the author[Hui, 1989][Backhouse,1992]. It employs a MMR low temperature micro-positioner (model LTMP-3) cryogenic chamber. Samples up to 1.2 cm x 1 cm in size are placed on a temperature-controlled stage in a chamber which is evacuated to less than 10 mTorr using an adsorption pump. The range of temperatures accessible with the unit is from 80 K to 400 K, but in this work the range of temperature was intentionally limited to 250 K to 350 K, since this is the practical temperature range of the scanning system. In addition, limiting the scanning range saved time and the quantity of compressed ultra high purity nitrogen used per scan. The stage temperature is regulated using a combination of cooling by means of a Joule-Thompson refrigerator and heating with a resistive element heater.

The illumination for the stimulation was supplied by one of two LEDs, one with a centre frequency 660 nm and the other 935 nm. The current signals were measured using either a EG&G model 181 current sensitive preamplifier or a Keithley 427 current amplifier. The output of the current amplifier was then processed to separate the dark current and transient current information. This signal was then digitized using an appropriate gain using a Data Translation model DT-2828 A/D card and the data was then

stored in the memory of the PC. The illumination, sample temperature and the data collection were performed under the control of a PC.

This method stored one second of transient signal with a maximum temporal resolution of 50  $\mu$ s and amplitude resolution of 12 bits. This method, where all information of interest from a given transient signal is collected at once, has several advantages over methods reported in which temperature scans are repeated while stepping the values of the sampling times  $t_1$  and  $t_2$  to obtain a spectrum. The most significant disadvantage of repeating scans is that with repeated thermal cycling over temperatures ranging not infrequently from 77 K to 400K, the characteristics of the electrodes providing electrical contact to the sample could change which would mean that conditions for each scan were different. Moreover the effects of thermal cycling on the determination of a complete set of trap parameters could be found by repeating a measurement. Finally the amount of time and supplies such as the compressed nitrogen required were greatly reduced.

Since this work was intended to be used as an aid in the development of a scanning version of OTCS, the experimental conditions were varied such that there would be a continuity between measurements which were comparable to those reported in the literature and those which were used in the scanning experiments. In addition to characterizing the method, similar samples were examined using three different electrodes and two different wavelengths for the illumination. In addition, the effects of two different magnitudes of voltage applied across the electrodes were investigated. The objective of this strategy was to determine how the experimental conditions affected the

parameters of the deep levels which were detected.

### **6-1.1 Survey of Literature**

This section starts with a brief survey of the literature with regards to deep levels in SI GaAs and in particular, levels introduced by copper. Much of the work has focussed on studies of the chromium and EL2 levels. Both of these levels are used to compensate shallow levels to reduce the free carrier concentration at room temperature.

In LEC grown GaAs the major source of impurities is the graphite heaters used to melt the gallium and arsenic during the crystal pulling process. Carbon forms a shallow acceptor in GaAs. To compensate, EL2 a deep donor level, which involves an arsenic in a gallium site is introduced by growing the material under arsenic rich conditions. The concentration of EL2 is typically in the  $10^{15}$  /cm<sup>3</sup> range[Kirkpatrick et. al.,1985]. EL2 is reported to be located at about 0.82 eV from the conduction band with a capture cross section ranging from  $0.8-1.7 \times 10^{-13}$  cm<sup>2</sup>[Milnes, 1983].

In the material supplied by Johnson-Matthey levels due to EL2 were expected to be dominant. For the material which was doped with copper a number of additional levels could be expected. The most prominent copper level reported in the literature is located 1.36 eV from the conduction band. This level has been detected mainly by photoluminescence studies done at cryogenic temperatures. The band gap at this temperature is roughly 1.5 eV. This level is believed to be correlated with the acceptor level at 0.15 eV above the valence band. There have also been acceptor levels reported with energies ranging from 0.4 to 0.55 eV above the valence band due to copper.

A survey of copper levels found in the literature are given below. The energies reported are in reference to separation from the valence band.

Energy level	Reference	Material	$\sigma$ (cm <sup>2</sup> )
0.52	Tin et. al.,1989	Cu diff. SIB <sup>1</sup>	10 <sup>-17</sup>
0.44	Milnes, 1983	Cu doped LPE <sup>2</sup>	3.4 x 10 <sup>-14</sup>
0.42	Milnes, 1983	Cu diff. VPE <sup>3</sup>	3.0 x 10 <sup>-15</sup>
0.31	Venter, 1992	Cu diff. VPE	1.0 x 10 <sup>-16</sup>
0.41	Venter, 1992	Cu diff. VPE	2-3 x 10 <sup>-15</sup>
0.213	Zirkle, 1990	Cu diff. SIB	
0.14	Zirkle, 1990	Cu diff. SIB	
0.117	Zirkle, 1990	Cu diff. SIB	

<sup>1</sup> LPE (Liquid phase epitaxy)

<sup>2</sup> VPE (Vapour phase epitaxy)

<sup>3</sup> Semi-insulating bulk(SIB)

#### Copper Levels Reported in Literature

**Table 6-1**

Some of the differences in values for the energy can be attributed to differences in experimental method. For example it is believed that the capture cross section of the traps are dependent on electrical fields. In these studies, the electric field can be expected to vary significantly since the electrode geometries and the applied voltages are different. These differences have been reported to influence the determination of the energy level.

## **6-2 Experimental Results**

In the following section, OTCS results of copper diffused and untreated material are compared. Two methods of analyzing the OTCS data were used. In one a software equivalent of the double gated method was used to characterize the exponential parameters of the transient current. In the other a numerical fitting routine was used to fit sums of exponential terms to the transient while varying the amplitude and time constants of each of the terms.

Features observed in the OTCS spectra were different for both electrode materials and geometry. The differences in the spectra between different electrode configurations were found to be much larger than the differences between specimens. This was surprising since some of the samples were intentionally contaminated with copper.

In general there were relatively few peaks detected in the range of temperatures used. In the planar samples there were one or two peaks in the OTCS spectra with only minor negative transients which may have been due to noise in the signal or a small bias in the amplification system. Arrhenius plots of the peaks gave the expected linear dependence of  $\ln(1/T^2\tau)$  on  $1/T$ .

### **6-2.1 Co-planar Schottky Electrodes**

Using co-planar Schottky electrodes, there were noticeable changes in the OTCS spectra with changes in applied voltage and illumination wavelength. Three peaks were found in the spectra. For a time constant of 186 ms, the first was located between 260

K and 268 K, the second between 286 K and 298 K and the third near 320 K. For a applied bias of 7 V the peaks occurred at lower temperatures than in the spectra obtained with a bias of 2 V. The energy levels and capture cross sections determined from the temperature of the peaks and corresponding time constants in an Arrhenius plot are tabulated in Table 6-2. The parameters which were found in this work are comparable to those found in literature, however, a clear correlation between the levels found in this work and those reported other work could not be made. This is not surprising since it is well known that the determination of deep level parameters using DLTS methods is dependent on experimental conditions and reported results are rarely in agreement. In some of the spectra, the magnitude of the second peak between 286 K and 298 K was found to be larger for copper treated samples than for control samples. No separate peak due to copper was found.

Electrodes, illumination	Copper sample	Control sample
Schottky, visible, 2V	0.58 eV( $\sigma=5.5 \times 10^{-15} \text{cm}^2$ )	0.71 eV( $\sigma=5.1 \times 10^{-13} \text{cm}^2$ )
		0.46 eV( $\sigma=3.5 \times 10^{-16} \text{cm}^2$ )
Schottky, infra-red, 2V	1.1 eV( $\sigma=1.8 \times 10^{-8} \text{cm}^2$ )	
Schottky, visible, 7V	0.67 eV( $\sigma=6.6 \times 10^{-14} \text{cm}^2$ )	0.63 eV( $\sigma=2.9 \times 10^{-13} \text{cm}^2$ )
Schottky, infra-red, 7V	0.99 eV( $\sigma=6.2 \times 10^{-10} \text{cm}^2$ )	
	0.81 eV( $\sigma=1.2 \times 10^{-11} \text{cm}^2$ )	

Levels Detected Using Planar Al Electrodes and Double Gated Analysis

Table 6-2

### 6-2.2 Co-planar Ohmic Electrodes

In the OTCS data obtained using co-planar ohmic contacts there was less variation in the spectra than for Schottky electrodes. There were at most two distinct peaks per temperature scan. The first peak was found below 290 K and the other above 320 K for a time constants of 186 ms. There was also a shift in the position of the peaks with applied voltage, similar to that observed in experiments with aluminium electrodes. The energy and capture cross section calculated from this data are summarized in Table 6-3.

Electrodes, illumination	Copper sample	Control sample
ohmic, visible, 2V	0.67 eV( $\sigma=3.2 \times 10^{-13} \text{cm}^2$ )	0.70 eV( $\sigma=2.4 \times 10^{-12} \text{cm}^2$ )
		0.90 eV( $\sigma=2.0 \times 10^{-11} \text{cm}^2$ )
ohmic, infra-red, 2V	0.58 eV( $\sigma=5.0 \times 10^{-16} \text{cm}^2$ )	0.75 eV( $\sigma=3.3 \times 10^{-11} \text{cm}^2$ )
	0.82 eV( $\sigma=3.7 \times 10^{-11} \text{cm}^2$ )	
ohmic, visible, 7V		0.81 eV( $\sigma=1.5 \times 10^{-10} \text{cm}^2$ )
		0.86 eV( $\sigma=6.5 \times 10^{-12} \text{cm}^2$ )
ohmic, infra-red, 7V	0.73 eV( $\sigma=1.8 \times 10^{-12} \text{cm}^2$ )	0.69 eV( $\sigma=1.6 \times 10^{-14} \text{cm}^2$ )
	1.2 eV( $\sigma=2.3 \times 10^{-6} \text{cm}^2$ )	0.72 eV( $\sigma=6.4 \times 10^{-12} \text{cm}^2$ )

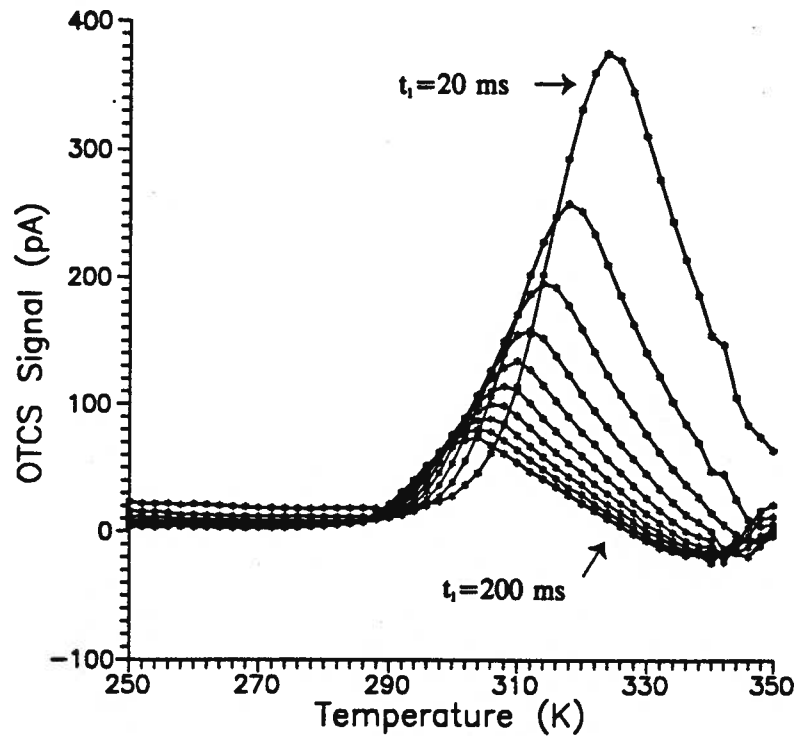
### Levels Detected Using Planar AuGe Electrodes and Double Gated Analysis

**Table 6-3**

### 6-2.3 Parallel Plate Electrodes

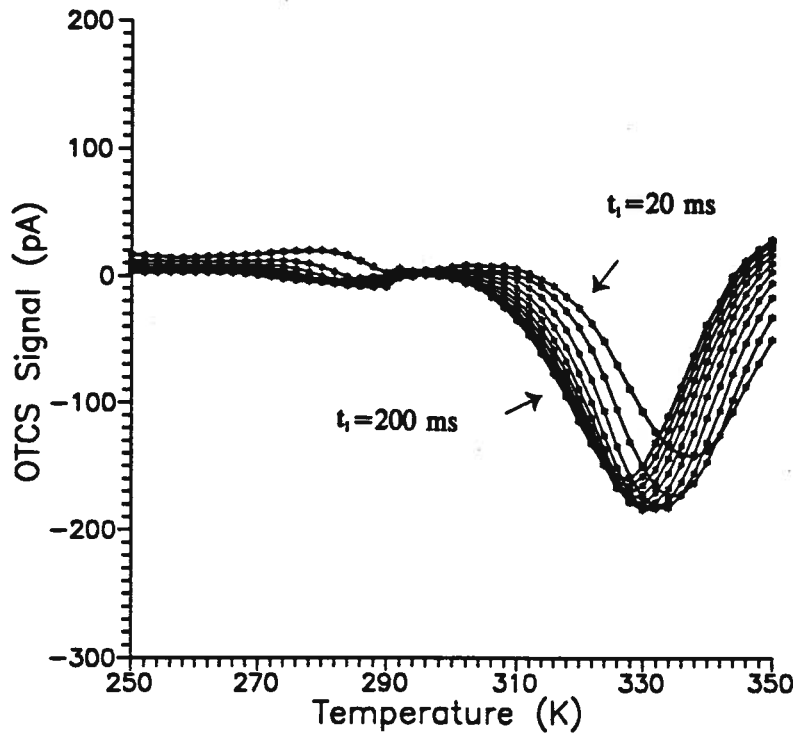
There was a marked difference in the spectra of copper diffused and untreated samples obtained using parallel plate electrodes. The negative peak dominated for samples which were not treated with copper. In the treated samples a positive peak which

was larger or of comparable magnitude to the negative peak was observed. Both positive peaks and negative peaks demonstrated a temperature dependence. Figure 6-1(a) and (b) show the signal versus temperature plots for copper treated and untreated sample respectively.



OTCS Spectra of a Copper treated Sample,  $t_2 = 5t_1$ ,  $t_1$  incremented in 20ms steps

Fig. 6-1 (a)



OTCS Spectra of a Untreated Sample,  $t_2=5t_1$ ,  $t_1$  incremented in 20 ms steps

**Fig. 6-1 (b)**

Illumination, $V_{\text{applied}}$	Copper sample	Control sample
Infra-red, 7V	0.73eV( $\sigma=3.97 \times 10^{-13} \text{ cm}^2$ )	1.12eV( $\sigma=3.18 \times 10^{-9} \text{ cm}^2$ )
Visible 3V		Neg. Peak. 1.30eV

Levels Detected Using Parallel Plate Electrodes and Double Gated Analysis

**Table 6-4**

#### **6-2.4 Effect of the illumination wavelength**

The absorption of light to create electron hole (e-h) pairs can be classified into two types. In the extrinsic case the energy of light,  $h\nu$ , is less than the band gap energy and most of the generation involves transitions between a band edge and deep levels. In this case the absorption coefficient of the light is quite small and the light penetrates an appreciable distance into the bulk. For light with a wavelength of 935 nm this was expected to be a few microns[Sze, 1981]. In the intrinsic case the carrier generation is dominated by band to band transitions. The associated absorption coefficient is large and the light is absorbed near the surface. For a wavelength of 660 nm the penetration depth of the light has been reported to be about 0.5  $\mu\text{m}$ .

#### **6-2.5 Negative transients**

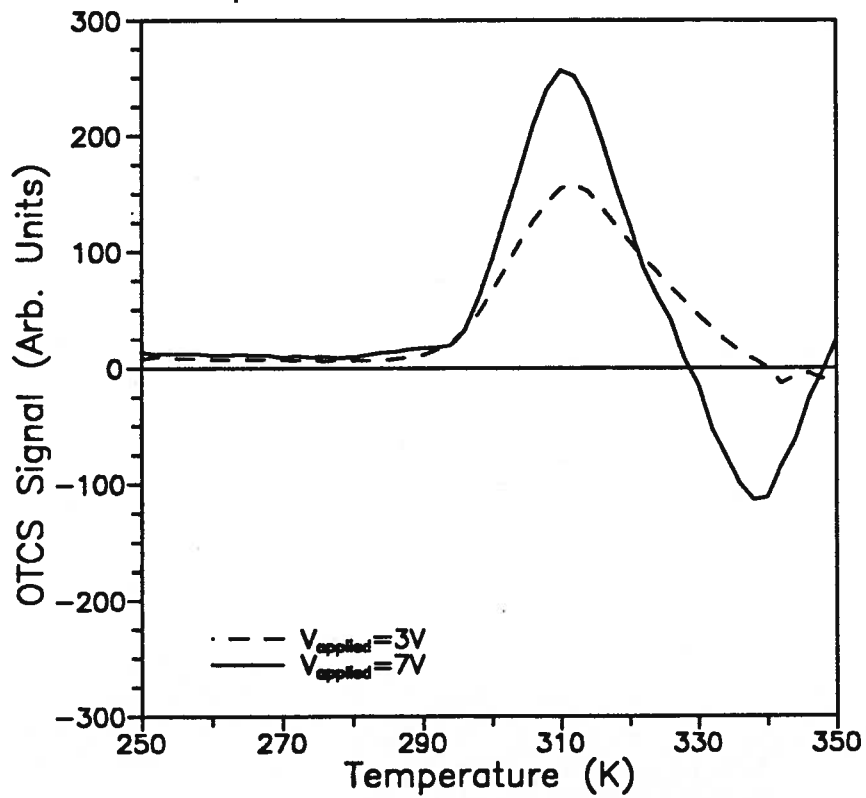
A negative transient is characterised by an initial decrease in the current following the removal of illumination which is then followed by an increase in the current. This feature was observed in all of the experiments conducted to some extent but was particularly noticeable with the parallel plate or "sandwich" structures. The cause of a negative peak in OTCS studies has been a topic of some controversy in the literature. For example it was claimed by Blight et. al., 1986, that negative peaks were due to charge exchange with surface states. However in work reported by Young et. al., 1986, and in this work, negative transients were found in structures in which the illuminated surface was completely covered with the metal. In such cases it is unlikely that there would be

a exchange of charge with surface states. Two other possible cause for the negative peak as proposed by Young et. al., 1986, are contained in the neutral semiconductor model and the in the insulator model. In addition, in work by Hui, 1989, the conditions under which negative peaks could occur were defined. In addition, a correlation was made between surface abrasion and the occurrence of the negative peak. In the neutral semiconductor model, it is assumed that charge neutrality is always maintained in the bulk of the sample with the contacts supplying the required carriers to maintain this neutrality.

In this work negative peaks were dominant only in the sandwich electrode structures and only occurred at temperatures above 310 K. The magnitude of the transient was dependent both on illumination, applied voltage and the presence of copper. ( In addition the spectra that was observed was qualitatively similar to the results obtained by Martin et. al., 1978, in which the samples were much thinner.) This suggests that the transient at least in the sandwich structure may be strongly affected by conditions near the surface.

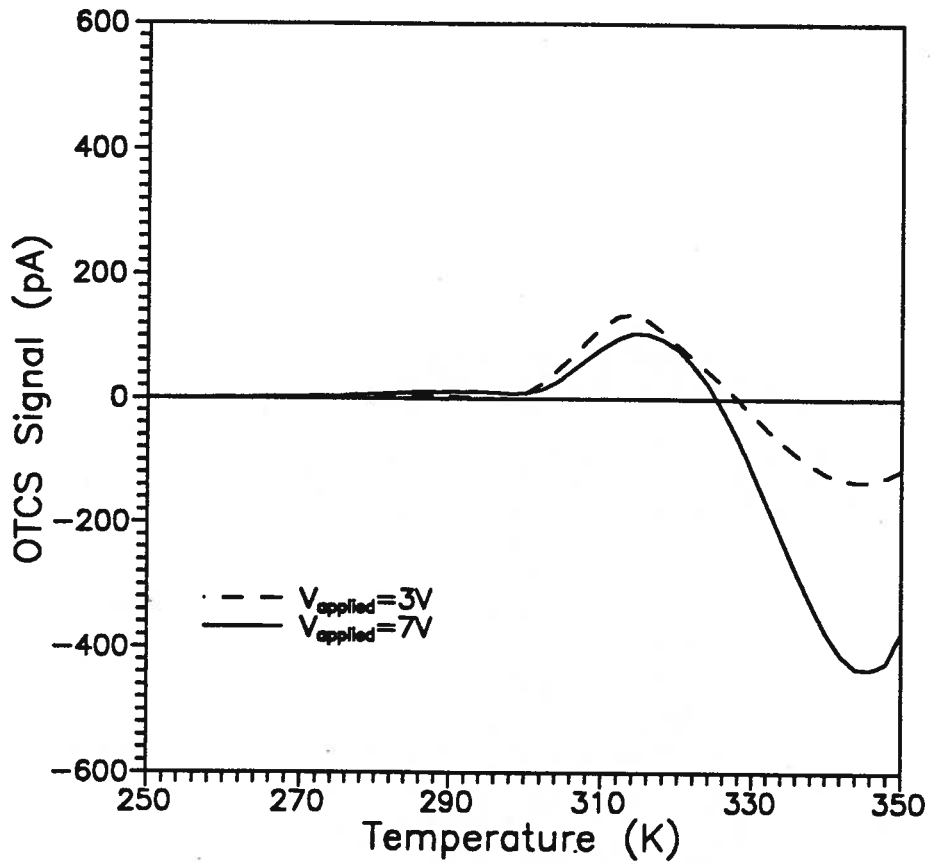
The magnitude of the negative transient peak with respect to the magnitude of the positive peaks was dependent on both applied voltage and the frequency of light used to generate carriers. In the copper-treated case, the magnitude of the transient was much larger. In Figure 6-2(a) are plots of the magnitude of the signal from the double gated analysis with respect to temperature for an OTCS scan carried out using 935 nm illumination with reverse bias voltages of 3 and 7 volts. With smaller applied voltages the magnitude of the peak due to the negative transient is much smaller relative to the positive peak than in the scan with the higher applied voltage. This was also found with

the visible 660 nm illumination, however the positive peaks were reduced even further. This is illustrated in Figure 6-2(b). In the case of the larger reverse bias, the depletion layer is larger which should presumably reduce the effect of the semi-insulating region. The change in depletion depth between the two applied voltages is expected to be in the order of microns.



Change in OTCS Spectra with Applied Voltage for 935 nm Illumination

Fig. 6-2 (a)



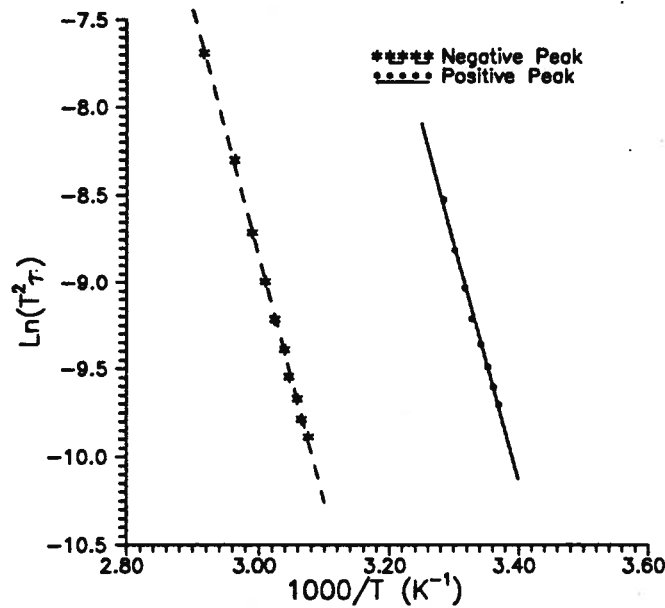
Change in OTCS Spectra with Applied Voltage for 660 nm Illumination

Fig. 6-2 (b)

Therefore it is more likely that differences in magnitude are due to mechanisms which take place in the depletion layer.

The negative peak also displayed a temperature dependency, as shown in the Arrhenius plot of Figure 6-3. Although the conventional concepts of activation energy are not meaningful, they were nevertheless calculated to determine what effect the negative peak could have on the determination of energies of the positive peaks. The

parameters for the negative peak were found to be 1.21eV with a capture cross section of  $1.3 \times 10^{-13} \text{ cm}^2$ . In many cases where a strong negative peak was observed, at certain temperatures the negative peak reduces the magnitude of the positive peak. In these regions any dependence of the positive peak position on temperature is likely to be distorted by the temperature dependence of the negative peak.



Arrhenius Plot for a Negative Peak

Fig. 6-3

To summarize, it was found in samples with sandwich structure electrodes that the relative magnitude of the negative peak to the positive peaks were higher for visible illumination and higher applied voltages. In addition the negative peaks for copper treated material were also larger in magnitude.

### 6-2.6 Exponential Fitting

Although the numerical fitting of exponential functions to data has the potential for higher resolution than a double-gated analysis as described above, there were difficulties encountered in using this method in this work. For the range of temperatures used in this work the number of peaks were few and relatively easy to distinguish using a double-gated method. Due to the sensitivity of the exponential fitting method, there were difficulties in analyzing data by using just the  $\chi^2$  values as an indicator of the fit. In most cases by fitting 3 to 6 terms to any given transient, the difference between the fitted function and the data could be reduced to a level comparable to the background noise in the collected signal. However, the terms which were fitted in this manner did not always follow a linear relation with respect to temperature when displayed on an Arrhenius plot. Moreover, the range of temperatures over which the relation was linear was found to be smaller than in the double gated-analysis. Furthermore, the temperature dependence of the time constant was such that there were several distinct lines with similar slopes. Physically this would correspond to several traps with similar energies but different capture cross sections. Also, the trap parameters obtained using this method were not consistent. For example, fitting a larger number of terms resulted in a better fit than using fewer terms, but the energy levels detected were found not to correspond with the fit using a smaller number of terms.

In conclusion, it was found that the application of the exponential fitting was not as easily applied as the double-gated method.

### 6-3 Conclusion

It was found that there were only a few peaks in the samples which were examined. The reasons for this may be that the more recently manufactured GaAs used in this work contains fewer defects in comparison to material used in previous studies.

Several characteristics of the negative peak were examined by altering the sample-electrode geometry, electrode material, copper contamination, and using two LED light sources with different wavelengths to stimulate free carrier generation. It was found that the negative peak was more prominent in the samples with parallel plate electrodes. In addition the relative magnitude of the negative peak with respect to the positive peak was also dependent on the applied field as well as the wavelength of the illumination which was used. Moreover, in comparing the double-gated with the exponential fitting routine, it became apparent that the transient signals were not exponential. This has been a recurring source of difficulty in much of the reported work. It was found that although good fits could be obtained by summing up to six exponential terms, the trap parameters which were collected were not always physically realistic. A possible explanation may be that there exist non-exponential components in the signal which vary in magnitude in proportion to the transient signal. Checks were made on the amplifiers, but no anomalies were found.

In further work, the possible sources for non-exponential components of the transient should be investigated. This would involve studies of the measurement apparatus as well as other current transport mechanisms such as surface current and surface recombination of carriers in the specimen.

## Chapter 7

### Conclusion and Suggestions for Future Work

In this work, many aspects of OTCS measurements which would need to be addressed in using OTCS to measure the spatial distribution of deep levels were examined. The choice of structure to be used in the scanning system was a parallel plate structure with a semi-transparent top electrode, as has been used in numerous OTCS studies. A comparative study of deep level trap parameters obtained using a variety of geometric variations of electrodes as well as different electrode materials was carried out. It was found that the contact characteristics play a significant role in the determination of trap parameters.

Variations in the OTCS signals were imaged and features comparable in size to dislocation networks imaged using CL were observed. However, the OTCS signals obtained using the scanning system were found to be different to those reported in previous work. To calibrate the system, copper was diffused into SI LEC GaAs to preferentially introduce deep levels in test samples. These were compared to control samples which were not exposed to copper. The diffusion of copper in GaAs was monitored using CL contrast imaging and observing changes in the I-V characteristics of specimens. Although copper diffuses into GaAs readily at higher temperatures it was found to be difficult to introduce an appropriate amount so that there would be a measurable increase in deep levels due to copper but not drastically alter the gross

material properties of SI GaAs. It was found that for samples exposed to copper at temperatures less than approximately 700°C there was a marked increase in the resistivity of the specimens. Much of this change was due to increases in contact resistance. This was found for both ohmic and Schottky electrodes.

It was found that the trap parameters obtained using OTCS measurements were sensitive to geometry and metal used in the experiment. This was especially apparent in the presence of a negative transient. It was found to increase with increasing applied voltage in the reverse bias direction. The negative transient was also larger for visible illumination which did not penetrate the sample beyond the depletion layer. This suggests that mechanisms other than those proposed in the neutral semiconductor model by Young et. al., 1986 and charging of surface states reported by Blight et. al., 1988, may be responsible.

In retrospect the choice of using levels due to copper as a means of calibrating a system to measure deep level traps was not efficient. Due to the complex nature of copper diffusion in GaAs a wide range of energy levels is possible. Moreover, copper has been reported to complex with other levels thus possibly reducing the signature of other levels as well as introducing new ones. Other choices such as the E3 electron level reported to be associated with the ion-implantation of protons in GaAs[Blood, 1992] may have provided a simpler case. Also by using an ion implantation process in conjunction with a masking procedure, the spatial distribution of the levels may have been more controllable than using a diffusion-based process. In addition since fewer process steps are required it may have been easier to control the experimental parameters from sample

to sample.

Other studies which may be of interest include using a variety of wavelengths of illumination in the scanning beam. To optimize the resolution of the system both spatially and with respect to energy, both the effects of sample size, beam size and intensity should be examined.

Experiments with a scanning beam could be performed on planar structures to determine if the contribution to the OTCS signal from all areas between the electrodes are equally weighted or dependent on the position with respect to the electrodes. In addition improved methods of forming contacts to SI material should be investigated. Methods which may be useful include creating a graded dopant profile such that there is a more gradual gradient than for diffused Ge layers in AuGe contacts.

## References

- Backhouse, C., Hui, D., Young, L., Comparison of Isothermal and Boxcar Methods of Analysis of Photocurrent Transients, *Semicond. Sci. Technol.* Vol. 7, 1992.
- Berger, H.H., Contact Resistance and Contact Resistivity, *J. Electrochem. Soc.: Solid State Science and Technology*, Vol. 119, No. 4, 1972, p. 507-514.
- Blanc, J., Bube, R.H., MacDonald H.E., Properties of High-Resistivity Gallium Arsenide Compensated with Diffused Copper, *J. Appl. Phys.*, Vol. 12 No. 9, 1961, p. 1666-1679.
- Blight, S.R., Page, A.D., Ladbrooke, P.H., Thomas, H., Detection of EL2 in Undoped LEC GaAs by a Novel Variation of Photo-induced Transient Spectroscopy, *Jpn. J. Appl. Phys.*, Vol. 26 No. 8, 1987, p. 1388-21389.
- Blight, S.R., Thomas, H., Investigation of the Negative Peak in Photoinduced Transient Spectroscopy of Semi-insulating Gallium Arsenide, *J. Appl. Phys.*, Vol. 65 No. 1, 1989, p. 215-226.
- Blood, P., Orton, J.W., *The Electrical Characterization of Semiconductors: Measurement of Minority Carrier Properties*, 1992, Academic Press, Toronto.
- Blood, P., Orton, J.W., *The Electrical Characterization of Semiconductors: Majority Carriers and Electron States*, 1990, Academic Press, Toronto.
- Breitenstein, O., Heydenreich, J., Scanning Deep Level Transient Spectroscopy(SDLTS), *Scanning*, Vol. 7, 1985, p.273-289.

- Breitenstein, O., Giling, L.J., Scanning-DLTS Investigations on Semi-Insulating GaAs:Cr,In Containing "Streamers", *Phys. Stat. Sol. (a)* Vol. 99, 1987, p. 215-223.
- Bube, R.H., *Photoelectronic Properties of Semiconductors*, Cambridge University Press, Cambridge, 1992.
- Chin, A.K., Camlibel, I., Caruso, R., Young, M.S.S., Von Neida, A.R., Effects of Thermal Annealing on Semi-insulating Undoped GaAs Grown by the Liquid-encapsulated Czochralski Technique, *J. Appl. Phys.* Vol. 57 No. 6, 1985, p. 2203-2209.
- Dobrilla, P., Blakemore, J.S. Experimental Requirement for Quantitative Mapping of Midgap Flaw Concentration in Semi-insulating GaAs Wafers by Measurement of Near Infra-red Transmittance, *J. Appl. Phys.* Vol. 58 No. 1, 1985, p. 208-218.
- Eckstein, M., Jakubowicz, A., Bode, M., Habermeiner, H.U., Temperature Dependence of Electron Beam Induced Current and Cathodoluminescence Contrast of Dislocations in GaAs, SPIE, Vol. 1284, *Nanostructures and Microstructure: Correlation with Physical Properties of Semiconductors*, 1990, p.228-236.
- Fang, Z., Lei, S., Schlesinger, T.E., Milnes, A.G., Photo-induced Transient Spectroscopy PITS Study on LEC Grown Semi-insulating GaAs, *Solid State Electron.* Vol. 32, No. 5, 1989, p.405-411.
- Fuller, C.S., Whelan, J.M. Diffusion, Solubility and Electrical Behaviour of Copper in Gallium Arsenide, *J. Phys. Chem. Solids* Vol. 6, 1958, p. 173-177.
- Fuller, C.S., Wolfstim, K.B., Allison, H.W., Hall-Effect Levels Produced in Te-Doped GaAs Crystals by Cu Diffusion, *J. Appl. Phys.* Vol. 38, No. 7, 1967 p. 2873-2879.

- Grove, A. S., *Physics and Technology of Semiconductor Devices*, 1967, John Wiley & Sons, New York.
- Hall, R.N., Racette, J.H., Diffusion and Solubility of Copper in Extrinsic and Intrinsic Germanium, Silicon and Gallium Arsenide, *J. Appl. Phys.* **35** (2), 1964, p.397-379.
- Hiramoto, T., Ikoma, T., The Source of Copper in Commercial Semi-insulating GaAs Wafers, 5th Conference on Semi-insulating III-V Materials, Malmö, Sweden, 1988, Institute of Physics Publishing, Bristol, p.337-342.
- Holt, D.B., An Introduction to Multimode Scanning Electron Scanning Microscopy, *SEM Microcharacterization of Semiconductors*, Holt, D.B., Joy, D.C., Editors, 1989, Academic Press, Toronto.
- Hui, D.C.W., *Characterization of Semi-insulating Liquid Encapsulated Czochralski Gallium Arsenide for Device Fabrication*, Ph. D. Thesis, 1989, U.B.C.
- Hui, D., Kato, H., Backhouse, C., Young, L., Effects of Electrode Geometry and Polarity on the Occurrence of Negative Peaks in Optical Transient Current Spectroscopy Applied to Semi-insulating Gallium Arsenide, *Journal of Electronic Materials*, Vol. 21, No. 9, 1992, p. 902-909.
- Jahn, U., Menninger, H., The Influence of Copper on the Change of Cathodoluminescence in Semi-insulating LEC GaAs After Rapid Thermal Processing, *Phys. Stat. Sol.* (a) Vol. 128, 1991, p.145-152.
- Jaros, M., *Deep Levels in Semiconductors*, 1982, Adam Hilger Ltd, Bristol.

- Jay, P. R., Device Applications of III-V Materials: The Changing Demand, *Semi-insulating III-V Materials*, Proceedings of the 7th conference on semi-insulating III-V materials, 1992, Institute of Physics Publishing, Bristol, p.1-10.
- Kang, N.S., Zirkle, T.E., Schroder, D.K., A Stress Gettering Mechanism in Semi-insulating, Copper Contaminated, Gallium Arsenide, *J. Appl. Phys.*, Vol. 72 (1), 1992, P. 82-89.
- Kimpel, B.M., Schulz, H.J., Cathodoluminescence of Copper-doped GaAs and Its Relation to EL2 Centres, *Phys. Stat. Sol. (b)*, Vol. 174, 1992, p. 583-591.
- Kullendorff, N., Jansson, L., Ledebø, L.Å., Copper-related Deep Level Defects in III-V Semiconductors, *J. Appl. Phys.* Vol. 54, No. 6, 1983, p. 3202-3212.
- Larabee, G.B., Osborne, J.F., Anomalous Behaviour of Copper During Acceptor Diffusion into Gallium Arsenide, *J. Electrochem. Soc.*, Vol. 113, No. 6, 1966, p. 564-567.
- Lehovec, K., Pao, H., Built-in Space Charge at Junctions Between Heavily Doped and Semi-insulating GaAs Layers, *Solid-State Electron.* Vol. 31 No. 9, 1988, p.1433-1440.
- Look, D.C., *Electrical Characterization of GaAs Materials and Devices*, 1989, John Wiley & Sons, Toronto.
- Macquistan, D.A., *The Behaviour of Copper on Gallium Arsenide*, M.A.Sc. Thesis, 1989, U.B.C.

- Mares, J.J., Smid, V., Kristofik, P., Hubik, Sarapatka, T., Deep Levels in Semi-insulating GaAs Determined by PICTS and SCLC, 5th Conference on Semi-insulating III-V Materials, Malmö, Sweden, 1988, Institute of Physics Publishing, Bristol, p. 171-176.
- Martin, G.M., Bois, D., A New Technique for the Spectroscopy of Deep Levels in Insulating Materials, Application to the Study of Semi-insulating GaAs, *Semiconductor Characterization Techniques*, Proceedings of the Electrochemical Society, Vol. 78, No. 3, 1978, p.32-42.
- Milnes, A.G., Impurity and Defect Levels (Experimental) in Gallium Arsenide, *Advances in Electronics and Electron Physics*, Vol. 61, 1983, p. 63-160.
- Mitonneau, A., Martin, G.M., Mircea, A., Hole Traps in Bulk and Epitaxial GaAs Crystals, *Electronics Letters*, 1977, Vol. 13, No. 22, p. 666-667.
- Mitonneau, A., Martin, G.M., Mircea, A., Electron Traps in Bulk and Epitaxial GaAs Crystals, *Electronics Letters*, 1977, Vol. 13, No. 22, p. 664-666.
- Moore, W.J., Henry, R.L., Saban, S.B., Blakemore, J.S., EL2-copper Interaction in Heat Treated GaAs, *Physical Review B*, Vol. 46, No. 11, 1992, p. 7229-7231.
- Morrow, R.A., Influence of Dislocations and Annealing Cap on the Electrical Activation of Silicon in Semi-insulating GaAs: Implications for Field Effect Transistors, *J. Appl. Phys.* Vol. 64, No. 11, 1988, p.6254-6258.
- Palmstrøm, C.J., Morgan, D.V., Metallizations for GaAs Devices and Circuits, *Gallium Arsenide*, Howes, M.J., Morgan, D.V., Editors, 1985, John Wiley and Sons, Toronto.

- Reeves, G.K., Harrison, H.B., Obtaining the Specific Contact Resistance from Transmission Line Model Measurements, *Electron Device Letters*, Vol. EDL-3, No. 5, 1982, p. 111-113.
- Roush, R.A., Mazzola, M.S., Stoudt, D.C., Infrared Photoconductivity via Deep Copper Acceptors in Silicon-Doped, Copper-compensated Gallium Arsenide Photoconductive Switches, *IEEE Trans. Electron Devices*, Vol. 40, No. 6, 1993, p. 1081-1086.
- Sandroff, C.J., Nottenburg, R.N., Bischoff, J.C., Bhat, R., Dramatic Enhancement in Gain of a GaAs/AlGaAs Heterostructure Bipolar Transistor by Surface Chemical Passivation, *Appl. Phys. Lett.* Vol. 51, No. 1, 1987, p.33-35.
- Sze, S.M., *Semiconductor Physics*, 1981, John Wiley and Sons, Toronto.
- Third, C.E., Weinberg, F., Young, L., Examination of Rapid Thermal Annealed GaAs Using Cathodoluminescence, *Applied Physics Letters*, Vol. 54, No. 26, 1989, p. 2671-2673.
- Third, C.E., *The Effects of Short Term Anneals on the Cathodoluminescence of GaAs*, Ph. D. Thesis, 1989, University of British Columbia, Vancouver.
- Tin, C.C., Teh, C.K., Weichman, F.L., Photoinduced Transient Spectroscopy and Photoluminescence Studies of Copper Contaminated Liquid-encapsulated Czochralski-grown Semi-insulating GaAs, *J. Appl. Phys.* Vol. 62, No. 6, 1987, p. 2329-2336.
- Tin, C.C., Teh, C.K., Weichman, F.L., States of Copper During Diffusion in Semi-insulating GaAs, *J. Appl. Phys.* Vol. 63, No. 2, 1988, p. 355-359.-

- Tuck, B., *Atomic Diffusion in III-V Semiconductors*, 1988, Adam Hilger, Philadelphia.
- Venter, A., Auret, F.D., Ball, C.A.B., Electrical Characterization of Cu-Diffused n-GaAs Epitaxial Layers Using Deep Level Transient Spectroscopy, *J. Electron. Mater.* Vol. 21, No. 9, 1992, p. 877-882.
- Williams, R., *Modern GaAs Processing Methods*, 1990 Artech House, Massachusetts.
- Willmann, F., Blatte, M., Queisser, H.J., Treusch, J., Complex Nature of the Copper Acceptor in Gallium Arsenide, *Solid State Communications*, Vol. 9, 1971, p. 2281-2284.
- Yacobi, B.C., *Cathodoluminescence Microscopy of Inorganic Solids*, Plenum Press, 1990, New York.
- Young, L, Tang, W.C. Dindo, S., Lowe, K.S., Optical Transient Current Spectroscopy for Trapping Levels in Semi-insulating LEC Gallium Arsenide, *J. Electrochem. Soc.: Solid-State Science and Technology* Vol. 133, No. 3, 1986, p. 609-619.
- Young, M.L., Hope, D.A.O., Brozel, M.R., Electrical Inhomogeneity in 1" Partially Dislocation Free Undoped LEC GaAs, *Semiconductor Science and Technology*, Vol. 3, 1988, p.292-301.
- Yoshie, O., Kamihara, M., Photo-induced Current Spectroscopy in High Resistivity Bulk Material. I. Computer /Controlled Multi-channel PICTS System with High Resolution, *Jpn. J. Appl. Phys.*, Vol. 22, No.4, 1983, p. 621-628.

Yoshie, O., Kamihara, M., Photo-induced Current Spectroscopy in High Resistivity Bulk Material. III. Scanning-PICTS System for Imaging Spatial Distributions of Deep-Traps in Semi-insulating GaAs Wafers, *Jpn. J. App. Phys.*, Vol. 24, No. 4, 1985, p. 431-440.

Zirkle, T.E., Kang, N.S., Schroeder, D.K., Roedel, R.J., Comparison of Electrical and Optical Characterization in Cu-gettered, Semi-insulating GaAs, *Nanostructures and Microstructure Correlation with Physical Properties of Semiconductors*, Proceedings of the SPIE, 1990, p. 249-257.

## Appendix A

### Fabrication Procedure

#### Specimens for Cathodo luminescence Studies

1. Scribe wafers and cleave into approx. 1cm x 0.5 cm sections.
2. Immerse samples in 8:1:1\H<sub>2</sub>SO<sub>4</sub>:H<sub>2</sub>O<sub>2</sub>:H<sub>2</sub>O for 1min to etch approximately 1 $\mu$ m from surface.
3. Rinse samples in cascade DI water bath for 10 min.
4. Rinse in hot isopropyl alcohol for 5 min and blow dry using N<sub>2</sub>.
5. Spin on Shipley S1400-27 photo-resist @ 4000 rpm, bake at 70°C for 20 min.
6. Expose approximately one half of the sample to U.V. using a cleaved silicon wafer as a mask.
7. Soak in chlorobenzene for 8 min and blow dry. Develop in Shipley MF-319 developer for 2-3 min.
8. E-beam evaporate 100-200 Å of Cu using Veeco Vacuum chamber.
9. "Lift-off" Cu film by soaking in warm acetone. Rinse in isopropyl alcohol.
10. Encapsulate both faces of wafer with silicon nitride using Plasma-therm PK-1250 PECVD/Plasma Etch system.
11. Heat using AG Associates RTA or Mini-brute furnace.
12. Remove silicon nitride and cleave wafer and mount on SEM specimen holder.

#### Specimens for OTCS/I-V Studies

1. Perform steps 1 through 11 from above list.
2. Remove silicon nitride using Buffered Hydrofluoric Acid. Rinse in DI

cascade bath for 10 min.

3. Immerse in warm isopropyl alcohol and blow dry with N<sub>2</sub>.
4. Cleave samples in half.
  
5. Spin on Shipley S1400-27 positive photoresist on back side of wafer for "Sandwich" electrode specimens and front side for planar ohmic electrode specimens at 4000 rpm for 40 s and bake at 70° C for 20 min.
6. Expose using AuGe electrode mask. Repeat steps 6 and 7 from previous procedure.
7. Deposit approx. 2000Å AuGe, 200Å Ni, 1000Å Au. "Lift-off metal using warm acetone and isopropyl alcohol.
8. Heat in Mini-brute furnace for 2 min at 435° C.
9. Deposit 80-120Å of Al on "Sandwich" samples.
10. Repeat steps 4 and 5 above using Al electrode mask with planar Schottky electrode samples. Mask off "Sandwich" specimens using glass slide to evaporate probing strip.
11. "Lift-off" Al using warm acetone and isopropyl. Blow dry using N<sub>2</sub>.

## Appendix B

```
/* ----- */
/*           Scanning OTCS Program           */
/*                                           */
/* This program controls the micromanipulator and performs data */
/* acquisition. The micromanipulator must be connected to the IEEE 488 card.*/
/* The current transient signal must be connected to A/D */
/* channel 0. The file created by the program can be input */
/* into the SURFER plotting program as an ASCII text file. */
/* ----- */
```

```
#include <stdio.h>           /* standard io header file           */
#include <math.h>            /* math functions header file        */
#include <conio.h>           /* inp(), outp() header files        */
#include <stdlib.h>          /* standard library header file      */
#include <graphics.h>        /* graphics header file              */
#include <string.h>
#include <alloc.h>
#include <bios.h>
#include <dos.h>
#include "c:\cec\ieee-c.h"   /* use local version (Turbo C specific) */
#include "c:\atlc\atldefs.h"
#include "c:\atlc\atlerrs.h"
#define reference 0
#define crntchan 1
#define reflect 2
#define positive 1
#define negative 0
#define micro_add 30
#define gpib_add 21
double xlength, ylength;
double x, y;                /* dimensions of rectangular scan area */
AL_CONFIGURATION configuration;
float convert, darkcurrent, reflectance;
float diff, netphoto,transient,photocurrent;
unsigned numdat =200;
int list[512],*buffadd,usable,offset;
int i, j, jj, buffnum,scan_count,channel_count;
int channels[16]={0};
int gains[16]={1};
int readings,t1,t2;
DEV_FLAGS device_flags;
```

```

float period = 5e-4;          /*time between samples*/
/*.....*/
void init_a_d()      /* sets up a/d card*/
{
    int i,j;
    AL_INITIALIZE();
    AL_SELECT_BOARD(1);
    AL_RESET();
    AL_GET_CONFIGURATION(&configuration);
    AL_SET_PERIOD(period);
    scan_count=1;
    AL_FIND_DMA_LENGTH(list,&usable);
    fprintf(stdprn,"usable=%d ",usable);
    fprintf(stdprn,"starting address of list =%p\n ",list);
    DUMP_CONFIGURATION();
    if (usable > numdat)
        { buffadd=list;
          offset=0;
        }
    else
        { buffadd=list+1+usable;
          offset=1+usable;
        }
    AL_DECLARE_BUFFER(&buffnum,&(list[offset]),numdat);
    AL_LINK_BUFFER(buffnum);
    AL_SETUP_ADC(2,1,channels,gains);
    fprintf(stdprn,"offset= %d\r\n ",offset);
    } /* end init_a_d */
/*.....*/

void doburst(float *diff,float *netphoto) /*takes a set of readings*/
{
    AL_BURST_ADC();
    AL_WAIT_FOR_COMPLETION(buffnum);
    AL_RELEASE_BUFFER(1,&buffnum);
    for(i=offset; i <(offset+ numdat); i++) /* fprintf(stdprn,"%u ",list[i]);*/
    for(i=1;i<199;i++) /* fprintf(stdprn,"%u ",list[i]);*/
    *diff=(float)list[offset+t1]-(float)list[offset+t2];
    *netphoto=(float)list[198]-(float)list[98];
}
/*.....*/

void takereadings()
{

```

```

transient=photocurrent=0;
for (jj=0;jj<(readings);jj++)
{
doburst(&diff,&netphoto);
transient=transient+diff;
photocurrent=photocurrent+netphoto;
/* fprintf(stdprn, "difference t1-t2 and netphoto resp.= %f %f\n",diff,netphoto);*/
/* fprintf(stdprn,"r\n"); */
}
photocurrent=photocurrent/readings;
transient = transient/readings;
}

```

```

/* ----- */

```

```

init488()      /* initializes the IEEE 488 card */
{
char response[80];
int spflag;

clrscr();
printf("\n          SYSTEM INITIALIZATION... \n\n");
initialize(gpib_add,0);
setoutputEOS(13,10);

} /* end init488() */

```

```

/* ----- */
micromf()
/* waits until command sent to the micromanipulator is completed */
{
int status, spflag;
spflag=0;
do
{
spoll(micro_add, &spflag, &status);
delay(2);
}
while((spflag&16) || (spflag==0));
if (!(spflag & 64))
{printf("error has occured. Spflag=%d",spflag);}
}

```

```

/* end micromf() */

/* ----- */
void initmicrom() /* initializes the micromanipulator */

{
    char response[80];
    int status, temp, spflag;
    send(micro_add, "J0,EP1,UP",&status);
    micromf();
    send(micro_add,"FS1,H", &status);
    /* enter scanning parameters while
       waiting for the micromanipulator to move */
    printf( "\nInput the number of readings at each location: ");
    scanf ( "%d", &readings);
    micromf();
    send(micro_add,"U1",&status);
    micromf();
    send(micro_add,"XM75000.,YM75000.,A",&status);
    micromf();
    /* enter sampling periods while waiting for micromanipulator to move */
    printf( "\n t1 should be a multiple of the sampling period= 0.5msec.\n" );
    printf( "Input the multiple: ");
    scanf ( "%d", &t1 );
    printf( "\n t2 should be a multiple of the sampling period.\n" );
    printf( "Input the multiple for t2: ");
    scanf ( "%d",&t2 );

    send(micro_add,"BE1",&status); /* enable backlash, set to 1 micron */
    micromf();
    /* micromanipulator will not work reliably without the backlash enable set*/

} /* end initmicrom() */
/* ----- */
rectdefn(xsize, ysize) /* define size of rectangular scan area */
double *xsize, *ysize;
{
    int status;
    clrscr();
    printf("\n DEFINE THE RECTANGULAR SCANNING AREA \n\n");
    send(micro_add, "J1", &status); /* enable joystick */
    micromf();
    printf("Probe the bottom left corner of wafer.\n Press any key when ready.

```

```

\nposition
=");
    while (!kbhit()) /* update position until a key is pressed */
    {
        position(xsize, ysize);
        gotoxy(20,6);
        printf("( %5.0f , %5.0f ) ",*xsize,*ysize);
    }
    getch();
    /* define the micromanipulator zero position */
    send(micro_add,"Z",&status);
    micromf();
    printf("\n\nProbe the top right corner of the wafer.\n Press any key when ready. \n");
    printf("Area size = ");
    while (!kbhit()) /* update area size until a key is pressed */
    {
        position(xsize, ysize);
        gotoxy(13,10);
        printf("%5.0f X %5.0f  ",-*xsize,*ysize);
    }
    getch();
    *xsize = fabs (*xsize);
    *ysize = fabs (*ysize);
    send(micro_add, "J0", &status); /* disable joystick */
    micromf();
    send(micro_add, "XM0.,YM0.,A", &status); /* move to newly defined zero */
    micromf();
} /* end rectdefn() */

/* ----- */
position (px, py) /* reads (x,y) coordinate of the micromanipulator */
double *px, *py;
{
    char linepos[256];
    char strcoord[256];
    int i, len, status;
    char *point;
    send(micro_add, "U1,DP", &status);
    delay(5);
    enter(linepos,30,&len,micro_add,&status);
    micromf();
    /* convert the string from micromanipulator to floating point */
    for (i=0; linepos[i] != '\0'; i++)
        strcoord[i] = linepos[i];
    point = &(linepos[i+1]);
}

```

```

    strcoord[++i] = '\0';
    *px = atof(strcoord);
    *py = atof(point);
} /* position() */
/* ----- */
absolute (xpos, ypos)/* moves the micromanipulator to location (xpos,ypos) */
double  xpos, ypos;
{
    double  x1, y1;
    int delay, ndec, status;
    char MMXM[25], MMYM[12], x1str[8], y1str[8], *x1ptr, *y1ptr, *x2ptr, *y2ptr;
    x1 = xpos;
    y1 = ypos;
    x1ptr=strcpy(MMXM, "XM");
    y1ptr=strcpy(MMYM, "YM");
    ndec=8;
    x2ptr=gcvt(x1, ndec, x1str);
    y2ptr=gcvt(y1, ndec, y1str);
    x1ptr=strcat(MMXM, x1str);
    y1ptr=strcat(MMYM, y1str);
    x1ptr=strcat(MMXM, ".");
    y1ptr=strcat(MMYM, ".");
    x1ptr=strcat(MMXM, MMYM);
    x1ptr=strcat(MMXM, "A");
    send(micro_add, MMXM, &status);
    micromf();
} /* absolute () */
/* ----- */
main()
{
    int  w, z;
    int  Idark;
    int  xinc, yinc;
    int  lo, hi;
    int  ps, psv;
    float  xgridpts, ygridpts;
    FILE  *fp[4];
    x = y = 0.0; /* initialize the coordinates of the micromanipulator */
    convert= 1.; /*10.0/4096.; define the ratio for the conversion */
    init488(); /* initialize IEEE 488 card */
    initmicrom(); /* initialize micromanipulator */
    rectdefn(&xlength, &ylength); /* define rectangular area */
    /* create the data files */
    fp[0] = fopen("otcsphot.grd", "w");

```

```

fp[1] = fopen("otcstran.grd", "w");
fp[2] = fopen("otcsrefl.grd", "w");
fp[3] = fopen("otcsnorm.grd", "w");
printf( "\nInput the x direction step size in microns: ");
scanf ( "%d", &xinc);
printf( "\nInput the y direction step size in microns: ");
scanf ( "%d", &yinc);
xgridpts = floor( xlength / xinc ) + 1;
ygridpts = floor( ylength / yinc ) + 1;
init_a_d(); /*setup ad board*/
/* Write data needed by the SURFER plotting program to all the
output files. See appendix H of the SURFER REFERENCE
manual for more details. */
for (w=0; w<=3; w++)
{
    fprintf( fp[w], "DSAA \n" ); /* indicates an ASCII grid file */
    fprintf( fp[w], "%4.0f %4.0f \n", xgridpts, ygridpts ); /* # points */
    fprintf( fp[w], "%d %4.0f \n", 0, (xgridpts-1)*xinc ); /* x range */
    fprintf( fp[w], "%d %4.0f \n", 0, (ygridpts-1)*yinc ); /* y range */
    fprintf( fp[w], "-5 5 \n"); /* maximum readings */
}
/* clrscr(); */
printf(" SCANNING WAFER...\n\nnow scanning location:\n\nscanning up to
location
(%4.0f,%4.0f)",xlength,ylength);
for( y=0; y<=ylength; y=y+yinc ) {
    for( x=0; x<=xlength; x=x+xinc ) {
        /* move micromanipulator(MM) to next location. Note that the
MM's x-axis is defined backwards compared to cartesian
x-axis, therefore place the negative sign in front of x. */
        gotoxy(22,23);
        printf("(%4.0f,%4.0f)\n", x, y );

        absolute(-x,y); /* move micromanipulator */
        takereadings();
        /* fprintf(stdprn,"last transient = %f \n ",-transient);*/

        /* output the averaged values to the files */
        fprintf( fp[0], " %f ",photocurrent );
        fprintf( fp[1], " %f ",transient);
    } /* endfor x */
    for(w=0; w<=3; w++) /* add a carriage return to all files */
        fprintf( fp[w], "\n" );
} /* endfor y */

```

```
fcloseall();  
AL_TERMINATE();  
printf("\n\n\n\n\n\nScan complete.\n");  
} /* End of Main Program */
```